Abstract

The objective of this master thesis is to quantify how the estimated uncertainty, associated with the Hyme field, will change as more data becomes available. This will be done by identifying the key uncertainties and comparing the pre/post -production estimated ultimate oil recovery and hence the long term potential of Hyme. Hyme is classified as a fast-track development, which means that limited technical subsurface work has been performed before the production start-up. There are limited data available, and no cores where taken.

The objective was achieved through a process that involved three major tasks. The first task was to adjust geologic and reservoir simulation models to establish a working reservoir simulation model and to generate a model reference case to be used in the uncertainty analysis. Secondly, a stochastic pre-production uncertainty analysis was performed in order to quantify the range of ultimate estimated oil recovery and the governing parameters that affect this. The final task was to perform a post-production uncertainty analysis, which utilizes actual bottom hole pressure data with a computer assisted history matching process.

The study concludes that the uncertainty associated with the Hyme subsurface was reduced with early data. Based on the results of the pre-production uncertainty analysis, the ultimate estimated oil recovery can be described within the range of 3.40 to 5.44 million Sm^3. The post-production uncertainty analysis resulted in a range of 4.01 to 5.21 million Sm^3. Hence the uncertainty range for the ultimate estimated oil recovery and the risk concerning the long term potential of Hyme was reduced.

Acknowledgements

This report presents the results of a master thesis by Mats Betanzo Bratteli at the Department of Petroleum Engineering, University of Stavanger. The work has been performed from December 2012 through June 2013.

This thesis would not have been possible without the support of many people. Firstly, I wish to express my gratitude to my main supervisor, Sjur Arneson (Director Reservoir Evaluation, VNG Norge AS) who offered invaluable assistance, support and guidance. I would also like to express my very appreciation to my faculty supervisor Svein M. Skjæveland (Professor of petroleum engineering, University of Stavanger) for his expert advises and suggestions during this thesis work.

I am particularly grateful for the assistance given by Kevin Best (Reservoir Engineering Advisor, VNG Norge AS), for the great conversations, suggestions and technical support. A deep thank to Adrian Anton (Reservoir Engineer, Schlumberger) for hosting a great course in Petrel, and for continuous technical support. I would also like to thank Karl Ludvig Heskestad (Commercial Director, Resoptima) for a personal training course in Olyx, and for technical support during this study.

Special thanks to Andre Sætheren (Senior Reservoir Engineer, VNG Norge AS), Ali Jaffri (Geological Consultant, Applied Stratigraphix), and Margaret Åsly (Senior Reservoir Engineer, VNG Norge AS) for advises and inputs during this study.

I would like to express my profound gratitude and appreciation to VNG Norge AS for support and participation in this study. To be a part of the Hyme asset and to be allowed to contribute with subsurface technical work has been a great motivator during the study. I will also like to thank the companies Statoil ASA, E.ON Ruhrgas Norge AS, GDF Suez E&P Norge AS, Core Energy and Faroe Petroleum for permission to use the necessary data.

Finally, I wish to thank my common law wife for support, patience and encouragement throughout my study.

Stavanger 13th of June 2013

……..

Mats Betanzo Bratteli

Table of Contents

List of figures

List of tables

1. Introduction

The objective of this thesis is to describe and quantify static and dynamic uncertainty associated with the development of a new oil field named Hyme. In order to describe and quantify these uncertainties, existing tools and techniques are used in combination with available geophysical, geologic, petrophysical, reservoir, drilling, and production data. The study focuses on an uncertainty analysis both before and after production start-up of the field. The overall purpose of this thesis is to quantify how perceived uncertainty will change as more data becomes available. This will be done by comparing the estimated ultimate oil recovery before and after the field starts production. To reach the main objective, technical work was divided into 3 main tasks.

The first task was to adjust the geologic and reservoir simulation models provided by the operator to establish a working reservoir simulation model and to generate a model reference case to be used in the uncertainty analysis. A description of the different input parameters, how the reference case is established and the results of the reference case, are described in chapter 3.

The second task was to perform a stochastic pre-production uncertainty analysis in order to quantify the range of ultimate estimated oil recovery and the governing parameters that affect this. A sensitivity analysis was performed of selected input parameters and 200 simulations were run for investigating the estimated ultimate oil recovery. In chapter 4 the uncertainty ranges for the input parameters are described as well the methodology and results of this task.

The final task was to integrate production data into the uncertainty study, in order to perform a post-production uncertainty analysis. This is known as history matching, and it will integrate actual production data into the simulator. In this thesis the history matching will be performed with assisted history matching software (Olyx). The aim of history matching is to provide a more representative model. Methodology and results for this study are described and presented in chapter 5.

Mapping of uncertainty associated with field development in the petroleum industry has become more important over the years, as the costs for developing a field and to collect the

necessary data is becoming increasingly expensive. There are several available uncertainty studies that have been performed with simulations to predict future performance of a reservoir behavior (Walstrom et al., 1967), (Damsleth et al., 1992), (Steagall and Schozer, 2001), (Li-Bong et al,. 2006) and (Lisboa and Duarte, 2010).

Walstrom et al. (1967) presented a method that incorporates uncertainty in the input parameters to a reservoir simulation model. Uncertainty was included in that more simulation models were run with different input parameters to compare the results statistically. A more efficient approach was proposed by Damsleth et al. (1992), where a methodology with experimental design was presented. Experimental design can be considered as a plan that specifies the setting of each input parameter in a series of simulation runs.

Steagall and Schozer (2001) presented a methodology of defining a set of uncertain parameters, performing a sensitivity analysis of the parameters, and then generating a number of simulation cases with experimental design. After the simulations were done, the results were treated statistically. The study was performed on the appraisal stage applied to a real offshore field in Campos Basin in Brazil. A model based uncertainty analysis methodology presented by Li-Bong et al (2006) uses a similar methodology, however this model based methodology incorporates multiple geologic models as well. These methodologies are analogues and form the basis of the methodology used in this thesis.

Lisboa and Duarte (2010) present a study incorporating history matching with the uncertainty study. The study is performed on a deep water oil field in the Campos Basin, where the field has been in production for a few years.

This thesis adopts a mix of the methods mentioned above, but differ in the extent that it concerns a new oil field in the initial production phase, where uncertainty is assessed both before and after production start-up. In addition to this, the experimental design could be considered as unique when it comes to which input parameters that are integrated at the same time and the software used for history matching.

2. Background

The Hyme field is an oil field located in the Haltenbanken area (block 6407/8) on the Norwegian continental shelf northwest of Trondheim (Figure 2-1). The field is located offshore in water depth of 250m. It was discovered in May of 2009 with the exploration well 6407/8-5 S and its sidetrack 6407/8-5 A. Hyme is described as a fast track development which implies a rapid design, construction, and installation. Additionally, Hyme will be a tie in to the already producing field Njord. This means that production is to the Njord A platform, through a 19 km long pipeline south-east of Hyme. Production started on the 2nd of March 2013, and the field is operated by Statoil, which owns 20% of the license. Other companies that are partners in the development are E.ON Ruhrgas Norge AS (30%), GDF Suez E&P Norge AS (28%), Core Energy (12%), Faroe Petroleum (7.5%) and VNG Norge AS (2.5%).

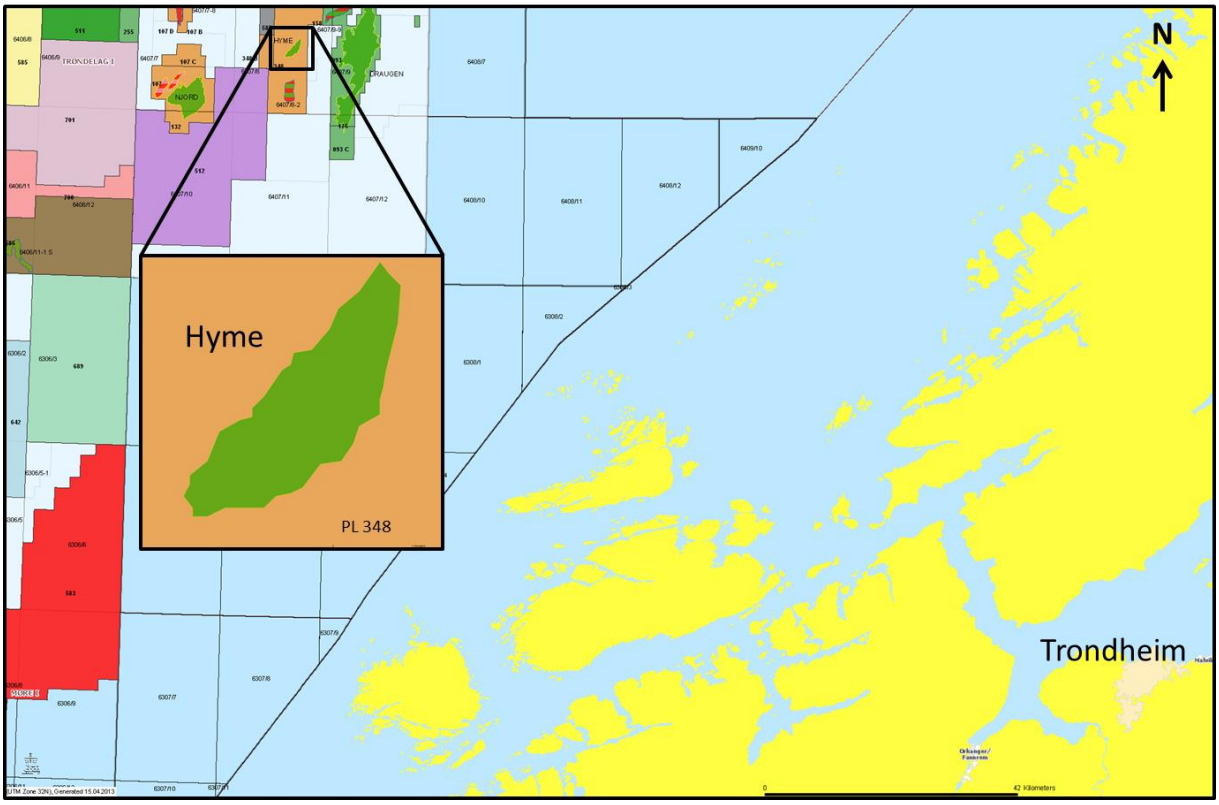

Figure 2-1: Location of the Hyme field on the Norwegian continental shelf.

Hyme has a limited volume of data available. Two seismic surveys with poor to moderate quality define the structure while well logs are used to describe the internal architecture of reservoirs. Cores were not extracted from the field, which means that analogue data from

nearby fields such as Njord and Heidrun which have similar geology will be used. Hydrocarbons were discovered both in Tilje and Ile formations, however more than 90% of the reserves are estimated to be located in Tilje. The field development is only focused on the Tilje reservoir.

The primary reservoir in the Hyme Field is the Lower Jurassic Tilje Formation (Dalland et al, 1988). The Tilje represents ancient tide-dominated delta sediments that were deposited in a rift-basin (Martinius et al ., 1999). Due to the complex interplay between river, tide, and to a lesser extent, wave processes, tidal deltas tend to produce extremely heterogeneous successions. Sands occur in tidal sand flats, channels, shore-normal tidal mouthbars, and subtidal dunes. The majority of these sand-prone lithofacies have internal mud-drapes. These mud-drapes can reach thickness of 1 cm and decrease vertical permeability. Studies performed on Tilje, based on pressure data from Heidrun, have identified these barriers (Reid et al.,1996). It is likely that these barriers also exist in Tilje formation of Hyme, making it one of the key uncertainties in this study. Besides internal flow barriers, another major uncertainty lies with the laterally discontinuous nature of sand bodies. Channels in tidal deltas have a low tendency to avulse, which means they do not meander freely, and do not produce sheet-like sand bodies. Tidal bars also form isolated sand bodies that are not connected. Therefore a borehole that intersects one of these compartmentalized sand-bodies may only drain that one particular unit.

There is one oil production well on Hyme and it is a multilateral with two branches. The main reason for the multilateral well is that the Hyme reservoir has a major fault dividing the reservoir into two parts, in eastern and western segment. The main bore is located in the largest segment, which is west, while the lateral bore is located in east. The eastern segment is smaller; therefore water breakthrough is predicted to come earlier in the lateral bore, compared to the main bore. This would result in a possible earlier shut in for this lateral and the model predicts this to occur in 2016.

To provide pressure support to the multilateral producer a water injector is planned. The injector is located in the northern part of the eastern segment, where the major fault has the smallest throw (Figure 2-2). Location of the injector was carefully decided by the license group based on a cross-disciplinary evaluation, including structural uncertainties. The

injector was located in the east to penetrate the water zone of the Tilje formation, and at the same time it assumed to pressure support both the segments. Currently, the estimated schedule for injection startup is 1st of June 2013 (Statoil, verbal communication).

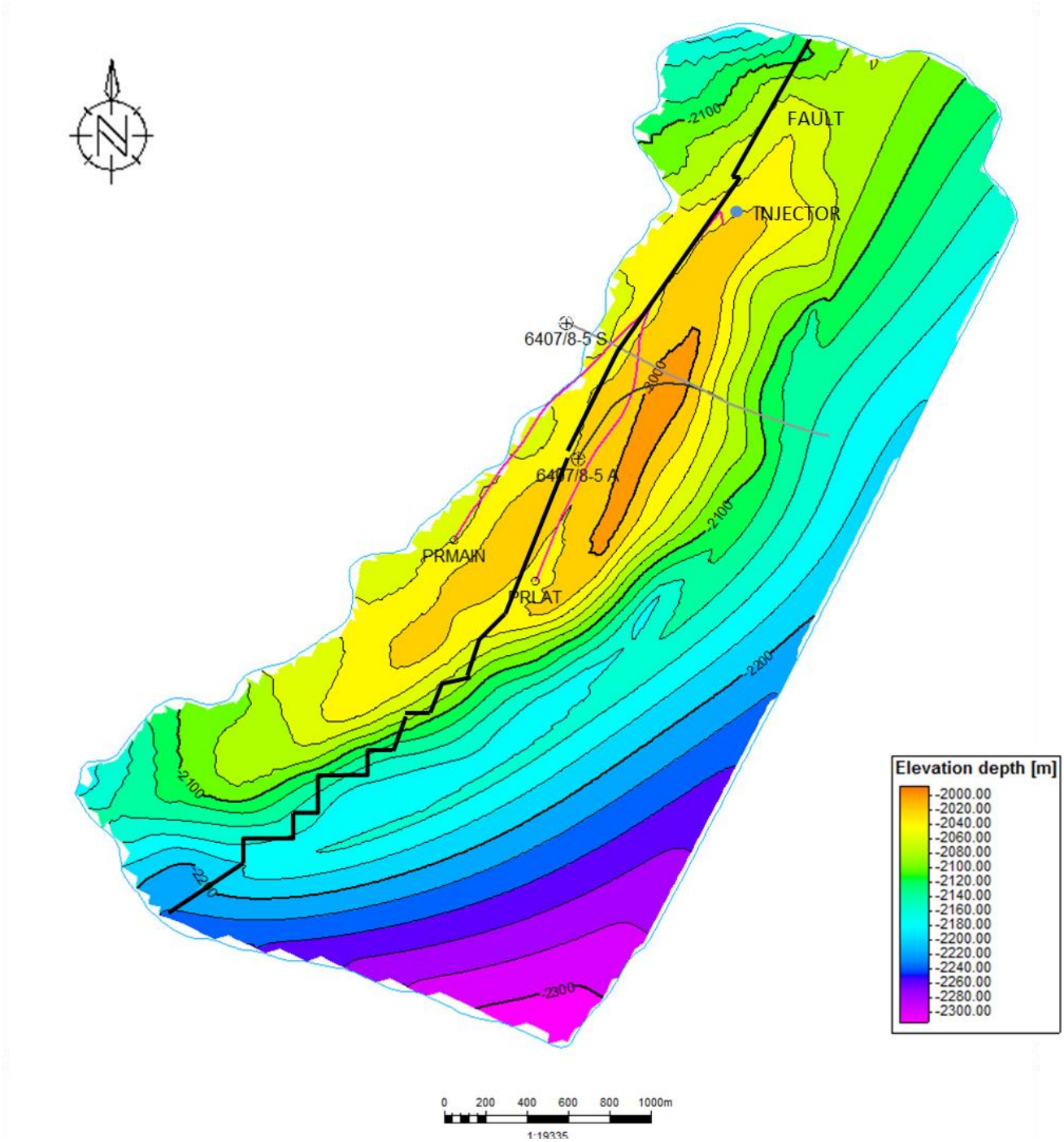

Figure 2-2: Geologic depth map of the Hyme reservoir.

3. Model Reference Case

Geologic and simulation models were provided by the operator Statoil. The models consist of static and dynamic input data, which is based on geologic, geophysical, petrophysical, reservoir engineering, production and drilling data. The first task was to create a reference case for prediction of future production performance of the Hyme reservoir (Figure 3-1). Based on these results, an uncertainty study was performed to investigate which parameters affect the initial in-place oil volume and the cumulative oil production.

3.0.1 Reservoir Simulation

Reservoir simulation is one of the most flexible and used tools in reservoir engineering. This is mainly because it is a tool that has the ability to predict the future production performance of oil and gas reservoirs over a wide range of operating conditions (Mattax and Dalton, 1990). To run a simulation model, it is necessary to have a model that represents the reservoir of interest. The model should contain information about the rock and fluid properties obtained by laboratory measurements of cores, well logs and seismic. All this information combined with interpretation of the results are called physical models (Kleppe, 2010). The input data for the Hyme reference case was provided by Statoil and are described in the reservoir and model description (section 3.1) of this thesis.

To be able to run a simulation on a physical reservoir model the model needs to be divided into a number of individual blocks, known as grid blocks. These blocks correspond to a unique location in the reservoir, with unique properties such as porosity, permeability and relative permeability that will represent the reservoir at this location. In a 3D grid, which will be used for the Hyme reference case, the grid blocks are assigned x, y and z coordinates (Mattax and Dalton, 1990).

A reservoir simulator can be defined as a computer program written to solve the equations for flow of fluids in a reservoir (Kleppe, 2010). During simulation, fluids can flow between neighboring grid blocks. The rate of this flow is determined by pressure differences between blocks and flow properties assigned to the interfaces between the blocks. This process will minimize the mathematical problem to a calculation of flow between grid blocks. For every interface between different grid blocks, a set of equations must be solved in order to calculate the flow of all mobile phases. In general, the equations include Darcy's law and the

concept of material balance and contain terms describing the permeability between grid blocks, fluid mobilities including relative permeability and viscosity, and compressibility of the rock and fluids (Mattax and Dalton, 1990).

There are several types of reservoir simulators, depending on which reservoir they are intending to simulate. For the Hyme reference case, a black oil model will be used. The simulator is Eclipse 100, developed by Schlumberger. Black oil model simulators are the most frequently used simulators in the petroleum industry, because it is the simplest model. The reason why it is considered as simple is the assumptions for the black oil model which are:

- Three phases, oil, gas and water.
- Three components; oil, gas and water.
- No phase transfer between water and hydrocarbons.
- Gas can be dissolved in oil and flow together with oil component in an oil phase.
- Oil cannot exist in the gas phase.
- Constant temperature.

Based on these assumptions, the black oil model consists of two hydrocarbon components. This is assumed to be appropriate for Hyme reference case, since changes in fluid compositions are not believed to play an integral part of the process. The three components are given the same names as the phases. That will not cause any problems for the water phase, since it is assumed to be no phase transfers between water and hydrocarbons. Between the oil and gas component there is a more complex relation since there is a one way transition. This means that it can exists gas in the oil phase, but not oil in the gas phase. Since Hyme is not a gas condensate field, these assumptions are expected to be valid. Additionally, the temperature is always assumed to be constant (Kleppe, 2010).

The final equations for the black oil model are based on differential equations for mass conservation for each component combined with Darcy's law. They are given by

water

$$\nabla \cdot \left[\frac{[k]k_{rw}}{\mu_w B_w} (\nabla P_w - \gamma_w \nabla d) \right] + Q_w = \frac{\partial}{\partial t} \left(\varphi \frac{S_w}{B_w} \right),$$

oil

$$\nabla \cdot \left[\frac{[k]k_{ro}}{\mu_o B_o}(\nabla P_o - \gamma_o \nabla d)\right] + Q_o = \frac{\partial}{\partial t}\left(\varphi \frac{S_o}{B_o}\right),$$

and gas

$$\nabla \cdot \left[\frac{[k]k_{rg}}{\mu_g B_g}\left(\nabla P_g - \gamma_g \nabla d\right)\right] + \left[\frac{[k]k_{ro}R_s}{\mu_o B_o}(\nabla P_o - \gamma_o \nabla d)\right] + Q_g = \frac{\partial}{\partial t}\left(\varphi \frac{S_g}{B_g} + R_s \varphi \frac{S_o}{B_o}\right),$$

where:

- Index o, w, c: oil, water and gas.
- *Q*: Source/sink term, positive for injection, negative for production
- *S*: Saturation
- *B*: Formation volume factor
- R_s: Gas Solubility
- K_r: Relative permeability
- [*K*]: Absolute permeability
- *P*: Pressure
- $\gamma: \rho g$
- ρ: Phase density
- g: Gravity acceleration
- d: Distance
- φ: Porosity

Before a reservoir simulator can run and predict future production performance, one must create a development strategy. This includes wells, production schedule and constraints. Number of producing and injecting wells must be specified, and under which conditions they can operate. Several wells can have group constraints, which can be flow rate or pressure related. The constraints can be economic limits or what the production facility actually can handle. The production schedule must also be specified, when production starts and for how long the run will last (Mattax and Dalton, 1990),(Kleppe, 2010). Development strategy for Hyme reference case was carefully created based on well and facility constraints provided by

Statoil. This will be further discussed in the development strategy section (section 3.5) of this thesis.

A standard procedure after the reservoir model is constructed is to test it against historical production data. The aim is to investigate if it is possible to duplicate past field behavior, running a simulator with historical data and compare the calculated production behavior with actual reservoir performance (Breitenbach, 1991), known as history matching. The Hyme reference case is a new development based on no production or pressure data, thus history matching was not considered. However, for the post uncertainty study, history matching will be applied.

Computer software (Petrel) was used for modeling, visualization, and post-processing. Petrel is a PC-based workflow application for subsurface interpretation, integration, and modeling. The software makes it possible for users to perform different workflows, from seismic interpretation to reservoir simulation. A benefit using this software is that geophysicists, geologists, and reservoir engineers can move across domains, rather than applications, through the Petrel integrated toolkit. Petrel is developed by Schlumberger, and uses the simulator Eclipse 100. (Schlumberger, 2012)

3.0.2 Workflow for development of Hyme reference case

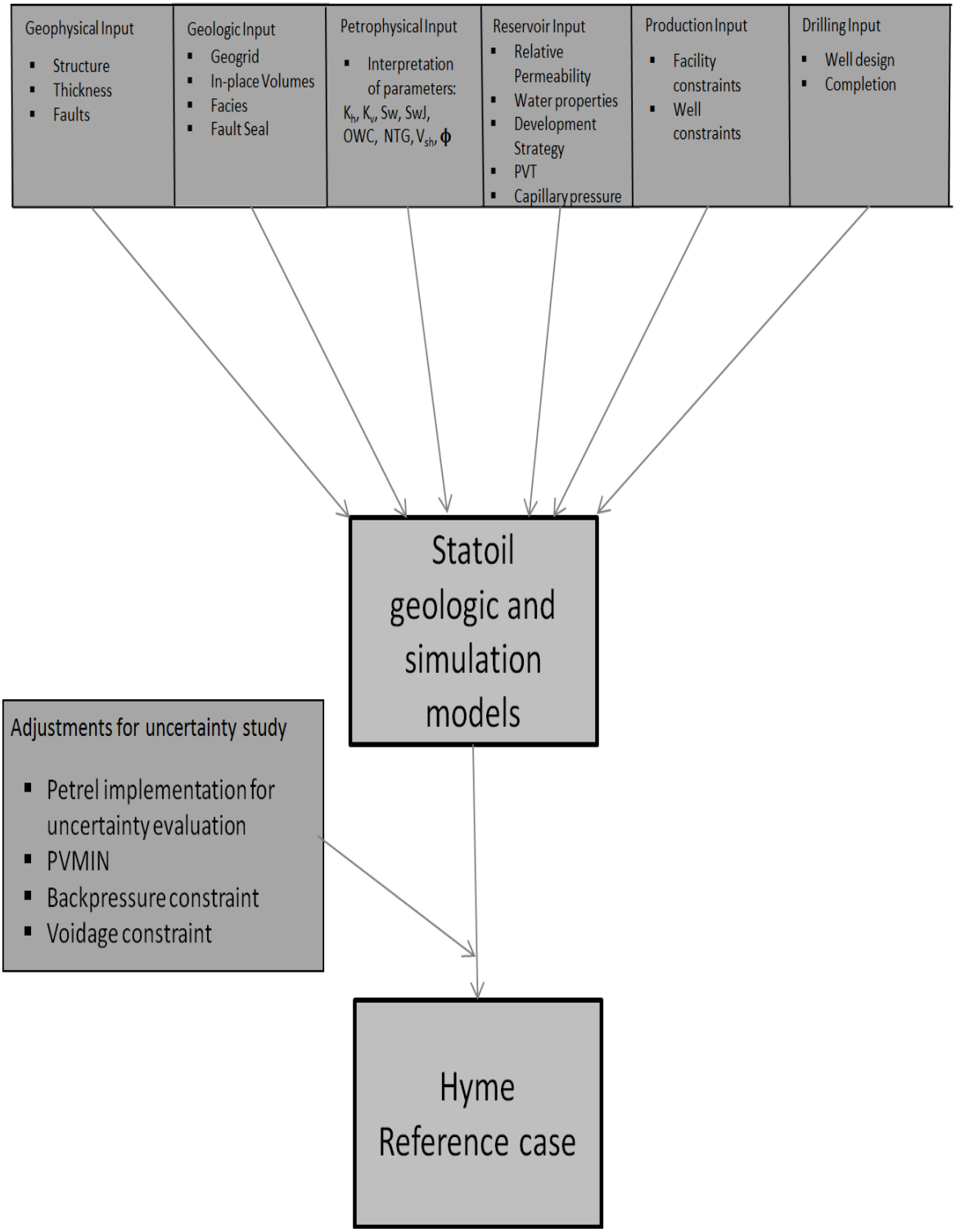

Figure 3-1: Schematic overview of the workflow for developing Hyme reference case.

3.1 Reservoir and model description

The input parameters used in this thesis, are based on Statoils early evaluation of the Hyme field. A geophysical study was performed by Statoil to generate a structural model for the Hyme reservoir. The structural model is based on seismic interpretations and it also includes location of the internal fault. From the seismic interpretations, the reservoir thickness was determined.

A geological evaluation of the Hyme field was performed by Statoil. The study has been simplified to meet the deadlines of the fast track work plan. The consequence is that parameters were modeled directly, without facies modeling. Another time saving decision was to build a geogrid that allows simulation without upscaling. The purpose for the geological evaluation has been to quantify the in-place volumes for the Tilje reservoir of the Hyme structure, create a grid for simulation, and quantify the uncertainties on in-place volumes. In addition a fault seal study was performed for investigating flow through the internal fault (Statoil, 2012).

A Petrophysical study was performed by Statoil to determine porosity, shale volume, oil-water contact, net sand, permeability, water saturation and a J function. The interpretation was based on the total porosity model using data from well logs and data from analogue fields in the area. The formation of interest in this study was Tilje (Statoil, 2012).

Reservoir data includes relative permeability, PVT and capillary pressure. Statoil performed an analogue study in order to obtain relative permeability and capillary pressure data. The PVT data were based on fluid lab analysis of samples from well 6407/8-5S and 6407/8-5A supplied by Statoil (Statoil, 2012).

In this thesis, the different input parameters are divided into two groups, static and dynamic input parameters. Static parameters include parameters that have an impact on volumes in place. Dynamic parameters include parameters that influence the flow of hydrocarbons and water and influences cumulative oil recovery.

3.2 Hyme static data

3.2.1 Rock properties

Thickness

The true vertical thickness was determined by geophysical interpretation of seismic. Combined with well logs, the thickness within each reservoir zone was determined, and is listed in Table 3-1 .

Table 3-1: Average true vertical thickness by reservoir zone.

Reservoir Zone	True vertical Thickness [m]
Tilje 4.2	5.7
Tilje 4.1	14.8
Tilje 3	44.0
Tilje 2.2	31.5
Tilje 2.1	2.9
Tilje 1	16.6
Tilje Total	115.5

Rock compressibility

Due to lack of core data, the rock compressibility was assumed to be constant (Table 3-2). It was estimated based on bulk modulus calculations for the nearby field Midgard, combined with Hyme average porosities.

Table 3-2: Rock compressibility

Parameter	Value	Unit
Rock compressibility	7.83×10^{-5}	bar^{-1}

Porosity

The interpretation of porosity was based on log data and the total porosity model, where the curve was computed from the density log. The following equation for total porosity where used

$$\phi_{D,tot} = \frac{\rho_{ma} - \rho_b}{\rho_{ma} - \rho_{fl}},$$

where $\varphi_{D,tot}$ is the total porosity, ρ_{ma} is the matrix density, ρ_b is the bulk density from logs and ρ_{fl} is the fluid density. Due to lack of core data on Hyme, the matrix density coming from core data from the relevant formation units from wells in the area, and then averaged over each formation.

Base case porosity function PHIT, is taken from the average porosity of Tilje in both wells. Since the locations of the two wells are close, it is assumed that the reservoir quality is similar. However, the TVD depth is deeper in the S well compared to well A, which could result in lower porosity. Results for porosity in the different reservoir zones are listed in Table 3-3.

Shale volume

The calculation of shale volume fraction was based on a minimum of two estimates. The first estimate from gamma-ray log and the second estimate from neutron porosity log data. The shale volume equation is given by

$$V_{sh} = Min(V_{sh,\gamma}, V_{sh,dn}),$$

with the volume shale fraction from gamma-ray given by

$$V_{sh,\gamma} = \frac{\gamma - \gamma_{min}}{\gamma_{max} - \gamma_{min}},$$

where γ is the read of the gamma-ray log, γ_{max} is the shale gamma-ray value, and γ_{min} is the clean sand gamma-ray value (Lehne, 1985).

The volume shale fraction from density neutron is given by

$$V_{sh,dn} = \frac{\phi_{Nc} - \phi_{D,tot} \times H_f}{\phi_{Nsh}},$$

where φ_{Nc} is the borehole corrected neutron porosity from log converted to sandstone porosity units, $\varphi_{D,tot}$ is the total porosity form the density log and φ_{Nsh} is the apparent shale neutron porosity from literature (Lehne, 1985). The H_f is the fluid hydrogen index. Shale volume fractions for the different reservoir zones are listed in Table 3-3.

Net sand

Since no core data were available, the Net sand cut-offs was defined to minimize loss of hydrocarbon volume, and at the same time estimate volumes that are clearly non net from logs. Statoil proposed a porosity cut-off of 14% and a shale volume fraction cut-off of 0.35%. The proposed cut-offs are reported to result in a loss of 3 % hydrocarbon volume.

Net to gross

The base case net to gross is based on the average porosity of Tilje in both wells. Without core data, net to gross was estimated based on the net sand calculation. Results for net to gross values in the different reservoir zones are listed in Table 3-3.

Table 3-3: Average Porosity, Shale volume fraction, and net to gross by reservoir zone.

Reservoir Zone	Porosity [Frac]	Shale volume fraction [Frac]	Net to gross [Frac]
Tilje 4.2	0.182	0.209	0.433
Tilje 4.1	0.219	0.237	0.702
Tilje 3	0.282	0.140	0.851
Tilje 2.2	0.281	0.129	0.929
Tilje 2.1	0.183	0.264	0.355
Tilje 1	0.212	0.128	0.878
Tilje Total	0.256	0.154	0.824

Water Saturation

Water saturation (Figure 3-2 and Figure 3-3) was based on resistivity logs and the Archie equation (Archie, 1942), which gives the total water saturation

$$Sw_t = \left(\frac{a \times R_w}{\phi_t^m \times R_t} \right)^{\frac{1}{n}},$$

where R_W is resistivity of formation water, R_t is the true formation resistivity, φ_t is the total porosity, a is lithology coefficient, m is cementation exponent, and n is saturation exponent.

The true resistivity R_t is based on the deep resistivity induction log. Due to high inclination and influence of neighboring layers, the uncertainty in the R_t curve is considered as moderate to high. R_w was generated using Arp's formula combined with a Baker Atlas approximation of R_w as a function of salinity. The base case R_W is coming from a water sample taken in Tilje, which makes the uncertainty low.

Cementation exponent m, is based on a Pickett plot of Formation Factor (Ro/Rw) versus log total porosity in a clean water zone. The value obtained were 2.00, which is a standard value for m, hence low uncertainty. Due to lack of core data, standard values for n and a where used. The saturation exponent n was set to 2, and the lithology coefficient a to 1. Changes in all these factors will have an impact on the water saturation. The average water saturation for the different reservoir zones are listed in Table 3-4.

Table 3-4: Average water saturation by reservoir zone.

Reservoir Zone	**Water Saturation [Frac]**
Tilje 4.2	0.686
Tilje 4.1	0.580
Tilje 3	0.385
Tilje 2.2	0.944
Tilje 2.1	0.183
Tilje 1	0.913
Tilje Total	0.441

Water Saturation height function

The water saturation height function SWJ, is used to predict water saturation. This is given by the equation

$$SWJ = a \times J^{-b},$$

where a and b are regression coefficients determined form cross plots of SW versus J, and J is given by the equation

$$J = H \times \sqrt{\frac{KLOGH}{\phi_t}},$$

where H is the height above free water level, KLOGH is the log derived horizontal permeability and φ_t is the log derived total porosity.

3.2.2 Fluid properties

Oil water contact

The base case oil water contact in Tilje (Table 3-5) is based on pressure points measured by MTD tool from the exploration well 6407/8-5 S. The pressure points were considered as good data, and clear gradients were established in both oil and water bearing zones.

Table 3-5: Average Oil water contact for the Tilje formation.

Parameter	Value	Unit
Oil water contact, Tilje	2132.5	m TVD MSL

From Figure 3-2 and Figure 3-3 it can be observed that the Hyme field does not have a gas cap, hence there exists no gas oil contact. Based on Figure 3-3, which shows a 3D cross section of the reservoir, one can observe the base case oil water contact which is the boundary between the oil saturated zone and water saturated zone.

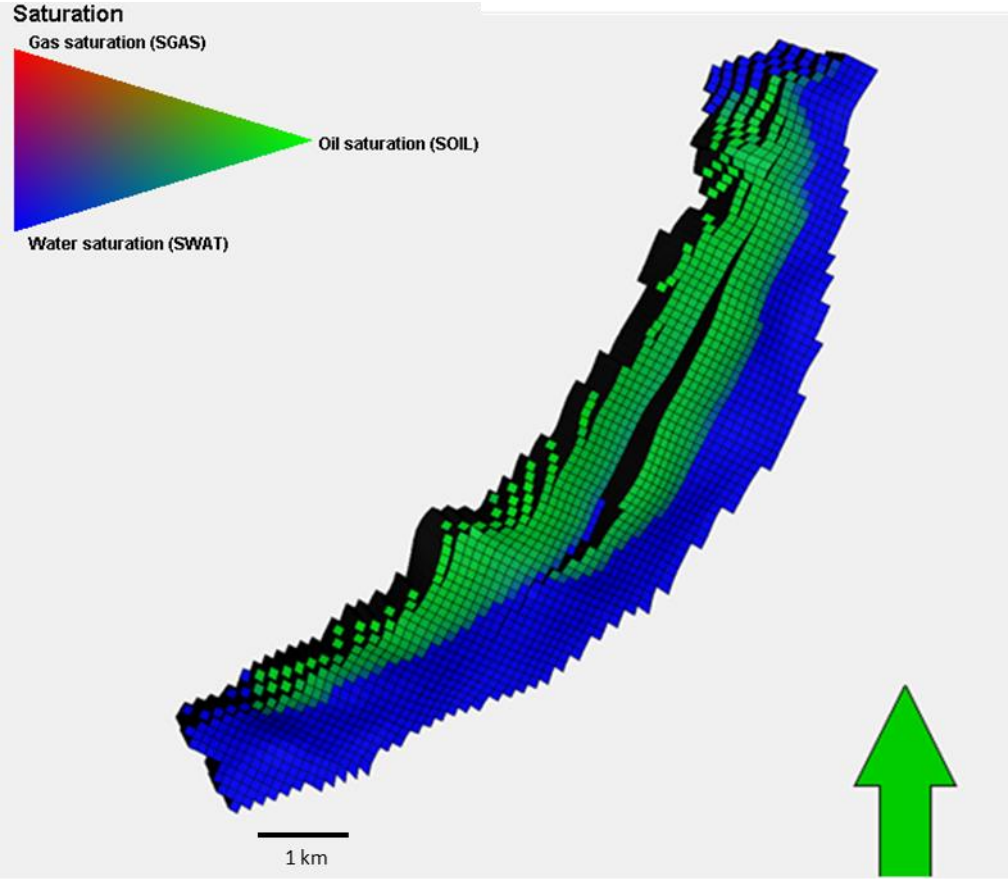

Figure 3-2: 2D overview of the initial saturations on the Hyme field.

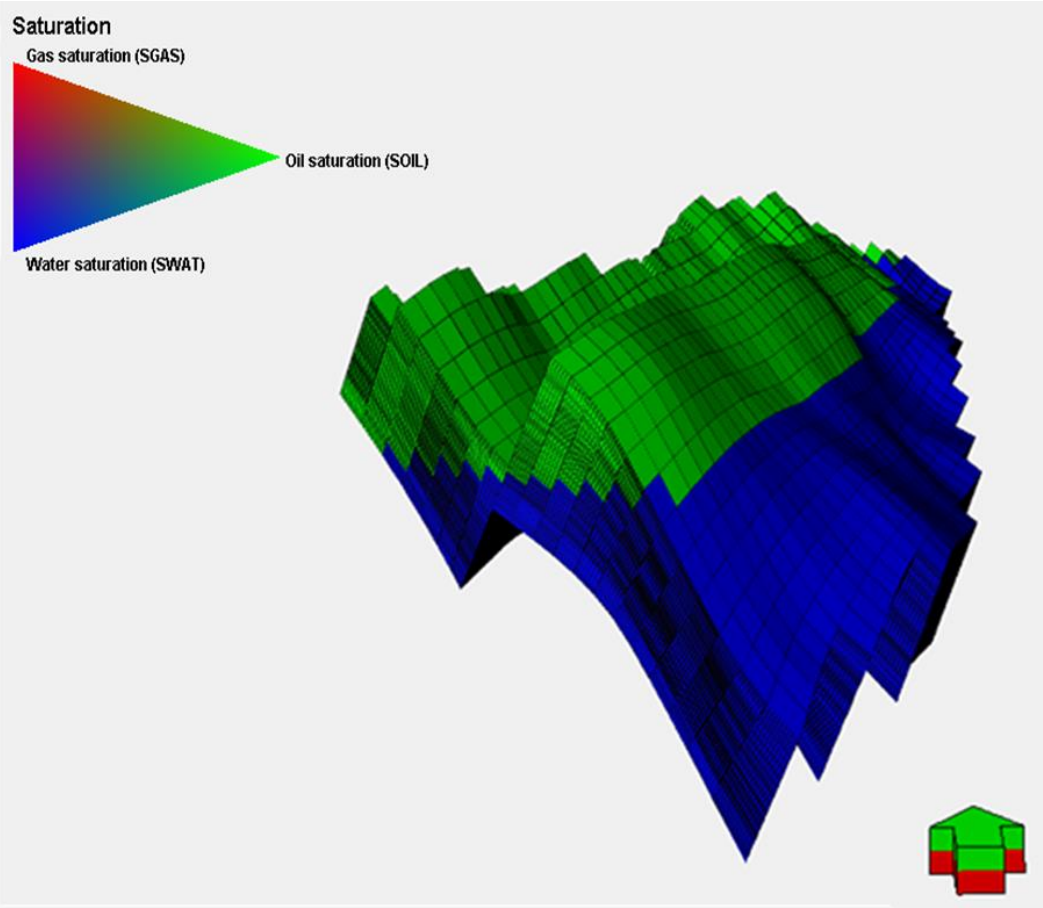

Figure 3-3: 3D cross section of the initial saturations on the Hyme field.

PVT

Based on fluid samples from Tilje formation, PVT data was measured and is reported in Table 3-6.

Table 3-6: PVT data from Tilje formation.

Parameter	Value	Unit
Solution GOR	187.3	Sm^3/Sm^3
Oil density	815.4	Kg/Sm^3
Gas Gravity	1.1042	Kg/Sm^3
Water Sp. Gravity	1.02841	Sp. Gravity
Water Salinity	41234.5	ppm
Oil formation volume factor	1.62884	Rm^3/Sm^3
Oil viscosity	0.214	cP
Reservoir temperature	96.5	°C
Bubble point pressure	198.2	Bara

3.3 Hyme dynamic data

3.3.1 Faults

There have been interpreted four faults on Hyme based on seismic data, but only one of them is integrated in the Hyme reference case, which is the internal fault G2. The internal fault G2 is considered as the most important fault because this fault divides the reservoir into two segments; western and eastern segment (Figure 2-2 and Figure 3-10). Other faults were not included due to limited time and the importance of these faults was considered as low.

For volume and recovery calculations, the location and sealing of the internal fault G2 is crucial. The fault is interpreted on two picks. One pick in well 6407/8-5 A based on log interpretation, and the other in well 6407/8-5 S based on image log results. Due to the bad seismic, there is a lot of uncertainty connected to the fault location. However, the main focus of this thesis will be the sealing capacity of the fault. The location will not be investigated further. To account for the limited vertical resolution, the fault was extended to a likely throw/length relationship.

Fault Seal

A fault seal analysis was performed by Statoil for investigating how fluids flow through the internal fault. One of the objectives in the fault analysis was to calculate fault permeabilites and exporting fault transmissibility multipliers to the reservoir simulator. Input data where based on sample analysis of micro faults in core from analogue fields Njord and Heidrun. For the Hyme reference case, the internal fault G2 is modeled with transmissibility multipliers for each gridblock where the fault may exist. The internal fault G2 is assumed to be open in the Hyme reference case.

3.3.3 Vertical communication

Vertical communication is based on analogue data from Heidrun and Njord, where there is a long production experience from the Tilje reservoir. According to Heidrun and Njord data, there should be barriers or baffles to flow between most of the reservoir zones in Tilje. This is most likely clay drapes and lenticular bedding (Reid et al., 1996). For the Hyme reference case vertical communication between the reservoir zones in Tilje (Figure 3-4) is modeled with transmissibility multipliers (Table 3-7).

Table 3-7: Transmissibility multipliers between the different reservoir zones.

Transmissibility multiplier	Reservoir zones [From-To]	Multiplier value
Z1	Tilje 4.2- Tilje 4.1	0
Z2	Tilje 4.1- Tilje 3	0
Z3	Tilje 3 - Tilje 2.2	0.0001
Z4	Tilje 2.2- Tilje 2.1	0

From Figure 3-4 it can be observed that the transmissibility multipliers (Z1, Z2, Z3, Z4) are applied on the boundaries between the different layers. There are vertical multipliers between all zones, except between Tilje 2.1 and Tilje 1.2, where it is assumed to be communication. Note that the multipliers in Table 3-7 are zero or really close to zero, which implies no communication.

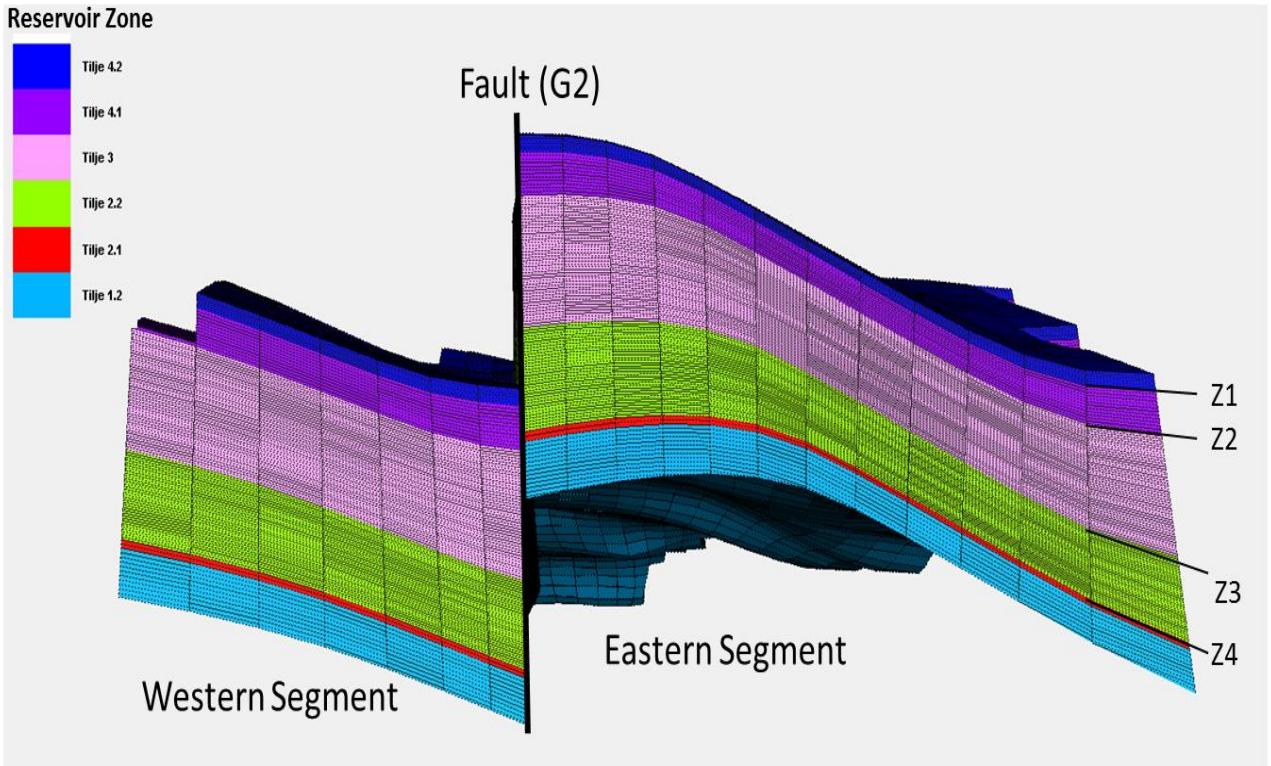

Figure 3-4: Vertical cross section of the 3D Grid displaying the different reservoir zones, location of transmissibility multipliers (Z1, Z2, Z3, Z4), the two segments and the internal fault G2.

3.3.4 Permeability

In the absence of core data, Statoil created a simple permeability model. This model is based on relations between porosity and permeability taken from core data from representative formations. This includes the Tilje formation, from nearby Njord field and Galtvort field. The porosity-permeability model is given by the expression;

$$KLOGH = 10^{(a_k + b_k \times \phi_{D,tot})},$$

where KLOGH is the horizontal permeability, $\varphi_{D,tot}$ is the total porosity, a_k and b_k is regression constants. a and b are calculated by linear regression of porosity and permeability and nearby wells.

Vertical permeability is modeled using the K_v/K_h relationship of 0.1 which is based on the analogue fields. There are almost always uncertainties connected to permeability calculations, due to lack of information. Since there is no core data available for Hyme, the uncertainty in permeability are considered as large. The nearest analogue data for Tilje formation is located on the Njord field, which is several hundred meters deeper than the Tilje formation on Hyme. Average vertical and horizontal permeability for the different reservoir zones are listed in Table 3-8.

Table 3-8: Average horizontal and vertical permeability for the different reservoir zones.

Reservoir Zone	Horizontal Permeability [mD]	Vertical Permeability [mD]
Tilje 4.2	45.2	4.5
Tilje 4.1	135.4	13.55
Tilje 3	1364.9	136.5
Tilje 2.2	905.8	90.6
Tilje 2.1	16.5	1.7
Tilje 1	60.5	6.1
Tilje Total	795.7	79.6

3.3.5 Relative permeability

It has been recommended to use relative permeability in the Hyme simulation model for both oil/water and gas/oil two phase flow. Since cored wells are not available, analogue data was used as basis for the relative permeability. Njord is used as analogue due to a common main reservoir Tilje, with similar PVT and petrophysical properties.

The analogue study gave few clear trends, but some parameters seemed to be dependent on permeability. Additionally permeability was compared with porosity for Tilje on Njord, and the data tend to gather in two trends or rock types. This resulted in the use of two saturation regions for addressing relative permeabilities, for absolute permeabilities above and below 500mD. The regions were named SATNUM 1 (K<500mD) and SATNUM 2 (K>500 mD). Based on experimental data, it was hard to justify more saturation regions, therefore the parameters are kept constant within each SATNUM. The study provided a base case, which will be used in the Hyme reference case. Properties for the base case are listed in Table 3-9 and Table 3-10. Base case is based on mixed wettability and Corey type equations (Schlumberger, 2012)

for oil-water system

$$k_{ro} = k_{ro}(s_{wmin}) \left[\frac{s_{wmax} - s_w - s_{orw}}{s_{wmax} - s_{wi} - s_{orw}} \right]^{C_{o/w}},$$

$$k_{rw} = k_{rw}(s_{orw}) \left[\frac{s_w - s_{wcr}}{s_{wmax} - s_{wcr} - s_{orw}} \right]^{C_w},$$

for gas-oil system

$$k_{rg} = k_{rg}(s_{org}) \left[\frac{1 - s_w - s_{gcr}}{1 - s_{wi} - s_{org} - s_{gcr}} \right]^{C_g},$$

$$k_{ro} = k_{ro}(s_{gmin}) \left[\frac{s_w - s_{wi} - s_{org}}{1 - s_{wi} - s_{org}} \right]^{C_{o/g}},$$

where

- K_{ro}: Relative permeability of oil
- K_{rw}: Relative permeability of water
- K_{rg}: Relative permeability of gas

- S_{wmin}: Minimum water saturation
- S_{wmax}: Maximum water saturation
- S_{wi}: Initial water saturation
- S_{wcr}: Critical water saturation
- S_{orw}: Residual oil saturation to water
- S_{gcr}: Critical gas saturation
- S_{org}: Residual oil saturation to gas.
- S_{gmin}: Minimum gas saturation.
- C_w: Corey water exponent
- $C_{o/w}$: Corey oil to water exponent
- $C_{o/g}$: Corey oil to gas exponent
- C_g: Corey gas exponent

These equations are used by Petrel for calculating the relative permeability curves, and are listed in the Petrel help manual (Schlumberger, 2012).

Table 3-9: Relative permeability input for the Hyme reference case.

SATNUM 1		**SATNUM 2**	
K<500mD		**K>500mD**	
Oil-Water		**Oil-Water**	
S_{orw}	0,17	S_{orw}	0,12
$K_{rw}(s_{orw})$	0,45	$K_{rw}(s_{orw})$	0,6
C_w	3,5	C_w	2,5
$C_{o/w}$	4,5	$C_{o/w}$	5
Gas-Oil		**Gas-Oil**	
S_{org}	0,12	S_{org}	0,08
$K_{rg}(s_{org})$	0,75	$K_{rg}(s_{org})$	0,85
C_g	2	C_g	2
$C_{o/g}$	4,5	$C_{o/g}$	4,5

Table 3-10 Constant endpoint properties for relative permeability

Constant endpoint properties	
S_{wmin}	0
s_{wmax}	1
S_{wcr}	0.02
S_{gcr}	0
S_{gmin}	0
$K_{rg}(s_{wmin})$	1
$K_{ro}(s_{omax})$	1
$K_{rw}(s_{wmax})$	1

The critical water saturation (S_{wcr}) is reported as 2 %, also known as the irreducible water saturation, is apparently low. The reason for this value to be that low is unknown since it was not documented by Statoil. Based on Table 3-9 and Table 3-10 four different sets of relative permeability curves were created. That includes oil-water and gas-oil relative permeability curves for both SATNUM1 and SATNUM 2. For SATNUM 1 oil-water relative permeability curve are shown in

Figure 3-5 and the gas-oil relative permeability are shown in Figure 3-6. For SATNUM 2 oil-water relative permeability curve are shown in Figure 3-7 and the gas-oil relative permeability are shown in Figure 3-8.

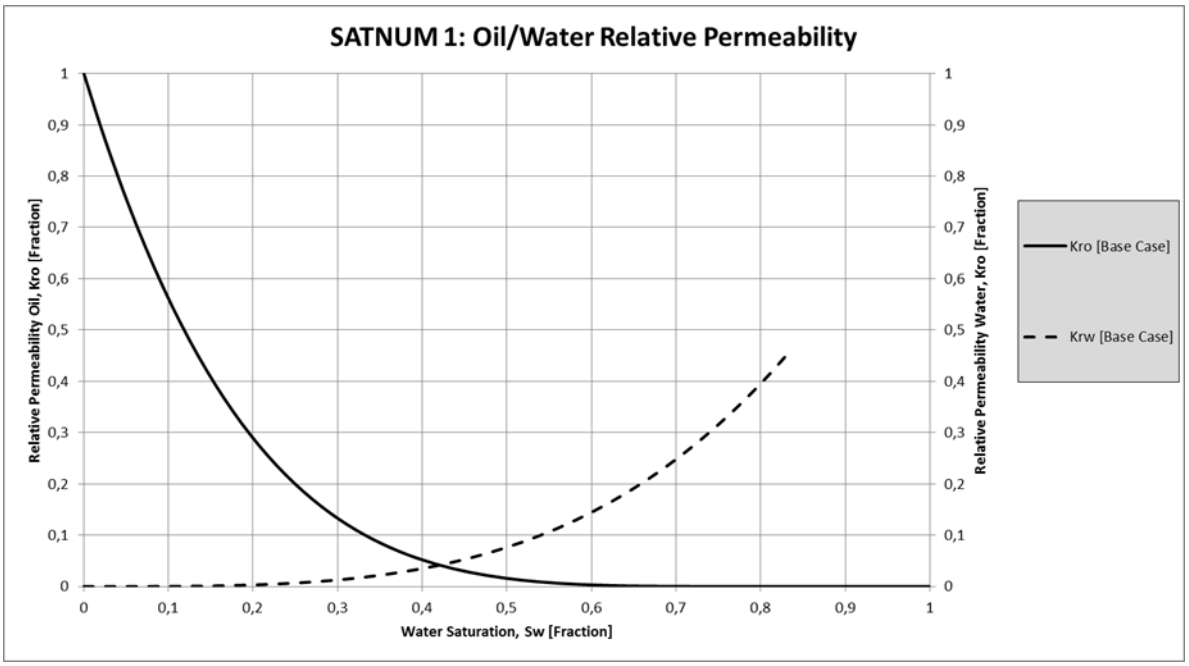

Figure 3-5: Oil-Water relative permeability for SATNUM 1

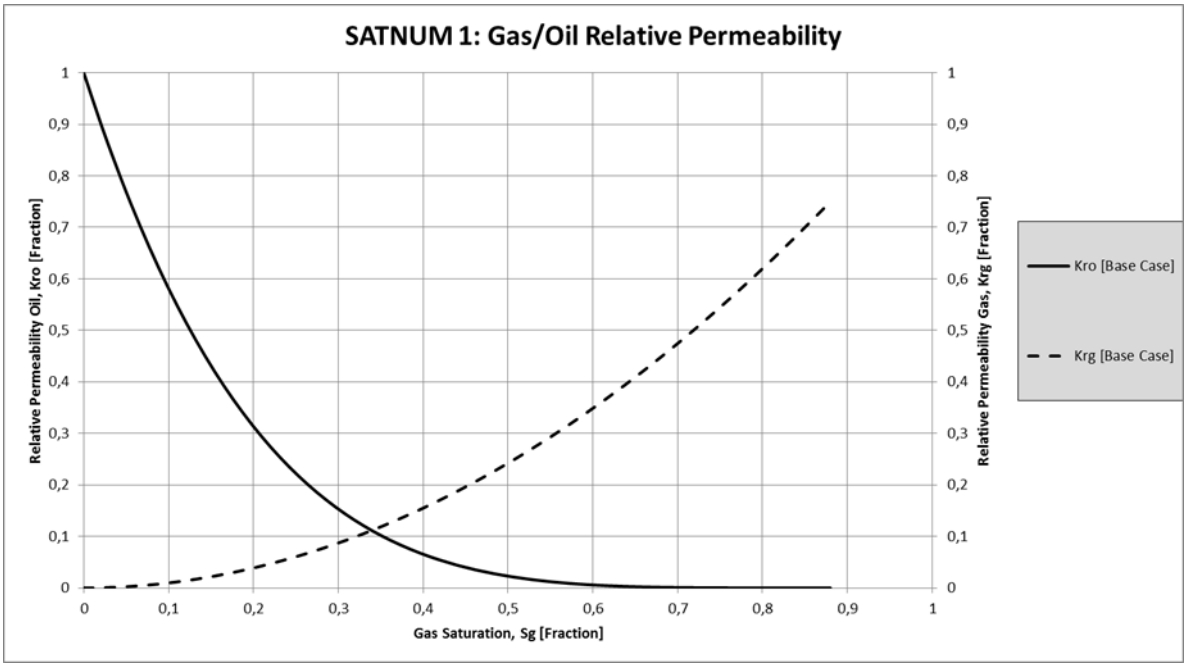

Figure 3-6: Gas-Oil relative permeability for SATNUM 1

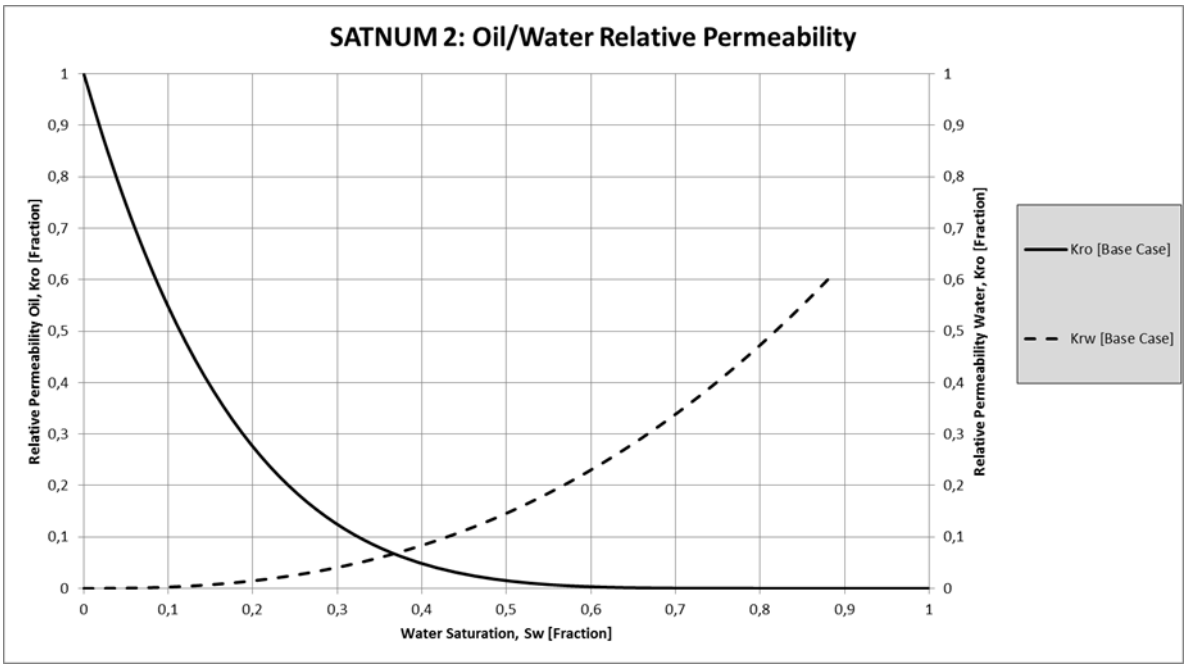

Figure 3-7: Oil-Water relative permeability for SATNUM 2.

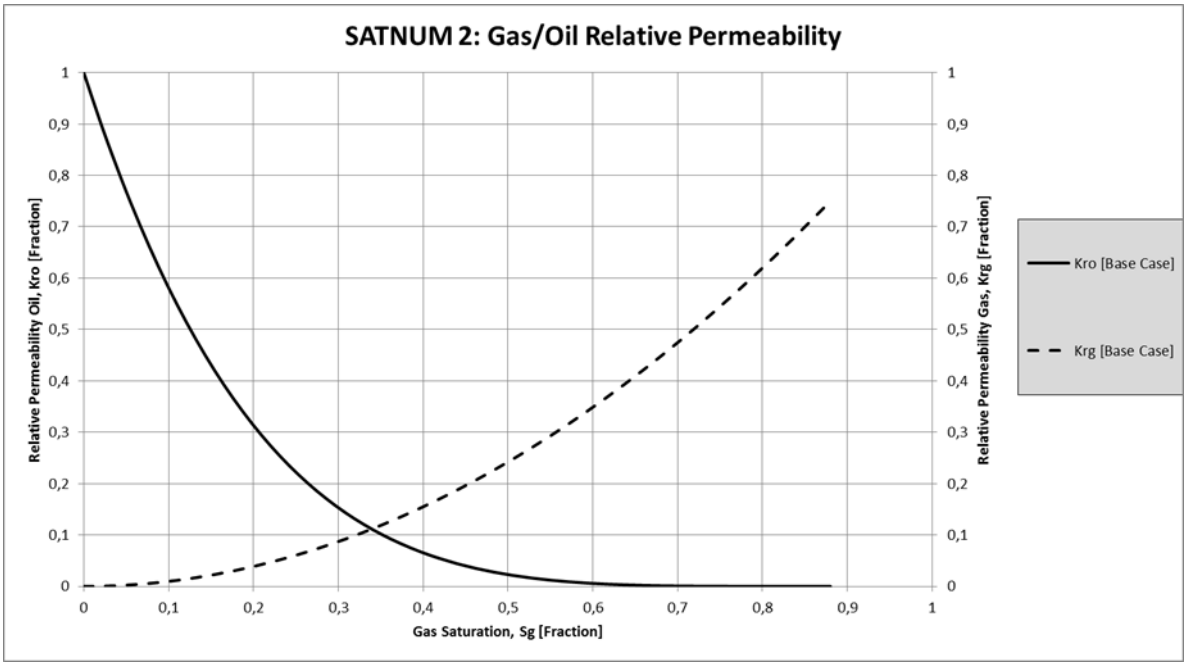

Figure 3-8: Gas-Oil relative permeability for SATNUM 2.

3.3.6 Capillary pressure

Capillary pressure are not a dynamic parameter, however it was placed in this section since it was measured in the same study as relative permeability. The water-oil capillary pressure curves are also based on analogue studies. Two curves were created, one for SATNUM1 and one for SATNUM2. Both of the curves are shown in Figure 3-9. Due to lack of information, the gas-oil capillary pressure was assumed to be zero.

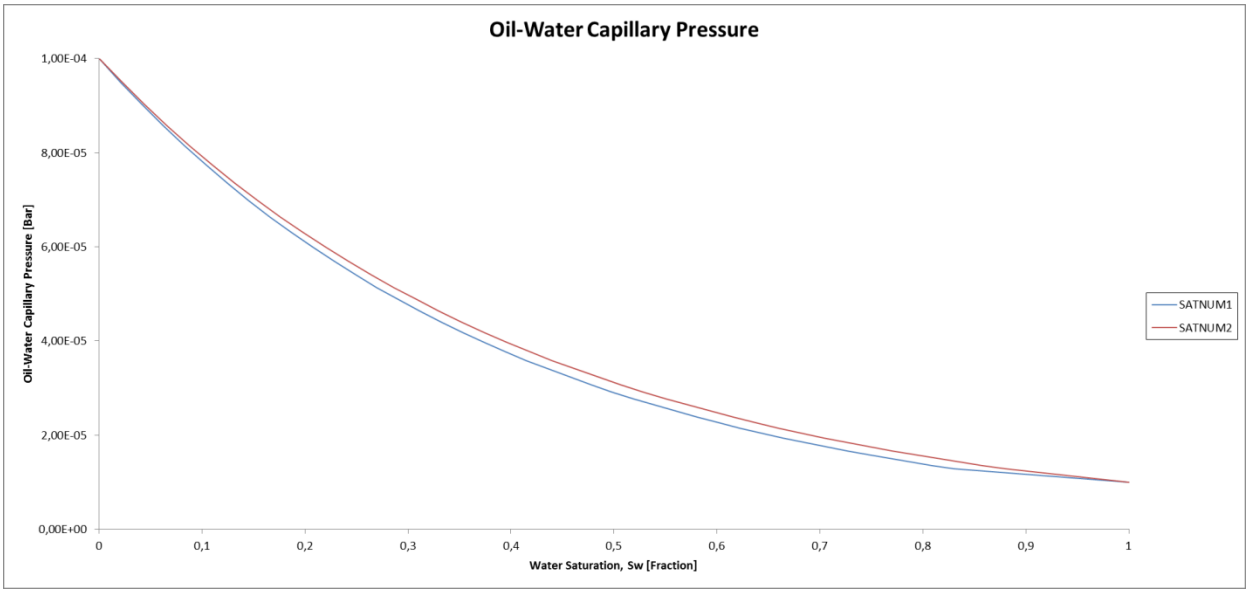

Figure 3-9: Oil-Water capillary pressure curve for both SATNUM 1 and SATNUM 2.

These capillary pressure curves (Figure 3-9) seem to have some unrealistic values. Capillary pressure for mixed-wet reservoirs should exhibit an asymptote at the residual saturation of water (S_{wcr}) and of oil where the capillary pressure goes to plus and minus infinity, respectively (Skjaeveland et al., 2000). This does not occur with these curves, because the minimum water saturation has a value of zero. Minimum water saturation is defined as the lowest value of water saturation that Petrel can handle (Schlumberger, 2012). The reason why these curves still are included in the simulation model is because the Petrel model requires oil-water capillary pressure curves in order to run. However, the capillary pressures are close to zero which suggests that they probably are not decisive for the results in this thesis.

3.4 Hyme simulation model

3.4.1 Simulation Grid

A simulation grid for Hyme was created during the geological evaluation, and the grid dimensions are given in Table 3-11.

Table 3-11: Grid dimensions for the Hyme reference case.

Direction	X	Y	Z	Total
Number of Gridblocks	77	114	156	1 369 368

Not all the gridblocks in Table 3-11 are active. An active gridblock can be defined as a gridblock that has volume and where fluid can flow. There are 167 787 active gridblocks in the model representing 12 % of the total gridblocks. To optimize the simulation run, a keyword MINPV was used to remove small grid blocks that cause problems during the simulation run. The keyword was set to remove gridblocks with a volume less than of 200 rm^3. This caused a reduction of 13 170 grid blocks, which resulted in a STOIIP reduction of 1.8%. For the purpose of this study, this change is considered appropriate. This change resulted in a total number of active gridblocks equal to 154 617.

3.4.2 In-Place volumes

To quantify the in-place volumes of Tilje, a static uncertainty study was performed by Statoil. Structural, petrophysical, and PVT uncertainties were included. The study resulted in determination of pore volume (PV), stock tank oil initially in place (STOIIP) and associated gas. Due to the major fault (Figure 3-10), that divides the reservoirs into two segments, results are divided into western and eastern segment (Table 3-12). Changes made by the MINPV keyword are also included.

Table 3-12: In-place volumes for Hyme reference case

Segment	Pore volume [10^6 Rm^3]	STOIIP [10^6 Sm^3]	Associated Gas [10^9 Sm^3]
Western	39.96	8.13	1.52
Eastern	44.34	2.62	0.49
Total	84.30	10.75	2.01

3.4.3 Wells

The Hyme field is developed with one multilateral producer and one deviated injector (Figure 3-10). Performance of the multilateral producer and the injector was modeled by using constraints and assumptions described in the development strategy section. The mainbore of the producer is located in the western segment while the lateral is located in the eastern segment. The water injector is located in the north of the eastern segment intended for pressure support of both segments.

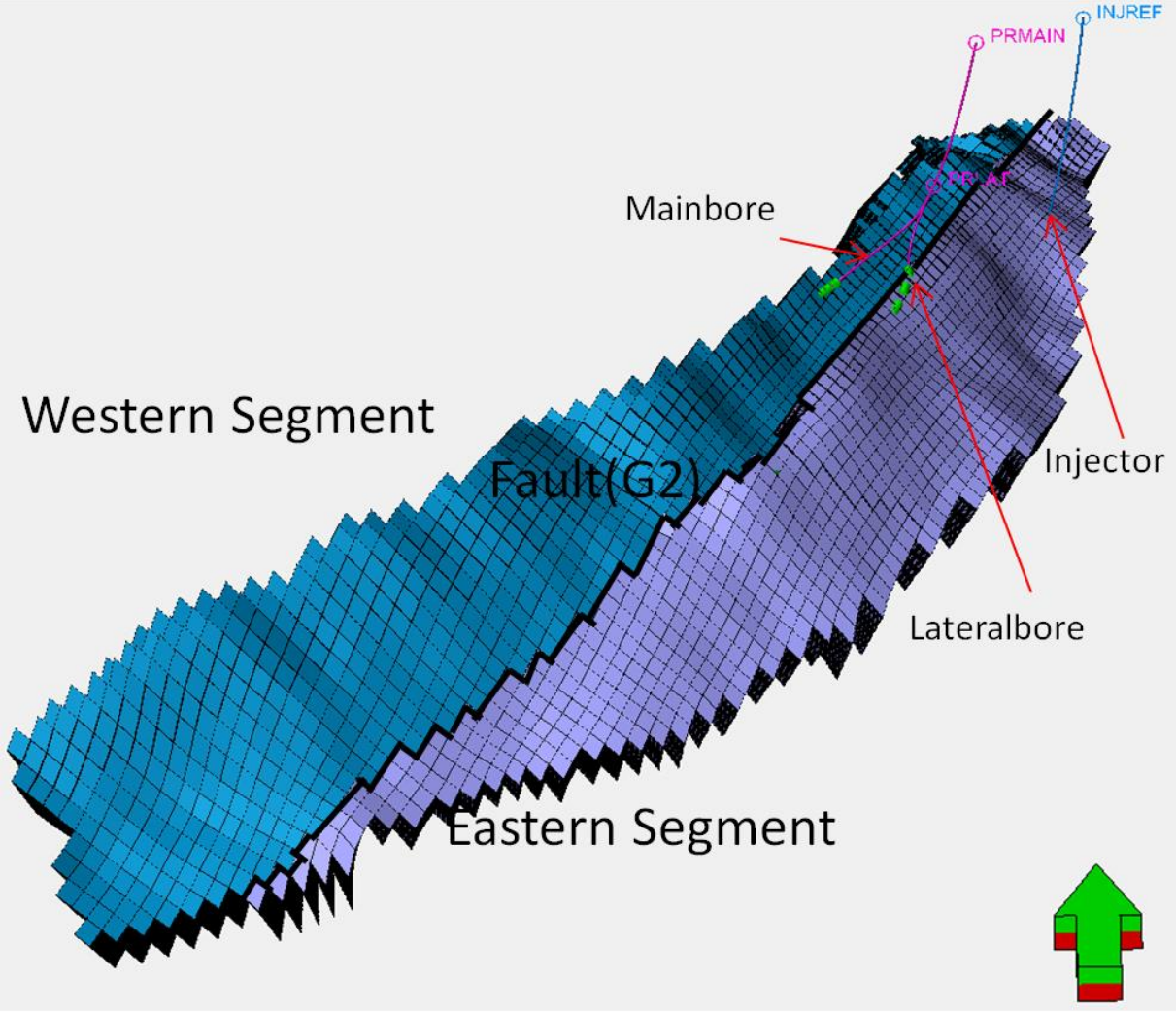

Figure 3-10: 3D grid of western and eastern segments with well locations and the internal fault (G2) dividing the reservoir into the two parts.

3.5 Development Strategy

Production start for Hyme was March 2nd 2013, with the multilateral producer as the only active well. The water injector was at the time this study was performed, estimated to start up 1st of June 2013. The simulation run will last until January 1st 2030. Both of the wells where set up with rules based on constraints and assumptions provided by Statoil (Table 3-13).

Table 3-13: Well and production constraints

Constraint	Unit	Value
Platform back pressure production	Bar	70
Platform water injection pressure	Bar	290
Maximum oil production rate	Sm^3/d	2500
Maximum injection rate	Sm^3/d	5000
Maximum liquid production	Sm^3/d	4000
Maximum water production	Sm^3/d	3500
Maximum water cut lateral bore	Sm^3/sm^3	0.70

A normal approach would be to generate lift curves for the different wells for controlling the bottom hole pressures. For this study, the approach will be to use the constraints provided by Statoil (Table 3-13). This includes the platform back pressure the producer needs to have and the platform water injection pressure that constraints maximum injection rate. These rules were implemented as well constraints.

The multilateral producer was assigned production rate constraints, which includes maximum oil production rate, maximum water production rate and maximum total liquid rate. On the lateral bore, a maximum water cut of 70 % was added for economic reasons. Additionally, it was created a similar rule for the main bore. Here it was specified that perforations with water cut greater than 95 % will shut in. For the water injector, a maximum rate for injection was specified.

Additionally a group control was added to keep a stable reservoir pressure of 215 bar. This rule will maintain the reservoir pressure on a field basis, and control the production and injection to maintain this pressure. The aim of this rule is to avoid production below the bubble point pressure, and still inject and produce at realistic rates.

3.6 Hyme Reference case Results

This section describes the results for Hyme reference case. The results are based on the dynamic reservoir simulation model. Table 3-14 shows the cumulative annual production of oil, gas, and water as well as the recovery factor for oil. Figure 3-11 to Figure 3-13 shows predicted production profiles respectively oil, gas, and water. These production profiles show both rates and cumulative production. Water injection is shown in Figure 3-14, and reservoir pressure, gas oil ratio, and water cut are shown in Figure 3-15.

Table 3-14: Cumulative production results for Hyme reference case.

Cumulative Production				
Date	**Cum. Oil [10^6 Sm^3]**	**RF Oil [%]**	**Cum. Gas [10^9 Sm^3]**	**Cum. Water [10^6 Sm^3]**
01.01.2014	0.72	6.7	0.13	0.02
01.01.2015	1.59	14.8	0.30	0.23
01.01.2016	2.44	22.7	0.46	0.67
01.01.2017	3.02	28.1	0.57	1.48
01.01.2018	3.34	31.0	0.62	2.55
01.01.2019	3.54	33.0	0.66	3.73
01.01.2020	3.70	34.5	0.69	4.95
01.01.2021	3.84	35.7	0.72	6.16
01.01.2022	3.95	36.8	0.74	7.38
01.01.2023	4.05	37.7	0.76	8.59
01.01.2024	4.14	38.5	0.77	9.81
01.01.2025	4.22	39.2	0.79	11.02
01.01.2026	4.29	39.9	0.80	12.24
01.01.2027	4.35	40.5	0.82	13.45
01.01.2028	4.41	41.1	0.83	14.66
01.01.2029	4.47	41.6	0.84	15.88
01.01.2030	4.53	42.2	0.85	17.09

Table 3-14 shows that the recovery factor is up to 42.2% the 1st of January 2030. The cumulative oil production is at 4.53 million sm^3 while the cumulative water production is 17.09 million sm^3. This may be an indication that it is not economically appropriate to produce until 2030. The cumulative oil production is greater than water production until

2019, where water production is rising dramatically. Given that Hyme is classified as a fast track development, it is not believed that the depletion will last as far as 2030, which these results support.

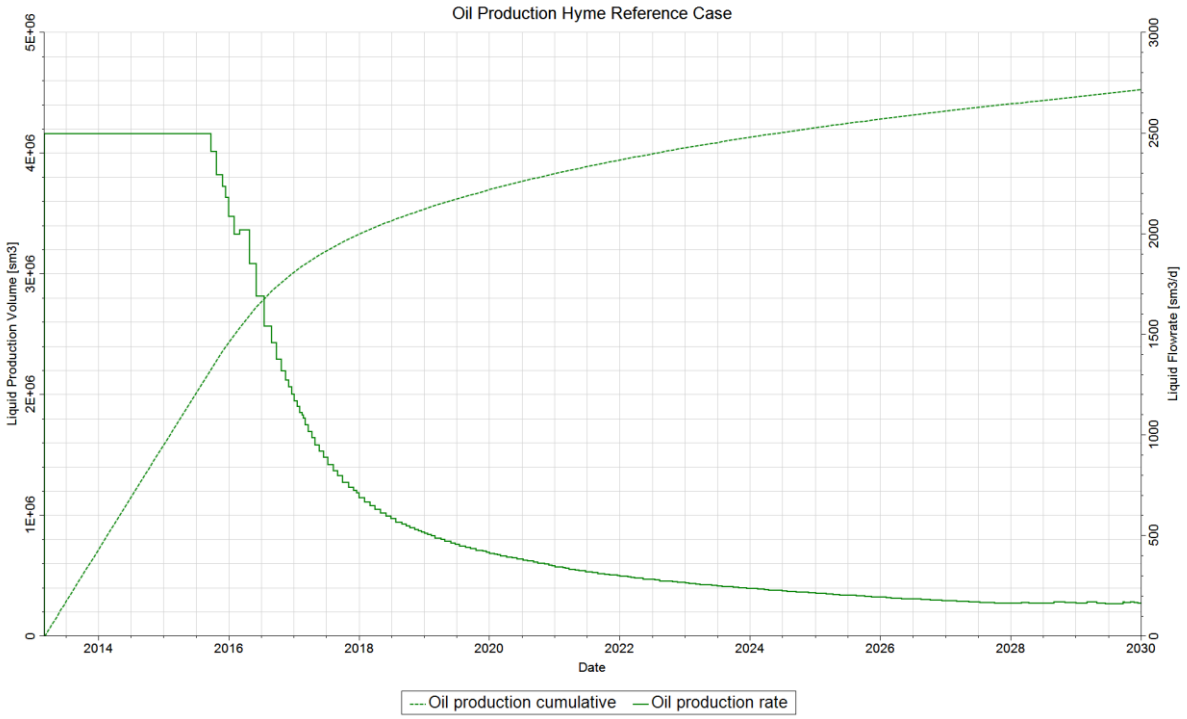

Figure 3-11: Predicted oil rate and cumulative oil production for Hyme reference case.

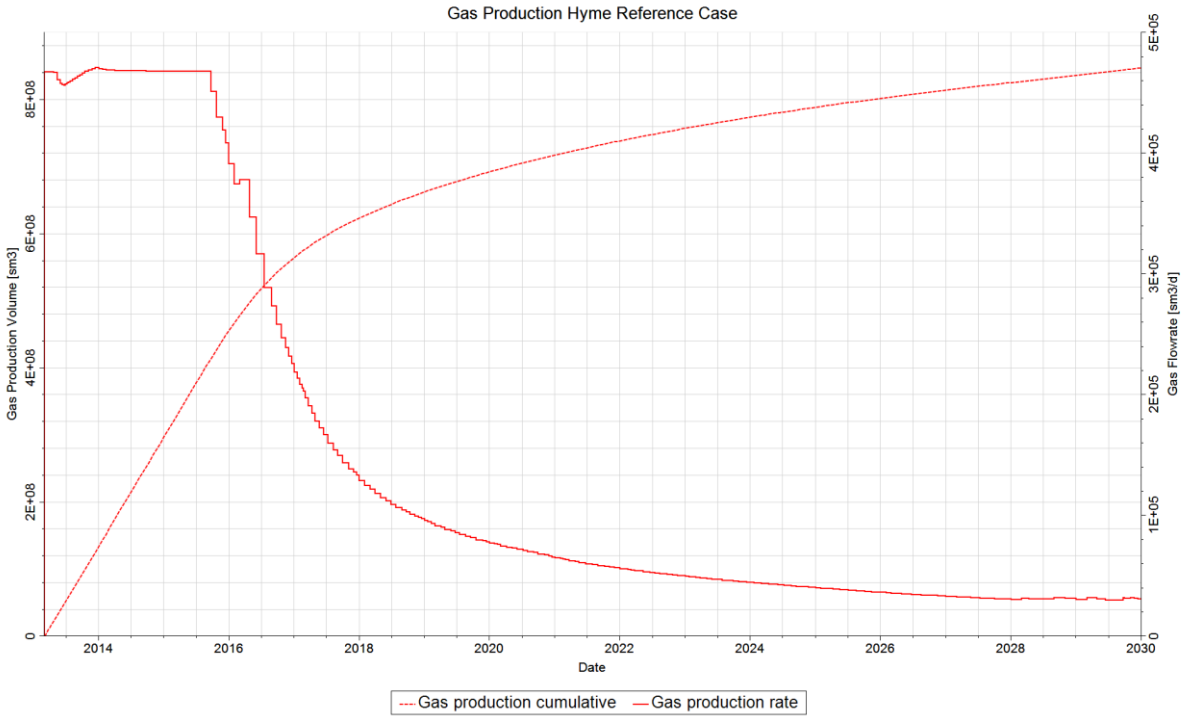

Figure 3-12: Predicted gas rate and cumulative gas production for Hyme reference case.

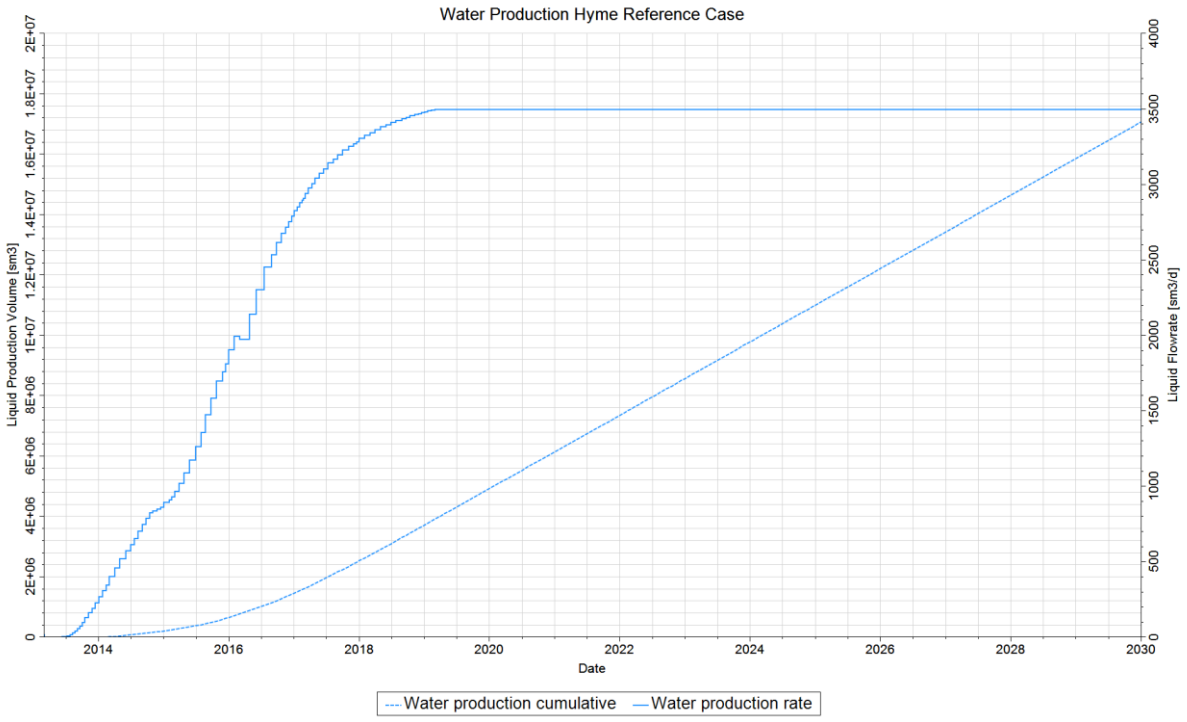

Figure 3-13: Predicted water rate and cumulative water production for Hyme reference case.

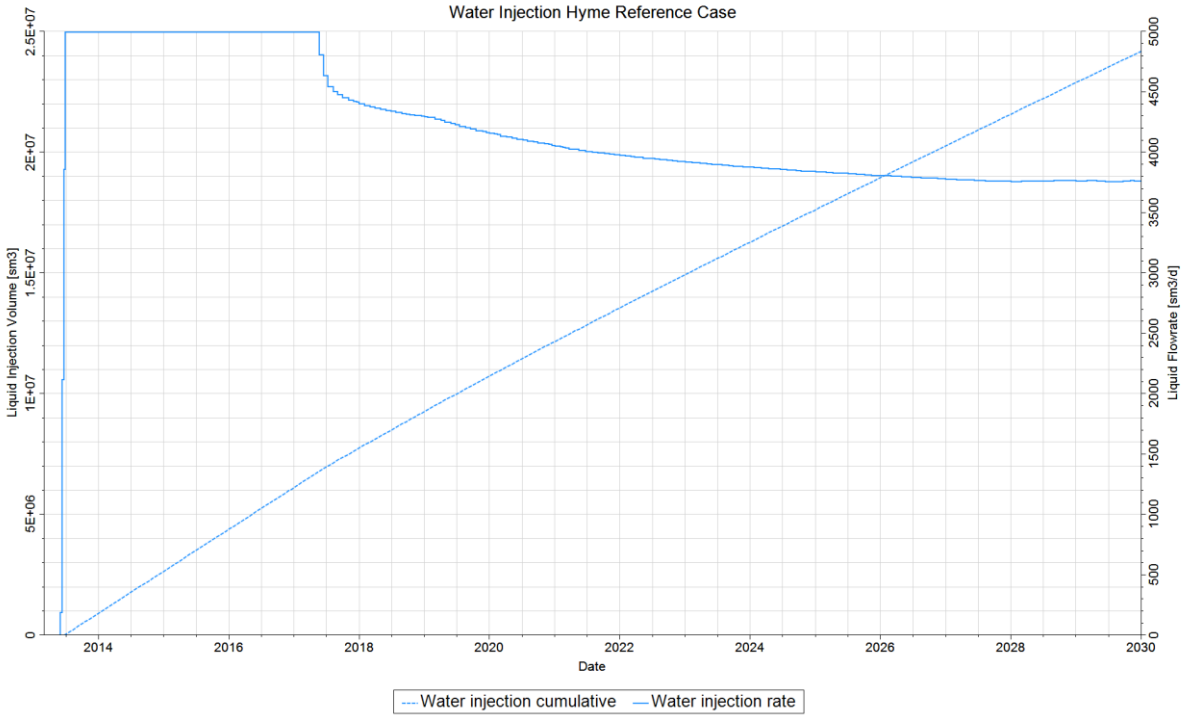

Figure 3-14: Predicted water injection rate and cumulative water injection for Hyme reference case.

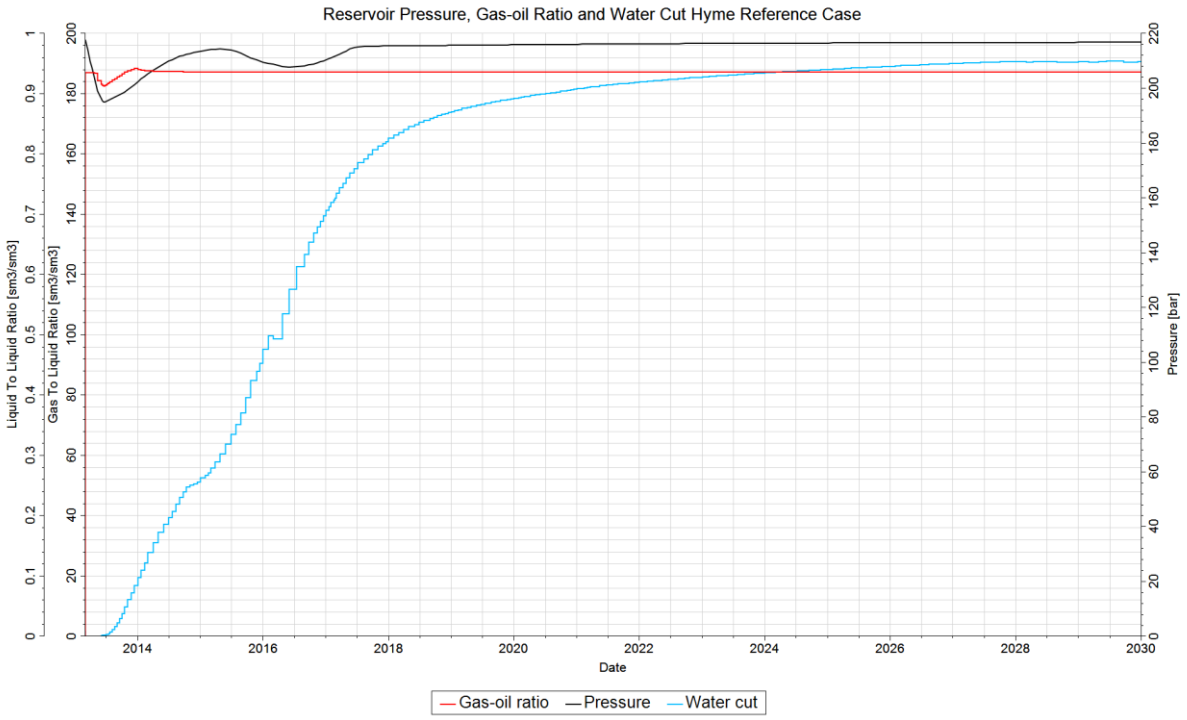

Figure 3-15: Predicted reservoir pressure, gas-oil ratio and water cut for Hyme reference case.

The model results show that the oil rate (Figure 3-11) is producing at plateau until late 2015, where it starts to decline due to increasing water production (Figure 3-13). Figure 3-13 also shows that water breakthrough is expected in early 2013 with a steep increase. This increase compared to the volume of liquid produced is also shown through the water cut (Figure 3-15). In 2020 the water cut reaches a value of 0.9, which suggest that 90% of all produced volumes are water.

Gas rate (Figure 3-12) follows the oil rate as the reservoir consists of undersaturated oil, with one exception in the very beginning of production. This exception is due to reservoir pressure (Figure 3-15) dropping below the bubble point pressure, which also can be observed from the gas-oil ratio. The cause of the pressure drop is that water injection (Figure 3-14) does not start until June 1st 2013, two months after the start of production. When water injection starts, the reservoir pressure is increased and stabilized after a while at a constant value of 215 bar.

Based on these results, water injection seems to be crucial for production maintenance at Hyme. Another important aspect is to determine the economic cut off for production, which seems to be after. However, this will not be considered further in this thesis.

4. Pre-production Uncertainty Study

A pre-production uncertainty study is performed based on the Hyme reference case. The first objective was to determine the uncertainty parameters of interest. The parameters chosen are parameters that are interpreted as uncertain, and with possibility to make a significant difference in terms of oil recovery and oil volume in-place. These parameters were provided by Statoil including the ranges for the uncertainty.

The next objective was to create an uncertainty workflow (Figure 4-1) in the Petrel software where the interpreted uncertainty ranges are integrated. From this workflow, sensitivities were generated based on the low and high cases for the interpreted uncertainty ranges. This generated 20 simulation cases that provided an overview of which parameters that are affecting the oil volumes in-place and the cumulative oil production and how much the impact is.

When the 20 sensitivity simulations were performed, a stochastic Monte Carlo based uncertainty study was made, where random selections of the parameters were combined in several simulation runs. In this study, 200 simulation cases were generated. The results from this study will aid in the understanding of the future performance and potential of Hyme.

4.0.1 Stochastic modeling

Almost all data used in reservoir simulation are uncertain. These uncertainties tend to be large, specifically away from the wells to spatially distribution parameters such as porosity and permeability. A consequence of this is that a production profile associated with any development scheme cannot be predicted exactly. In order to capture the behavior of the reservoir, the best thing to do is calculate a range of possible profiles (O.J Lèpine et al., 1999). For the Hyme reference case, only one production profile is obtained. In order to capture what impact different uncertainties will have on oil production and oil volume in place, a stochastic uncertainty study was performed.

Initially, a reservoir can be considered as deterministic. This means that the reservoir exists, and it has input parameters that can be observed and measured. Haldorsen and Damsleth presented a definition of stochastic phenomenon or variable in the JPT paper “Stochastic Modeling” April 1990: “A stochastic phenomenon or variable is characterized by the

property that a given set of circumstances does not always lead to the same outcome (so that there is no deterministic regularity) but to different outcomes in such a way that there is statistical regularity." An example would be; if we had used deterministic values for the input parameters in a reservoir description, we would obtain one answer. In this case, this would be Hyme reference case. Applying stochastic techniques enables the user to achieve uncertainty ranges. This can be considered as crucial to understand the subsurface with limited amount of data, which is the case for Hyme (Haldorsen and Damsleth, 1990).

The main reason for applying stochastic techniques is that we know that there are a lot of unknowns in the subsurface. Incomplete information about dimensions and geologic structures are a major reason. Another reason is spatial variations and distributions in the reservoir, which is really hard to predict. The parameters of interest can be divided into static and dynamic parameters. Static parameters can be considered as point values along the well, combined with seismic data, while dynamic parameters are time-dependent parameters such as pressure and rates. There could also be unknown relationships between the different petro physical input parameters and the volume of rock used for averaging (Haldorsen and Damsleth, 1990). Summarized, the main problem is that it exist a gap between observed and unsampled locations. In order to perform this stochastic uncertainty study, a Monte Carlo sampling approach will be used.

4.0.2 Monte Carlo sampling

Monte Carlo method can be defined as a study of a stochastic model which simulates, in all essential aspect, a physical or mathematical process. The method is a combination of sampling theory and numerical analysis, which gives the method a special contribution to the science of computing. This implies that Monte Carlo is a practical method that can solve problems by numerical operations on random numbers (Stoian, 1965). As mentioned, Statoil provided interpreted uncertainty ranges for some of the input parameters in Hyme reference model. These parameters will be further discussed in the uncertainty parameter section 4.1. By using Monte Carlo simulation, random values within these ranges will be sampled. This means that several simulation cases will be generated and run based on random sampling within each of the uncertainty ranges.

4.0.2 Workflow for Pre-production uncertainty study

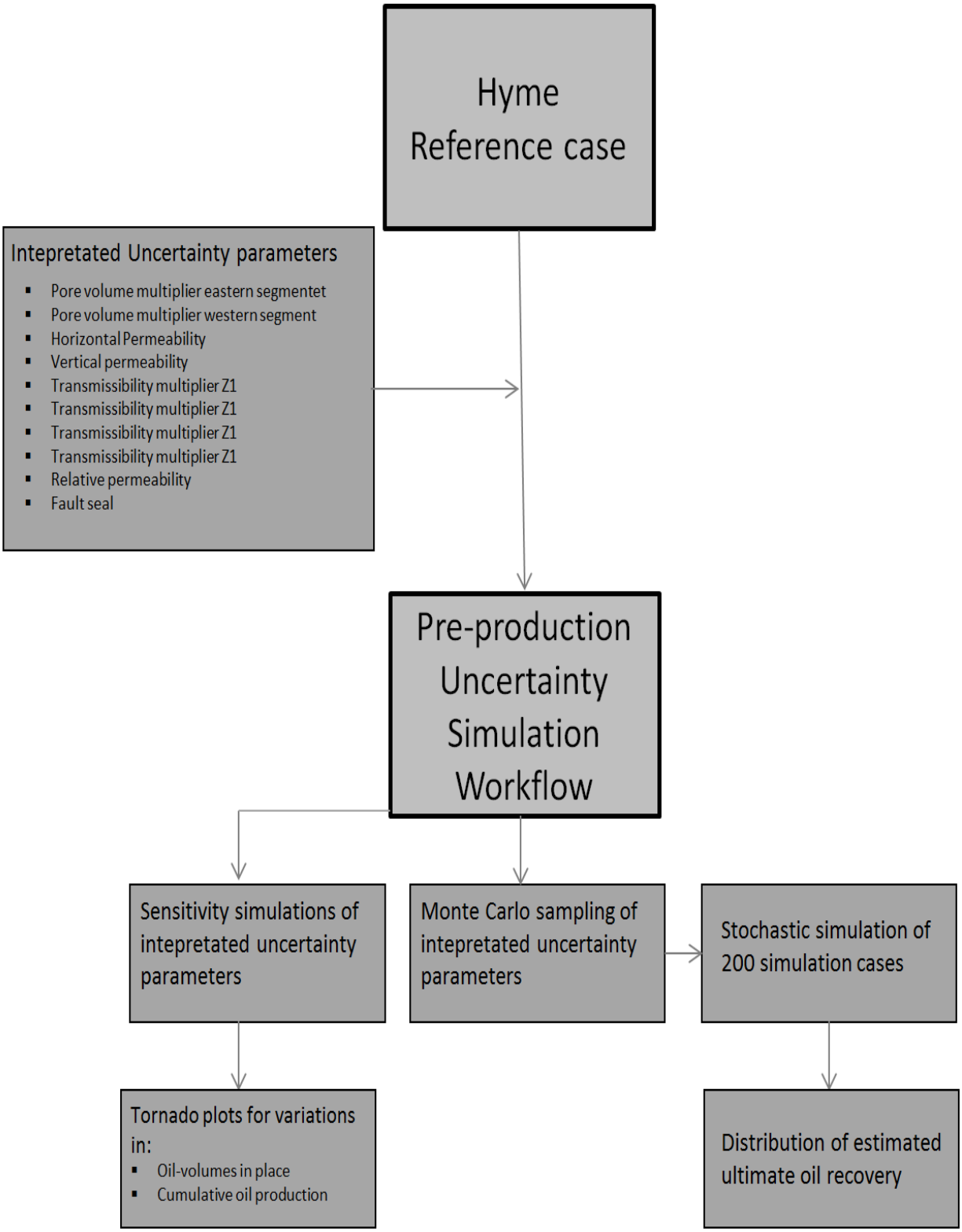

Figure 4-1: Schematic overview of pre-production uncertainty study.

4.1 Uncertainty Parameters

4.1.1 In-Place volumes

As input to the uncertainty study being performed, a pore volume uncertainty range will be used. The reason for this is to keep the volume calculation simple, without dependency of water saturation and formation volume factor. Pore volume is a function of gross rock volume (GRV), porosity and net to gross (NTG);

$$PV = GRV \times Porosity \times NTG.$$

Based on the uncertainty study performed by Statoil described in section 3.4.2, uncertainty ranges for this parameter were generated with respect to both eastern and western segment (Table 4-1).

Table 4-1: Uncertainty ranges for pore volume multipliers for eastern and western segment.

Pore volume multiplier	Low	Reference	High	Description
Eastern segment	0.5	1	1.62	Multiplier value
Western segment	0.2	1	1.4	Multiplier value

Notice that the uncertainties are multipliers, not actual volumes. The reason for using multipliers instead of actual volumes is for simplicity for input into the simulation model. In terms of volumes, the ranges will be as shown in Table 4-2.

Table 4-2: Uncertainty ranges for pore volume in eastern and western segment.

Pore volume	Low	Reference	High	Unit
Eastern segment	22.17	44.34	71.83	PV [10^6 Rm^3]
Western segment	7.99	39.96	55.94	PV [10^6 Rm^3]

The pore volume multipliers Table 4-1 will affect the stock tank oil initially in-place. However, as described in section 3.4.2, the oil in-place is much larger in the western segment compared to the eastern segment, even though the pore volume is significantly larger in eastern segment. This can be explained by that the initial oil saturation is larger in western segment (Figure 3-3).

4.1.2 Permeability

Based on the petrophysical evaluation of vertical and horizontal permeability, uncertainty ranges for the entire Tilje formation was interpreted (Table 4-3).

Table 4-3: Uncertainty ranges for horizontal and vertical permeability in the Tilje formation.

Parameter	Low	Reference	High Case	Unit
Horizontal Permeability	159.1	795.7	3978.5	[mD]
Vertical Permeability	15.9	79.6	397.9	[mD]

Table 4-3 shows that the uncertainty range for permeability in Tilje is large, and hence important for this study. To apply these ranges to the uncertainty simulation study, multipliers were created based on low, reference and high cases (Table 4-4).

Table 4-4: Uncertainty ranges for horizontal and vertical permeability multipliers in the Tilje formation.

Parameter	Low	Reference	High	Descriptiom
Horizontal Permeability	0.2	1	5	Multiplier value
Vertical permeability	0.01	0.1	0.6	Multiplier value

4.1.3 Relative permeability

As mentioned in section 3.3.5, Statoil performed an analogue study to determine the relative permeability. The study provided a base, high, and low case. Base case is based on mixed wettability and the optimistic case based on water-wet sand, with the pessimistic case based on oil-wet sand. The properties are given in Table 4-5.

Table 4-5: Uncertainty input data for relative permeability.

SATNUM 1				SATNUM 2			
K<500mD	**Base**	**Low**	**High**	**K>500mD**	**Base**	**Low**	**High**
Oil-Water				**Oil-Water**			
Sorw	0,17	0,1	0,25	Sorw	0,12	0,05	0,2
Krw(sorw)	0,45	0,7	0,25	Krw(sorw)	0,6	0,8	0,4
Corey krw	3,5	2,5	5	Corey krw	2,5	1,5	3
Corey krow	4,5	6	3,5	Corey krow	5	6,5	3,5
Gas-Oil				**Gas-Oil**			
Sorg	0,12	0,05	0,2	Sorg	0,08	0,04	0,15
Krg(sorg)	0,75	1	0,5	Krg(sorg)	0,85	1	0,6
Corey krg	2	1,3	2,6	Corey krg	2	1,3	2,6
Corey krog	4,5	5	3,5	Corey krog	4,5	5	3,5

Based on Table 4-5, Table 3-10 and the Corey type equations described in section 3.3.5, four sets of relative permeability curves were created (Figure 4-2 to Figure 4-5). This includes oil-water and gas-oil relative permeability curves for base, low, and high case within each SATNUM.

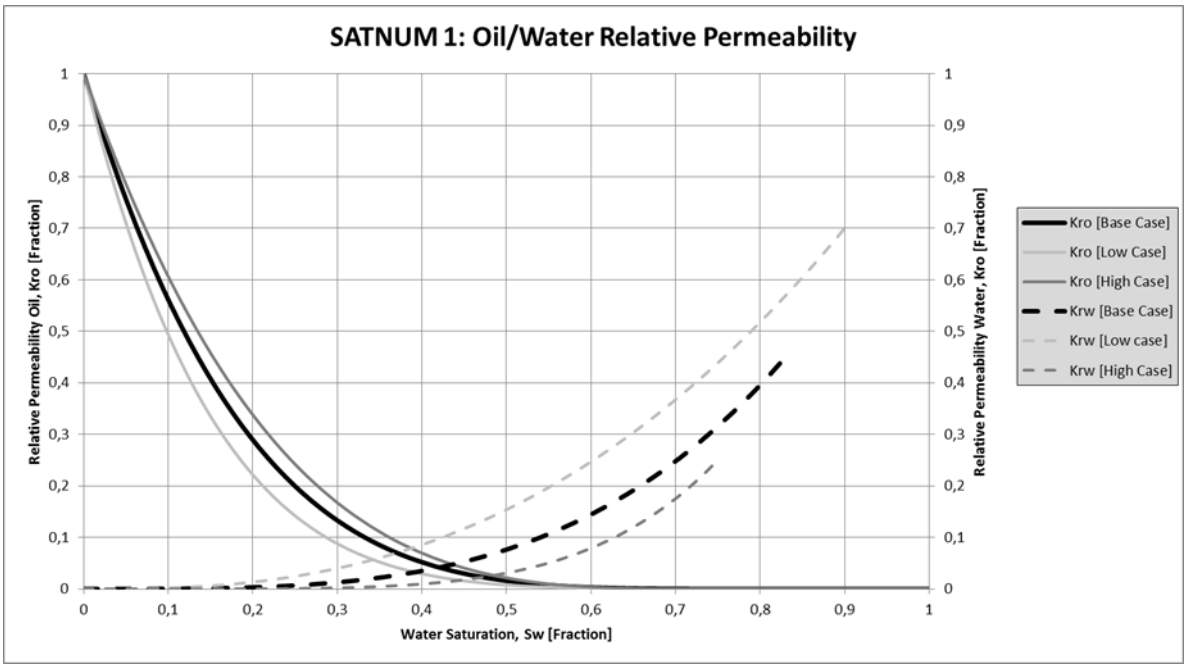

Figure 4-2: Oil-Water relative permeability for SATNUM 1 displaying base, low and high cases.

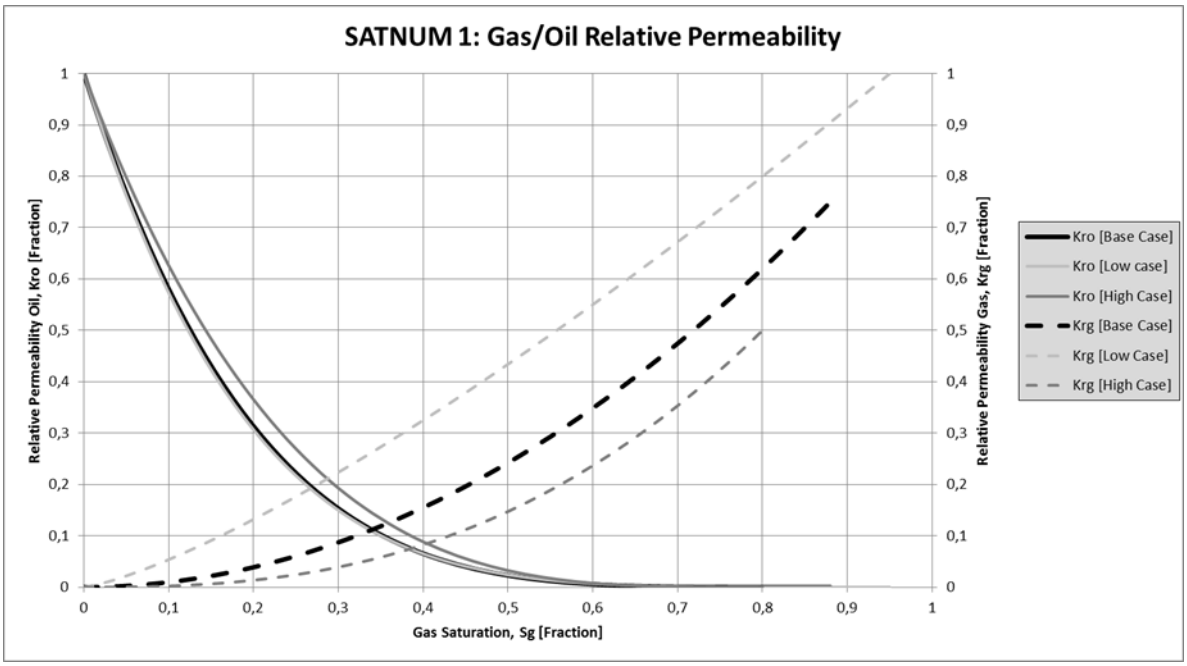

Figure 4-3: Gas-Oil relative permeability for SATNUM 1 displaying base, low and high cases.

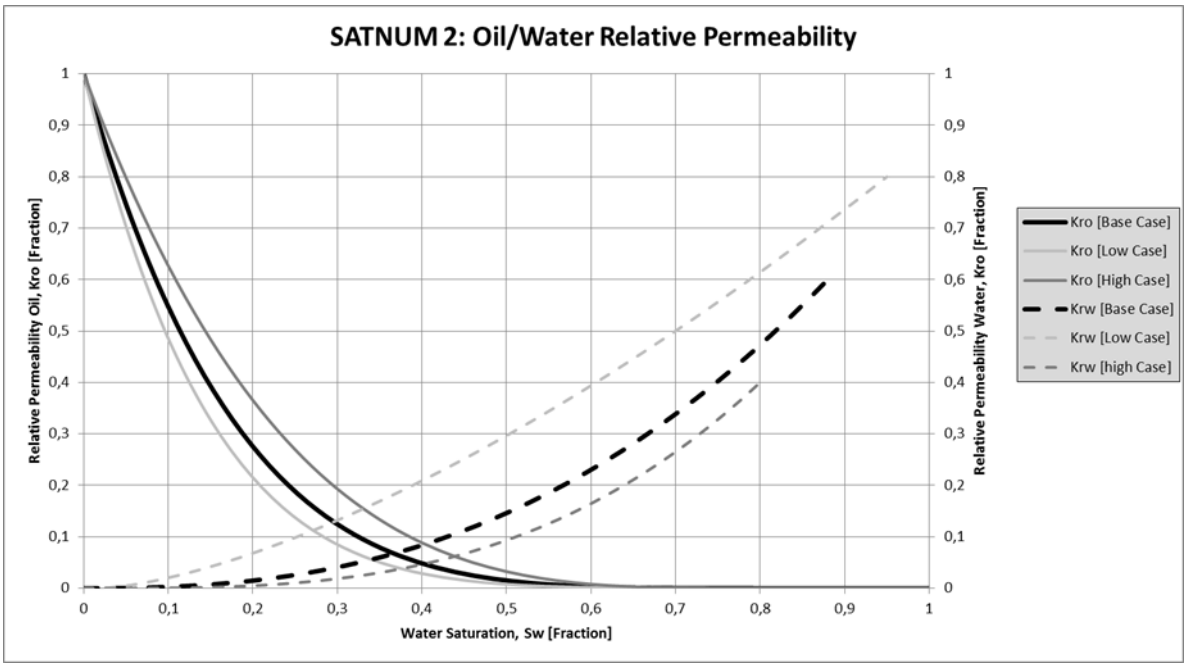

Figure 4-4: Oil-Water relative permeability for SATNUM 2 displaying base, low and high cases

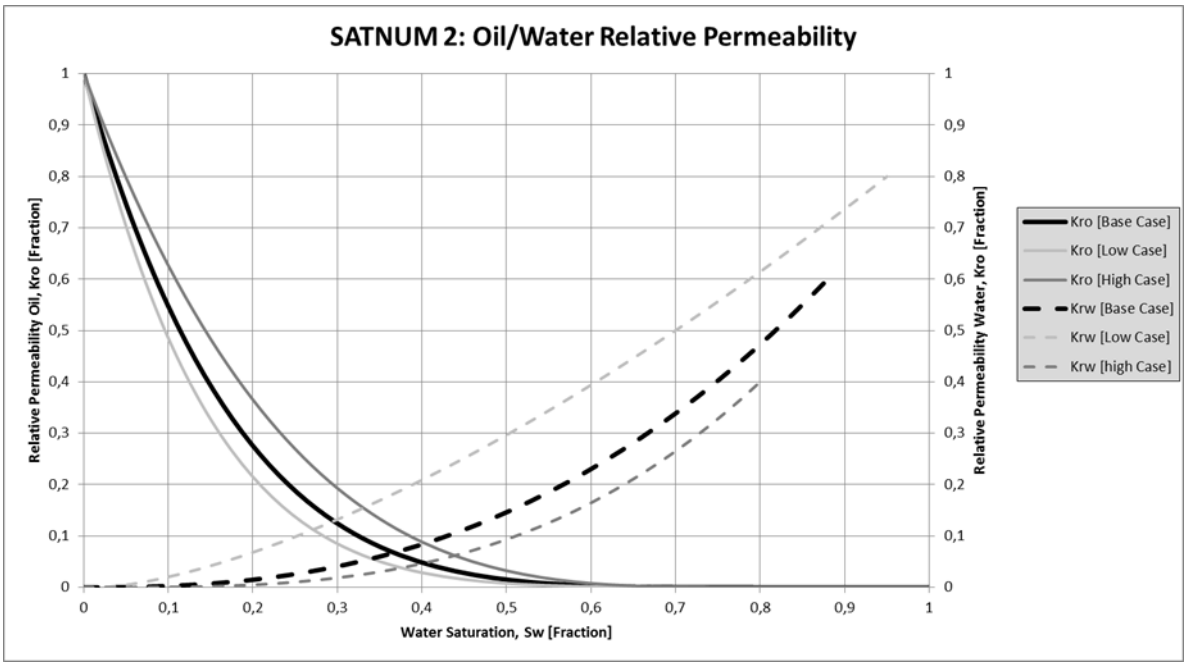

Figure 4-5: Gas-Oil relative permeability for SATNUM 2 displaying base, low and high cases.

The recommended relative permeability curves are being used as a discrete input to the uncertainty study (Table 4-6). The reason for keeping the curves as discrete inputs is to easily differentiate the cases that are used for base, low, and high case.

Table 4-6: Relative permeability discrete input parameters for uncertainty study.

Uncertainty	Low (oil-wet)	Base (mixed wet)	High (water-wet)
Relative Permeability	30%	40 %	30 %

Based on Table 4-6**,** 30% of all simulation cases will be generated with oil-wet curves, 40 % will be generated with mixed wettability curves and 30 % of the cases will be generated with water wet curves.

4.1.4 Fault Seal

The major fault is the internal fault G2, which divides the reservoir into two segments (Figure 2-2, Figure 3-4, and Figure 3-10). This fault was modeled as open in the reference case. For the uncertainty study both the reference case and high case suggest communication across the fault (Table 4-7). The low case is assumed to be sealed fault. This uncertainty will be used as a discrete input to the uncertainty study.

Table 4-7: Fault seal discrete input parameters for uncertainty study.

Uncertainty	Low (sealed)	Reference(open)	High (open)
Fault Seal	30%	40%	30%

Since both the reference case and high case suggest communication across the fault, 70% of all simulation cases will be generated with communication and 30 % will be generated without communication. The reason for listing both reference and high case in Table 4-7 is that the Petrel model requires low, base, and high variable values for uncertainty study.

4.1.5 Vertical communication

In the Hyme reference case, vertical communication between the zones in Tilje (Figure 3-4) was modeled with transmissibility multipliers (Table 4-8). This was based on analogue studies, which also provided uncertainty ranges for these transmissibility multipliers. The uncertainty ranges are shown in Table 4-8. It can be observed that all the low cases suggest there should be no communication between the layers, while the high case suggests. For the reference case, it is expected to be slightly communication between Tilje 3 and Tilje 2.2. For the intersection between Tilje 2.1 and Tilje 1.2 all cases suggest communication, hence they are not a part of the uncertainty study.

Table 4-8: Uncertainty ranges for transmissibility multipliers between the different reservoir zones.

Uncertainty	Reservoir zones [From-To]	Low	Reference	High
Transmissibility multiplier Z1	Tilje 4.2- Tilje 4.1	0	0	0.1
Transmissibility multiplier Z2	Tilje 4.1- Tilje 3	0	0	0.1
Transmissibility multiplier Z3	Tilje 3 - Tilje 2.2	0	0.0001	0.1
Transmissibility multiplier Z4	Tilje 2.2- Tilje 2.1	0	0	0.1

4.1.6 Summary of input parameters to uncertainty study

A summary of all parameters used in this uncertainty study are listed in Table 4-9. Based on the table, the majority of the input parameters are continuous multipliers. The reason multipliers are input for uncertainty study, is because it makes it easier to implement the uncertainty into the simulation model. The other parameters are modeled as discrete variables; this is mainly to explore the various scenarios in the various parameters. Monte

Carlo sampling of continuous parameters will result in random sampling within the perceived ranges. For the discrete variables, it will select either low, high or reference case.

Table 4-9: Summary of input parameters to uncertainty study.

Uncertainty	Low	Reference	High	Description
Pore volume eastern segment	0.50	1	1.62	Multiplier
Pore volume western segment	0.20	1	1.40	Multiplier
Horizontal Permeability	0.20	1	5.0	Multiplier
Vertical Permeability	0.01	0.1	0.6	Multiplier
Transmissibility multiplier Z1	0	0	0.1	Multiplier
Transmissibility multiplier Z2	0	0	0.1	Multiplier
Transmissibility multiplier Z3	0	0.0001	0.1	Multiplier
Transmissibility multiplier Z4	0	0	0.1	Multiplier
Relative permeability	30 % (oil-wet)	40 % (mixed wet)	30 % (water-wet)	Discrete
Fault seal	30 % (tight)	40 % (reference)	30 % (open)	Discrete

4.2 Pre-production uncertainty study results

Results for the pre-production uncertainty study are divided into three parts. The first part (section 4.3) deals with a sensitivity analysis of the various parameters that were input to this study. The second part (section 4.4) consist plots of the stochastic simulation results and the third part (section 4.5) shows the statistical treatment of the results for cumulative oil production.

4.3 Sensitivities

Sensitivities were created based on the interpreted uncertainty ranges. This will provide a low case and a high case for the 10 different input parameters respectively. The aim of the sensitivity was to investigate which parameters that affect the oil volume in-place, and cumulative oil production.

4.3.1 Sensitivities for oil volumes in-place

The results from the oil volumes in-place sensitivities are listed in Table 4-10.

Table 4-10: Oil volumes in-place by sensitivities.

Oil Volume in-Place			
Uncertainty	**Low Case**	**High Case**	**Unit**
Pore volume eastern segment	9.26	12.44	[10^6 Sm^3]
Pore volume western segment	2.63	14.09	[10^6 Sm^3]
Horizontal Permeability	10.75	10.75	[10^6 Sm^3]
Vertical Permeability	10.75	10.75	[10^6 Sm^3]
Transmissibility multiplier Z1	10.75	10.75	[10^6 Sm^3]
Transmissibility multiplier Z2	10.75	10.75	[10^6 Sm^3]
Transmissibility multiplier Z3	10.75	10.75	[10^6 Sm^3]
Transmissibility multiplier Z4	10.75	10.75	[10^6 Sm^3]
Relative permeability	10.75	10.75	[10^6 Sm^3]
Fault seal	10.75	10.75	[10^6 Sm^3]

As described in section 3.4.2, the total oil volume in-place for Hyme reference case was determined to be 10.75 million Sm^3. From Table 4-10 one can observe that the majority of the sensitivities are having the same oil volume in-place, with exception of the pore volume multipliers. The reason why, is that the pore volume multipliers are the only parameters that affect the pore volume, hence the in-place volume. To illustrate the difference between the sensitivities and the Hyme reference case, a tornado plot was created (Figure 4-6). A Tornado

Plot is a plot with vertical bars, with the largest bar on top with decreasing values downwards. The bars are attached to a given uncertainty range with a high and low value. Each bar indicates how much the uncertainty affecting a given output value, such as oil volume in-place and cumulative oil production. For this thesis, the different tornado plots indicate how much percentage deviation it is between the selected output of the Hyme reference case and the different uncertainty parameters.

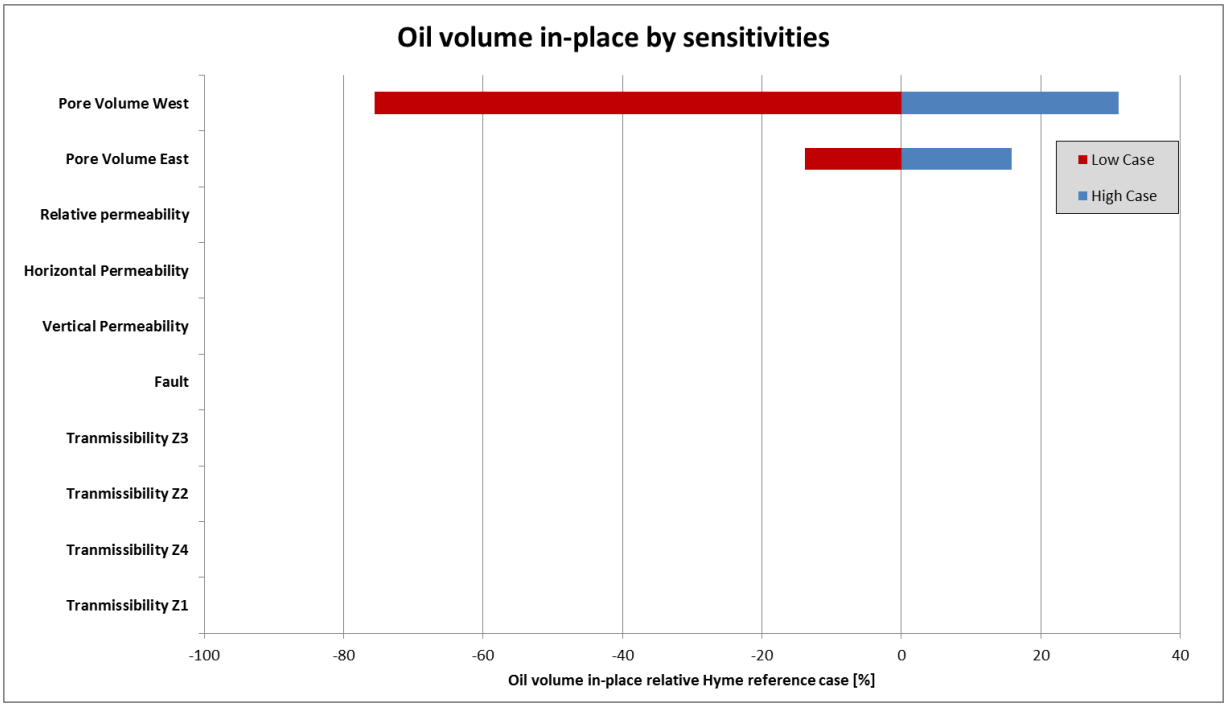

Figure 4-6: Tornado plot of difference in oil volume in-place between sensitivities and the Hyme reference case.

Figure 4-6 shows that changes in pore volumes in western segment are more sensitive than changes in the eastern segment. The major reason for this is that the oil volume in-place is much larger in western segment compared to eastern. In addition to this, the main bore of the producer are located in the western segment, which implies that the majority of the production will be from this segment.

4.3.2 Sensitivities for cumulative oil production

The simulation runs for the sensitivity analysis were run until 2030. For cumulative oil production, the different sensitivities were investigated in the years 2018 (Table 4-11), 2020 (Table 4-12), 2025(Table 4-13), and 2030(Table 4-14). For each of the years, a tornado plot was created in order to illustrate the difference between the sensitivities and the Hyme

reference case (Figure 4-7 to Figure 4-10). The reason for this is mainly that some parameters can affect the cumulative oil production at different times. Nevertheless, this thesis will have a main focus on the year 2030.

Table 4-11: Cumulative oil production by sensitivities at 01.01.2018.

Cumulative Oil Production 01.01.2018			
Uncertainty	**Low Case**	**High Case**	**Unit**
Pore volume eastern segment	2.92	3.69	[10^6 Sm^3]
Pore volume western segment	0.75	3.83	[10^6 Sm^3]
Horizontal Permeability	3.09	3.51	[10^6 Sm^3]
Vertical Permeability	3.23	3.44	[10^6 Sm^3]
Transmissibility multiplier Z1	3.34	3.34	[10^6 Sm^3]
Transmissibility multiplier Z2	3.34	3.36	[10^6 Sm^3]
Transmissibility multiplier Z3	3.34	3.39	[10^6 Sm^3]
Transmissibility multiplier Z4	3.34	3.34	[10^6 Sm^3]
Relative permeability	2.81	3.37	[10^6 Sm^3]
Fault seal	3.51	3.34	[10^6 Sm^3]

Table 4-12: Cumulative oil production by sensitivities at 01.01.2020.

Cumulative Oil Production 01.01.2020			
Uncertainty	**Low Case**	**High Case**	**Unit**
Pore volume eastern segment	3.22	4.80	[10^6 Sm^3]
Pore volume western segment	0.75	5.13	[10^6 Sm^3]
Horizontal Permeability	3.40	4.63	[10^6 Sm^3]
Vertical Permeability	3.59	4.34	[10^6 Sm^3]
Transmissibility multiplier Z1	3.70	4.22	[10^6 Sm^3]
Transmissibility multiplier Z2	3.70	4.24	[10^6 Sm^3]
Transmissibility multiplier Z3	3.70	4.26	[10^6 Sm^3]
Transmissibility multiplier Z4	3.70	4.25	[10^6 Sm^3]
Relative permeability	3.11	4.25	[10^6 Sm^3]
Fault seal	3.88	4.22	[10^6 Sm^3]

Table 4-13: Cumulative oil production by sensitivities at 01.01.2025.

Cumulative Oil Production 01.01.2025			
Uncertainty	**Low Case**	**High Case**	**Unit**
Pore volume eastern segment	3.66	4,80	[10^6 Sm^3]
Pore volume western segment	0.75	5.13	[10^6 Sm^3]
Horizontal Permeability	3.85	4.63	[10^6 Sm^3]
Vertical Permeability	4.09	4.34	[10^6 Sm^3]
Transmissibility multiplier Z1	4.22	4.22	[10^6 Sm^3]
Transmissibility multiplier Z2	4.22	4.24	[10^6 Sm^3]
Transmissibility multiplier Z3	4.22	4.26	[10^6 Sm^3]
Transmissibility multiplier Z4	4.22	4.25	[10^6 Sm^3]
Relative permeability	3.56	4.25	[10^6 Sm^3]
Fault seal	4.39	4.22	[10^6 Sm^3]

Table 4-14: Cumulative oil production by sensitivities at 01.01.2030.

Cumulative Oil Production 01.01.2030			
Uncertainty	**Low Case**	**High Case**	**Unit**
Pore volume eastern segment	3.97	5.15	[10^6 Sm^3]
Pore volume western segment	0.75	5.55	[10^6 Sm^3]
Horizontal Permeability	4.17	4.96	[10^6 Sm^3]
Vertical Permeability	4.40	4.65	[10^6 Sm^3]
Transmissibility multiplier Z1	4.53	4.53	[10^6 Sm^3]
Transmissibility multiplier Z2	4.53	4.55	[10^6 Sm^3]
Transmissibility multiplier Z3	4.53	4.58	[10^6 Sm^3]
Transmissibility multiplier Z4	4.53	4.57	[10^6 Sm^3]
Relative permeability	3.86	4.56	[10^6 Sm^3]
Fault seal	4.70	4.53	[10^6 Sm^3]

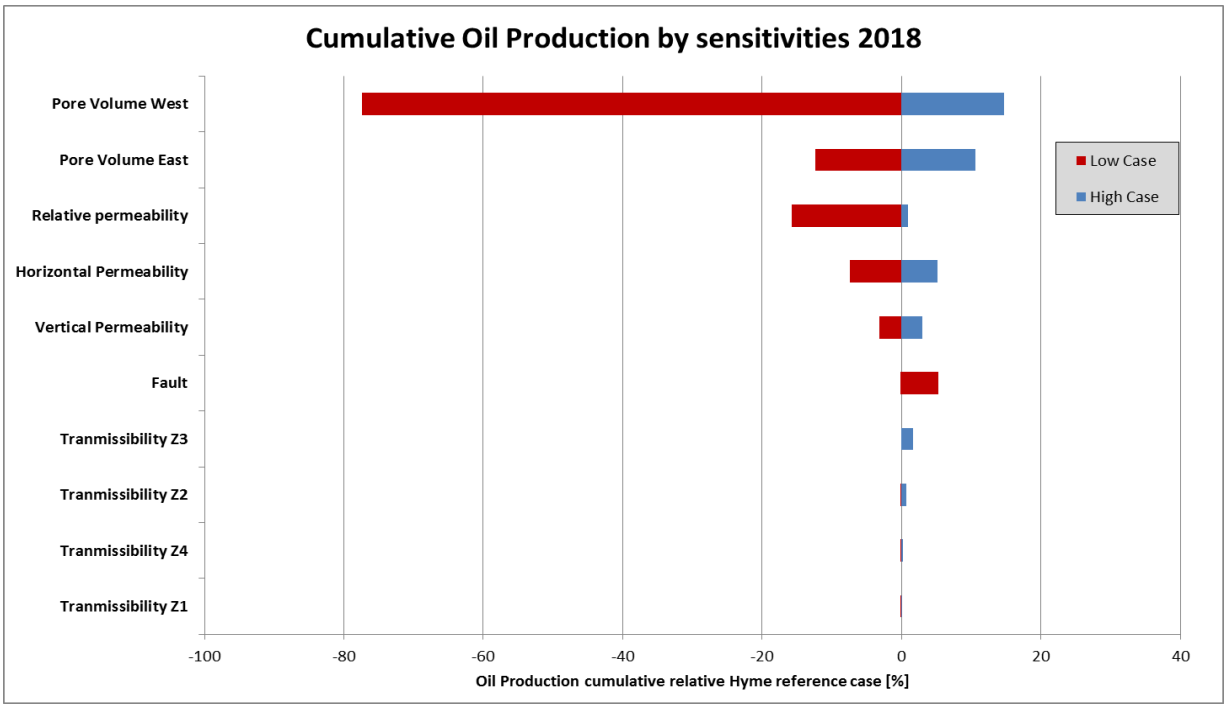

Figure 4-7: Tornado plot of difference in cumulative oil production between sensitivities and the Hyme reference case at 01.01.2018.

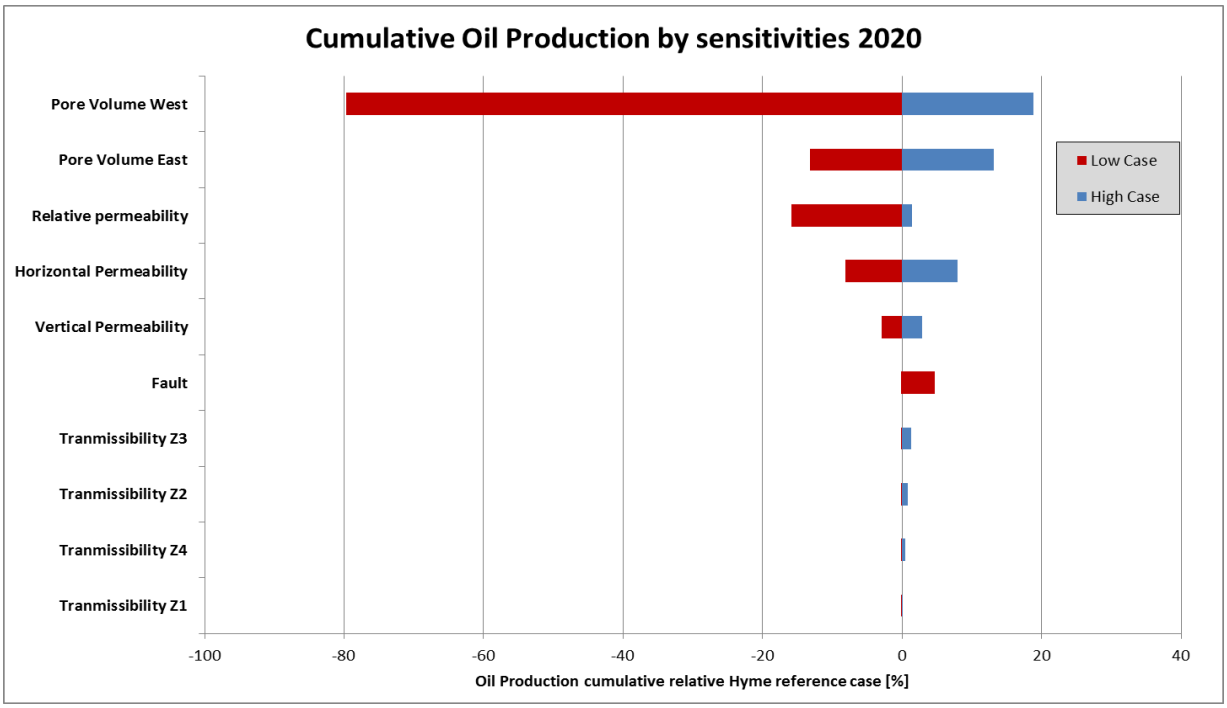

Figure 4-8: Tornado plot of difference in cumulative oil production between sensitivities and the Hyme reference case at 01.01.2020.

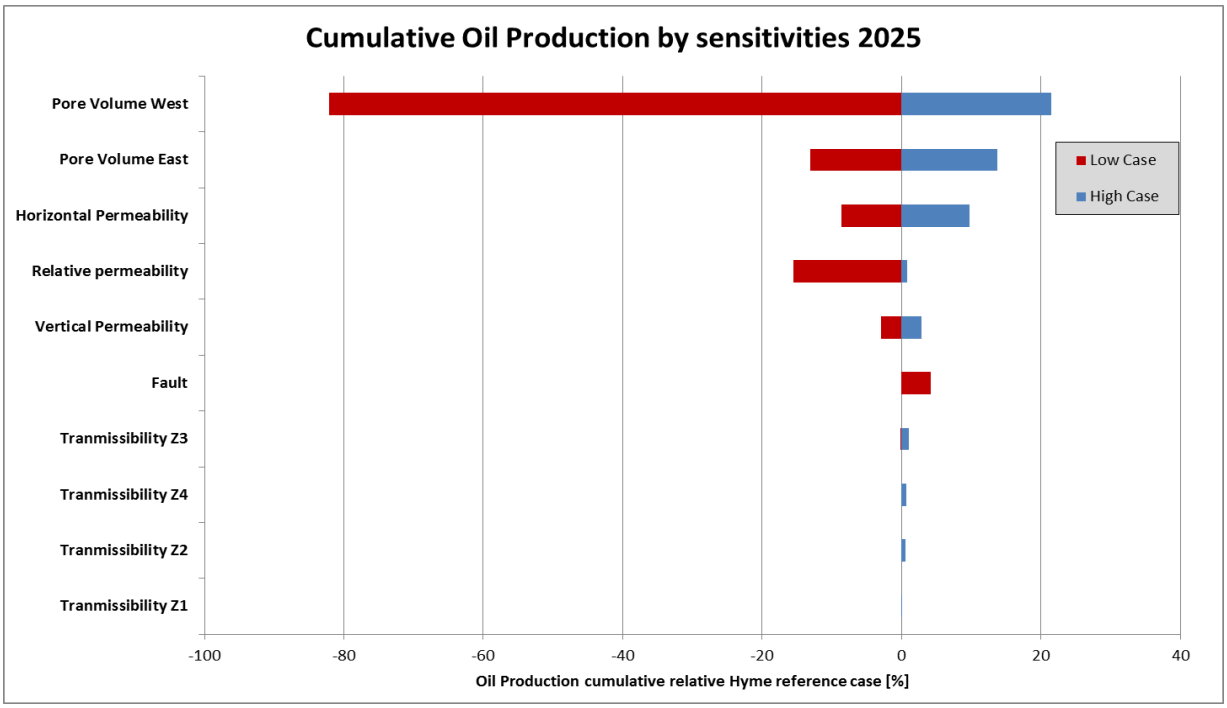

Figure 4-9: Tornado plot of difference in cumulative oil production between sensitivities and the Hyme reference case at 01.01.2025.

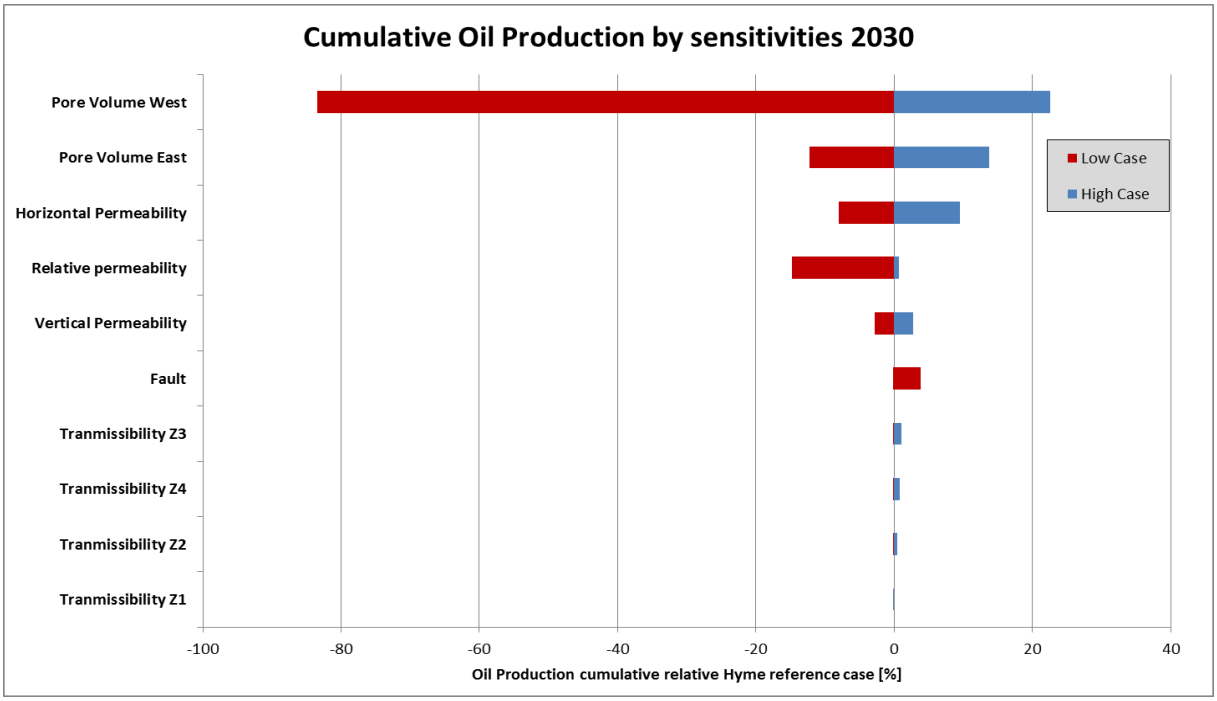

Figure 4-10: Tornado plot of difference in umulative oil production between sensitivities and the Hyme reference case at 01.01.2030.

Table 4-11 shows the results for cumulative oil production by sensitivities at 2018. A key observation here is the cumulative oil production for low case for pore volume western segment. The production here is predicted to be only 0.75 million Sm^3, which is fairly low compared to the other cases. The reason for this is that the oil volume in-place (Table 4-10) is not sufficient to keep production for longer than 2 years. This will affect the long term production for this sensitivity and Table 4-14 which is cumulative oil production at 2030, shows the same value of 0.75 million Sm^3.

Another key observation from the tables (Table 4-11 to Table 4-14) is the fault seal sensitivities. Here the low case gives a larger oil production than the high case. From the tornado plots in can be observed that the low case has about 5% larger oil production than the reference and high case. As described in section 4.1.4 the high and reference case for fault seal was communication between the two segments, while the low case was tight. The reason why the low case has a larger oil production could be that less water moves from eastern to western segment. This will result in less water production through the main bore, which again will result in higher oil production. However, this could also imply that the model has some limitations.

The major observation from the tornado plots (Figure 4-7 to Figure 4-10) is how much the pore volume multipliers affect the cumulative oil production. As described earlier, the low case for western segment can be explained by to low oil volumes in-place for production maintenance. For the high case, the oil production is about 15% larger than the reference case in 2018(Figure 4-7) and over 20% larger in 2030 (Figure 4-10). For the eastern segment, the low case is about 15% less than the reference case through all the four tornado plots. The high case is increasing with time, from about 10 to 15% larger than reference case.

Horizontal permeability is the third most uncertain parameter in 2030 (Figure 4-10), with a high case about 10% larger than the reference case, and low case about 8% lower. The low case is constant through all the tornado plots, while the high case slightly increases. The vertical permeability stays constant, with about 3% higher than reference case for high case, and 3% lower for the low case.

The relative permeability has a large influence when it comes to low case. It is constant through all tornado plots on a value about 17% lower than the reference case. The high case is slightly higher than reference case, about 1%.

For the vertical transmissibility multipliers, the difference between the reference case and the sensitivities is low. The largest difference is the transmissibility Z3 which is between the layers Tilje 3 and Tilje 2.2, with a high case about 1% higher than the reference case. A major reason for these results could be that the high case multipliers can be considered as low (Table 4-8), hence the communication is low.

4.4 Pre-production uncertainty simulation Results

Based on the 200 simulation cases that were run for the pre-production uncertainty analysis, 130 of them were successful. The reason why 70 of them did not complete is due to convergence failure with the material balance equations. In these cases, the simulator is reporting that it is unable to solve the material balance equations within the maximum numbers of iterations specified by the user. If the equations are not resolved within the maximum number of iterations, it will proceed if the value is less than the specified maximum. However, if the value exceeds the maximum value, computation is terminated and started again with a reduction in time step length (Kleppe, 2012). These maximum values could be considered as maximum flow in and out of a gridblock. If the value exceeds the maximum value too many times, the simulation case will be aborted.

There could be different physical reasons for why 70 of the cases are aborted due to convergence failure. The cases fails in different time periods, and has different production profiles, which eliminates the chance of systematic failures. For this pre-production uncertainty, several simulation cases were created based on Monte Carlo sampling of the desired input parameters. This results in simulation cases with large variations in pore volume and permeability. These are parameters that affect how much volume and how fast it flows between the different gridblocks. Based on the sensitivity analysis in section 4.3, it can be concluded that the pore volume multipliers have a large influence on the oil-volumes in place and cumulative oil production. The horizontal permeability has a large influence on cumulative oil production. On this basis, it is reasonable to conclude that variation in pore volume and permeability could cause convergence failure of the material balance equations.

The raw simulation results for the 130 cases are organized in plots and they are compared with the Hyme reference case. Due to the large magnitude of results, no tables are included. All simulation results are displayed with a grey color, while the Hyme reference case has an actual color. For the oil production, the Hyme reference case is displayed with green color for the oil production rates (Figure 4-11) and the cumulative oil production (Figure 4-12). The Hyme reference case is displayed with red color for gas rates (Figure 4-13) and cumulative gas production (Figure 4-14). For the water production and injection rates and cumulative production and injection (Figure 4-15 to Figure 4-18) the reference case has the color blue.

4.4.1 Production (Oil, gas, and water)

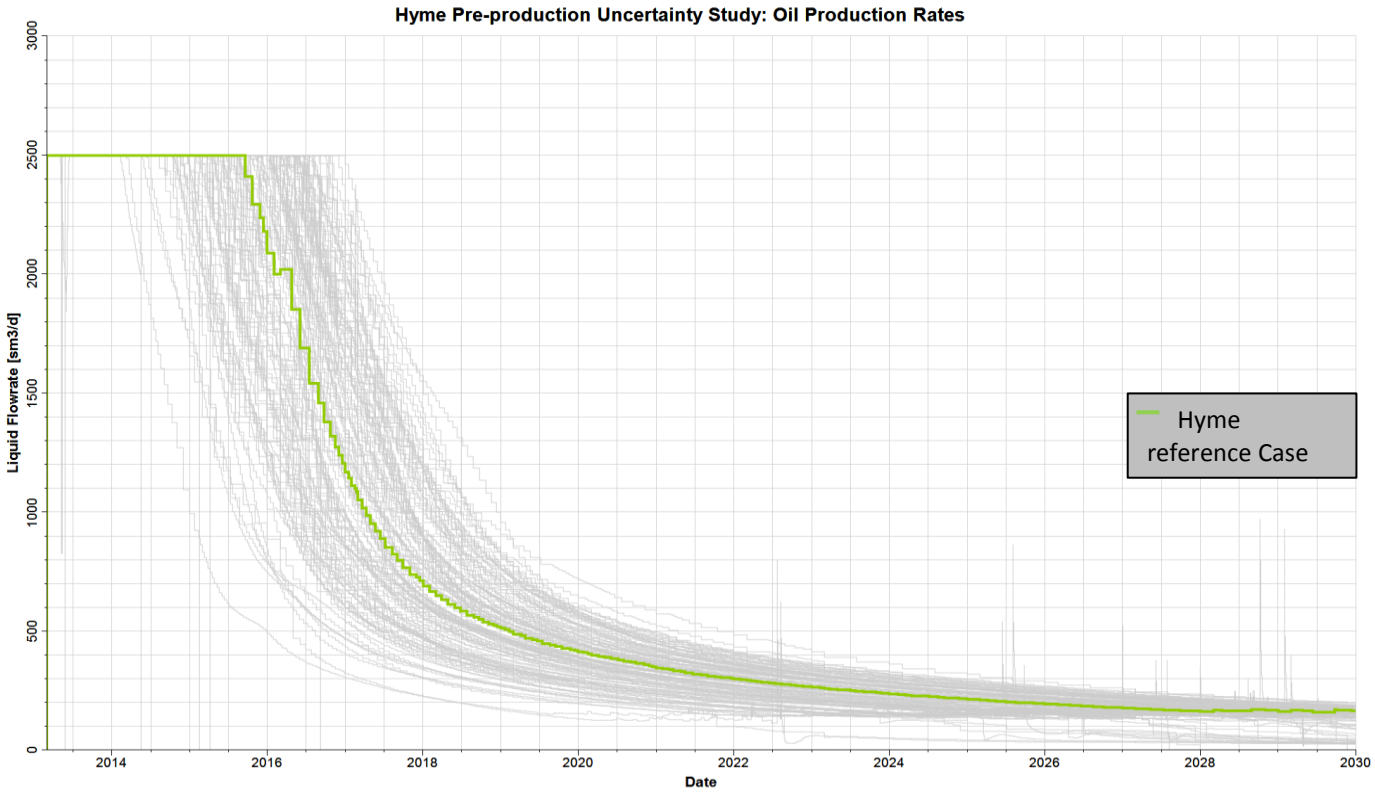

Figure 4-11: Oil production rates from pre-production uncertainty simulations.

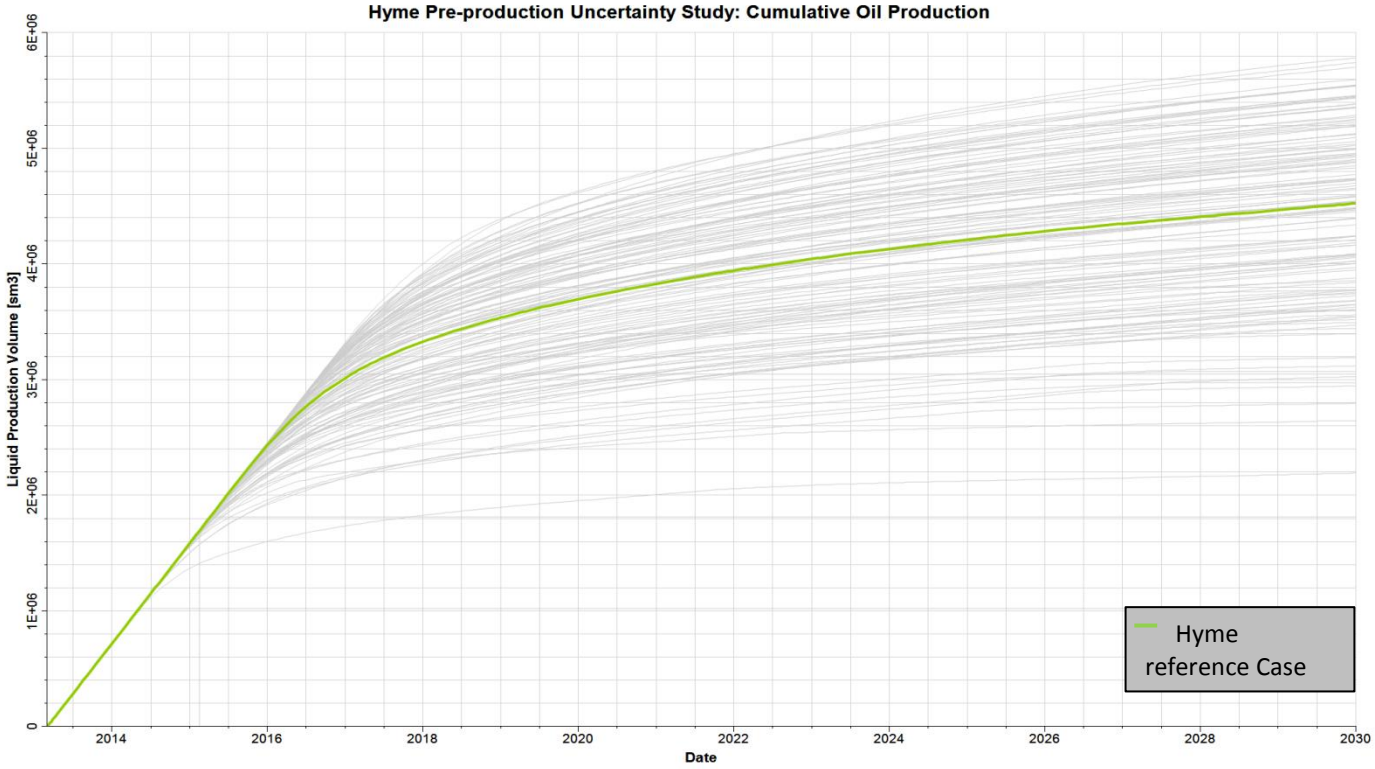

Figure 4-12: Cumulative oil production from pre-production uncertainty simulations.

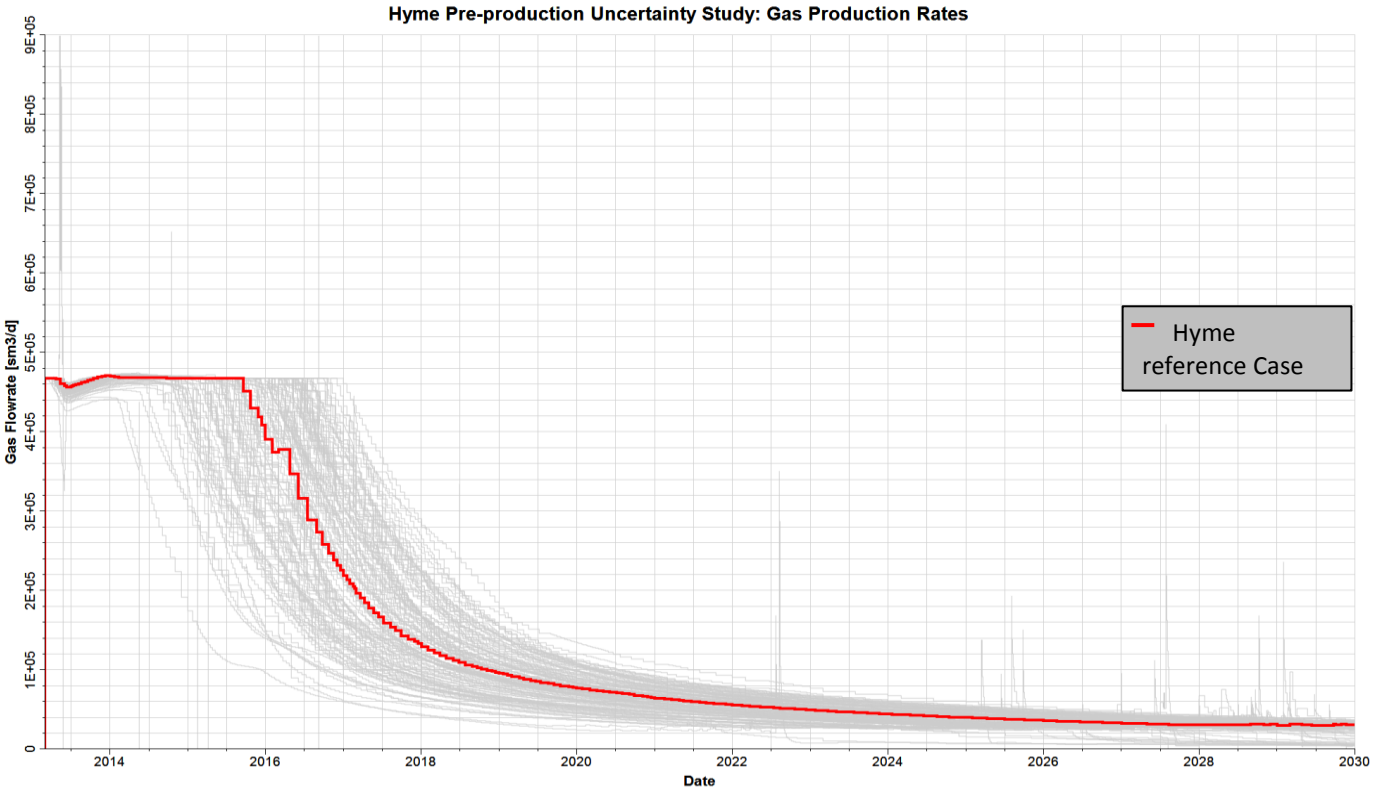

Figure 4-13: Gas production rates from pre-production uncertainty simulations

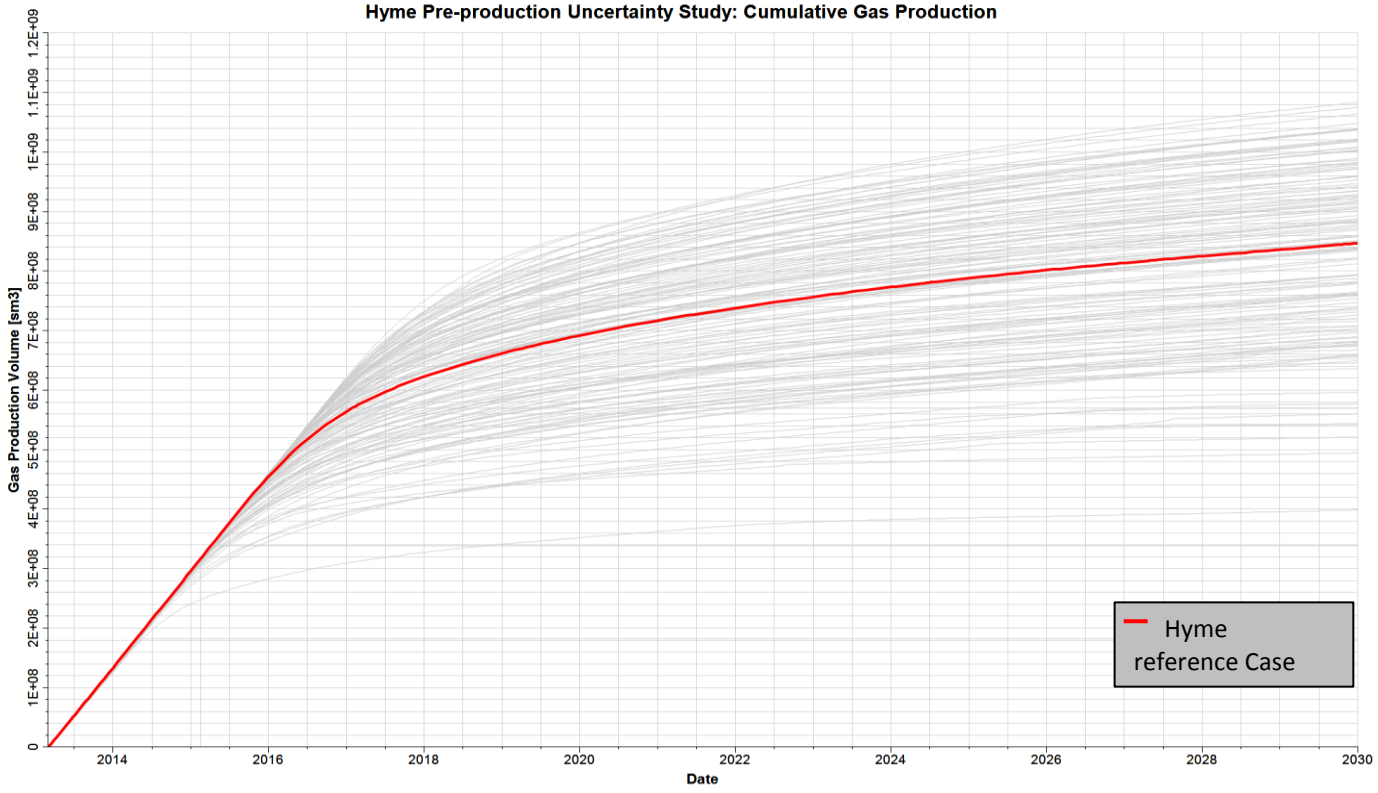

Figure 4-14: Cumulative gas production from pre-production uncertainty simulations.

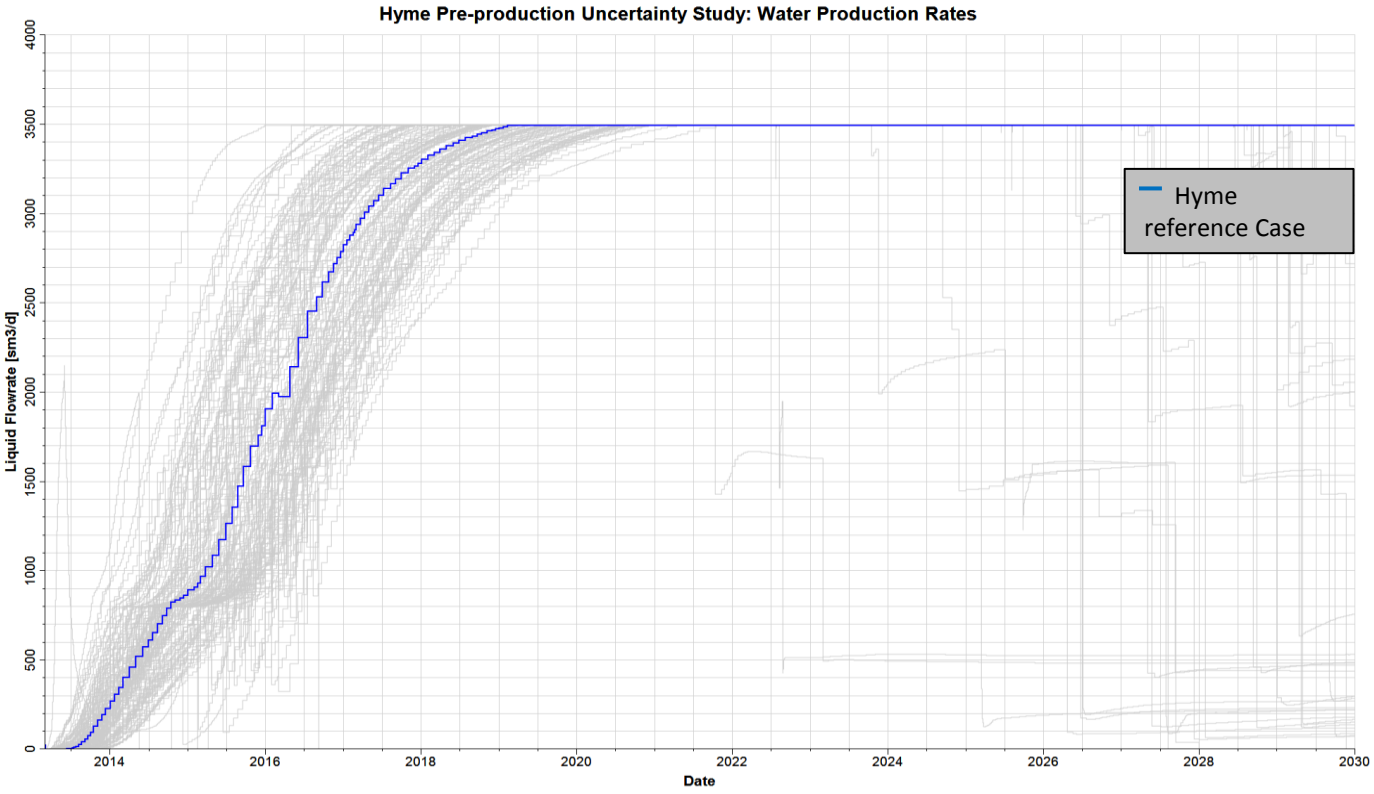

Figure 4-15: Water production rates from pre-production uncertainty simulations

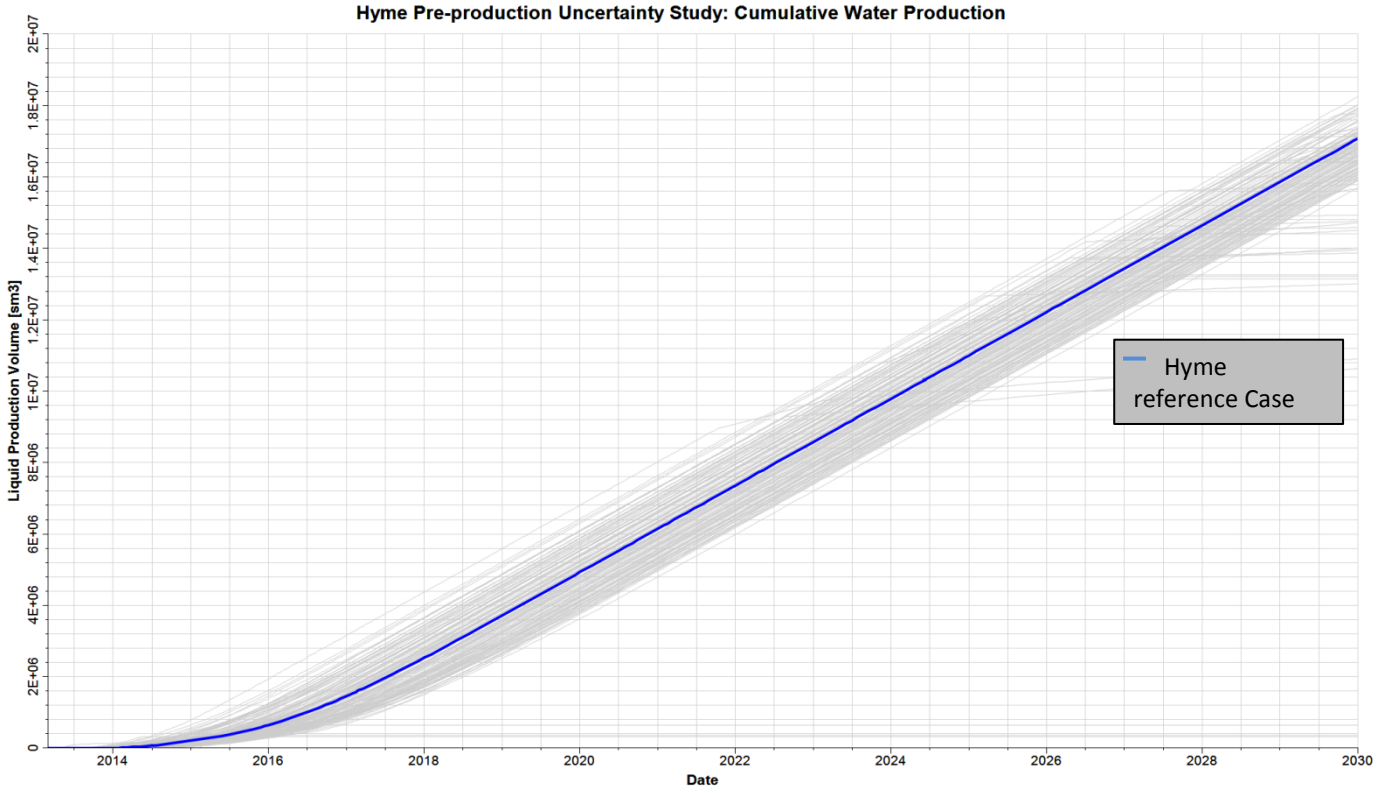

Figure 4-16: Cumulative water production from pre-production uncertainty simulations.

4.4.2 Injection (Water)

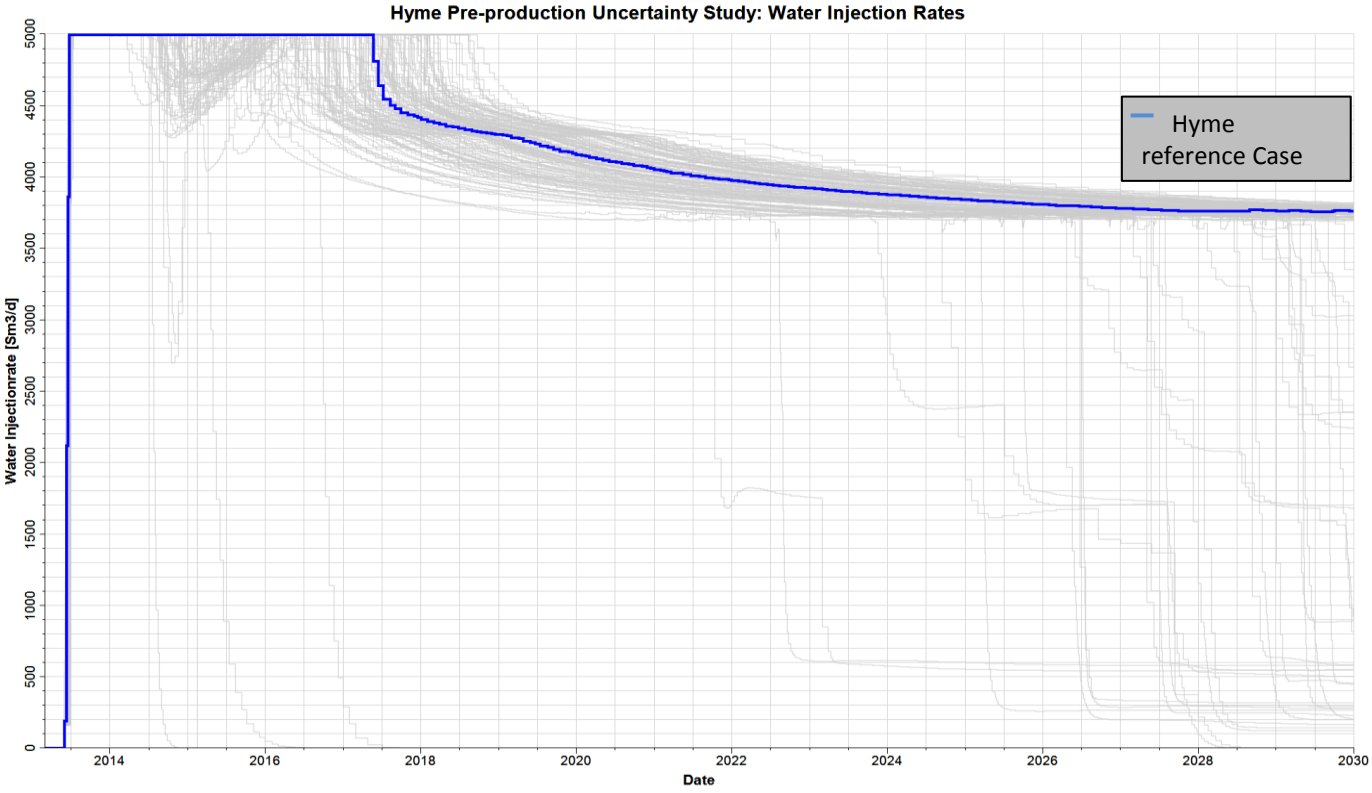

Figure 4-17: Water injection rates from pre-production uncertainty simulations

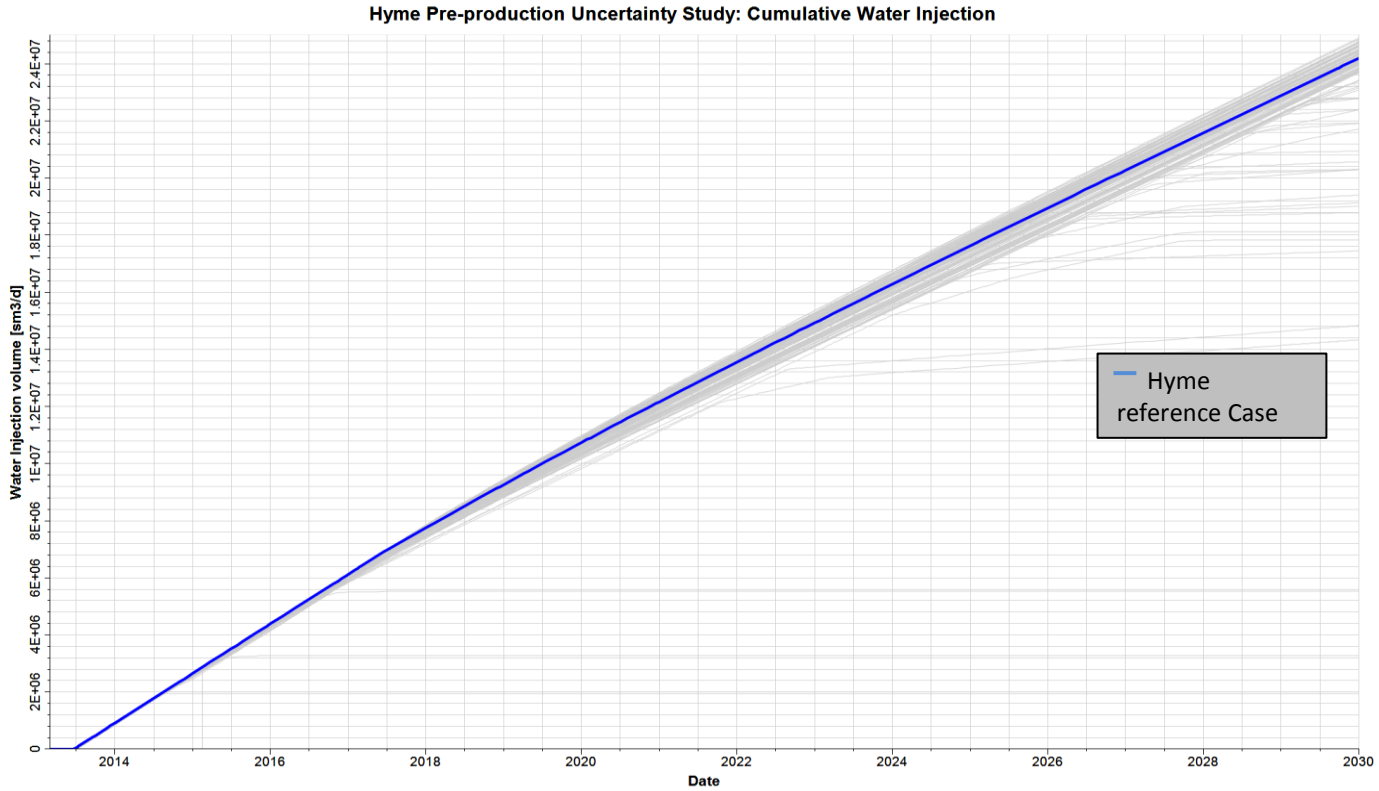

Figure 4-18: Cumulative water injection from pre-production uncertainty simulations.

4.4.3 Discussion concerning pre-production simulation results

In general, the Hyme reference case and the 130 pre-production uncertainty simulations show general alignment. The reference case seems to be an average curve in each of the plots (Figure 4-11 to Figure 4-18). For oil production rate (Figure 4-11) there are variations in how long the production is on plateau rate of 2500 Sm^3/d, with the following decline. This are reflected in the cumulative oil production (Figure 4-12), which also has variations. Since one of the main objectives in this thesis is to quantify the uncertainty ranges of the ultimate estimated oil recovery, this will be studied more in detail in section 4.5.

As expected, the gas production rates (Figure 4-13) follows the same trend as the oil production rates, since production most of the time are kept above the bubble point pressure. This gives approximately the same variations in cumulative gas production (Figure 4-14) as for the cumulative oil production.

For water production rates (Figure 4-16) there are variations in the first 6 years of the production, until the rate reaches the maximum water production rate constraint (Table 3-13) at 3500 Sm^3/d. From this point, all the cases are producing water at the maximum rate. This gives a cumulative water production with smaller variations compared with cumulative oil and gas production.

All injection rates (Figure 4-17) starts on the maximum injection rate constraint (Table 3-13) of 5000 Sm^3/d. There are some variations in terms of when injection rate are declining from this rate. Some of the cases have a decline in injection earlier, and then builds up to the constraint again. This can be explained by the fact that the injection is controlled by pressure maintenance. Nevertheless, the injection rate is in general large for each case, which gives high cumulative water injection (Figure 4-18) with small variations.

4.5 Pre-production estimated ultimate oil recovery

As described earlier, a major objective in this thesis is to quantify and reduce the uncertainty in the estimated ultimate oil recovery for the Hyme field, in order to investigate the long term oil production potential. Based on the 130 successful simulation runs from the pre-production uncertainty study, a distribution of the cumulative oil production was created.

The distribution consists of the average cumulative oil production and 10, 50 and 90 percentiles, which are based on the cumulative oil production at 1 of January 2030. The 50 percentile was chosen such that 50 percent of the cases have more cumulative oil production than the selected case, while 50 percent of the cases have less. For the 10 percent percentile, 10 percent of the cases have a larger production and thereby 90 percent have less. The 90 percentile indicates that 90 percent of the cases have larger production and 10 % have less. From this point the percentiles will be denoted as P10, P50 and P90. The results are listed in Table 4-15, and the Hyme reference case is included for comparison.

Table 4-15: Distribution of cumulative oil production based on pre-production simulation results.

Distribution of cumulative oil production						
Date	Mean	P90	P50	P10	Reference Case	Unit
01.01.2014	0.72	0.72	0.72	0.72	0.72	[10^6 Sm^3]
01.01.2015	1.58	1.59	1.59	1.59	1.59	[10^6 Sm^3]
01.01.2016	2.36	2.29	2.46	2.46	2.44	[10^6 Sm^3]
01.01.2017	2.93	2.63	3.10	3.29	3.02	[10^6 Sm^3]
01.01.2018	3.26	2.78	3.45	3.84	3.34	[10^6 Sm^3]
01.01.2019	3.47	2.89	3.67	4.17	3.54	[10^6 Sm^3]
01.01.2020	3.62	2.97	3.82	4.40	3.70	[10^6 Sm^3]
01.01.2021	3.75	3.04	3.95	4.57	3.84	[10^6 Sm^3]
01.01.2022	3.86	3.10	4.05	4.71	3.95	[10^6 Sm^3]
01.01.2023	3.95	3.15	4.13	4.84	4.05	[10^6 Sm^3]
01.01.2024	4.03	3.21	4.21	4.95	4.14	[10^6 Sm^3]
01.01.2025	4.10	3.26	4.28	5.05	4.22	[10^6 Sm^3]
01.01.2026	4.17	3.31	4.34	5.14	4.29	[10^6 Sm^3]
01.01.2027	4.23	3.34	4.39	5.22	4.35	[10^6 Sm^3]
01.01.2028	4.29	3.37	4.44	5.30	4.41	[10^6 Sm^3]
01.01.2029	4.35	3.39	4.49	5.37	4.47	[10^6 Sm^3]
01.01.2030	4.40	3.40	4.54	5.44	4.53	[10^6 Sm^3]

The results from Table 4-15 are illustrated in Figure 4-19.

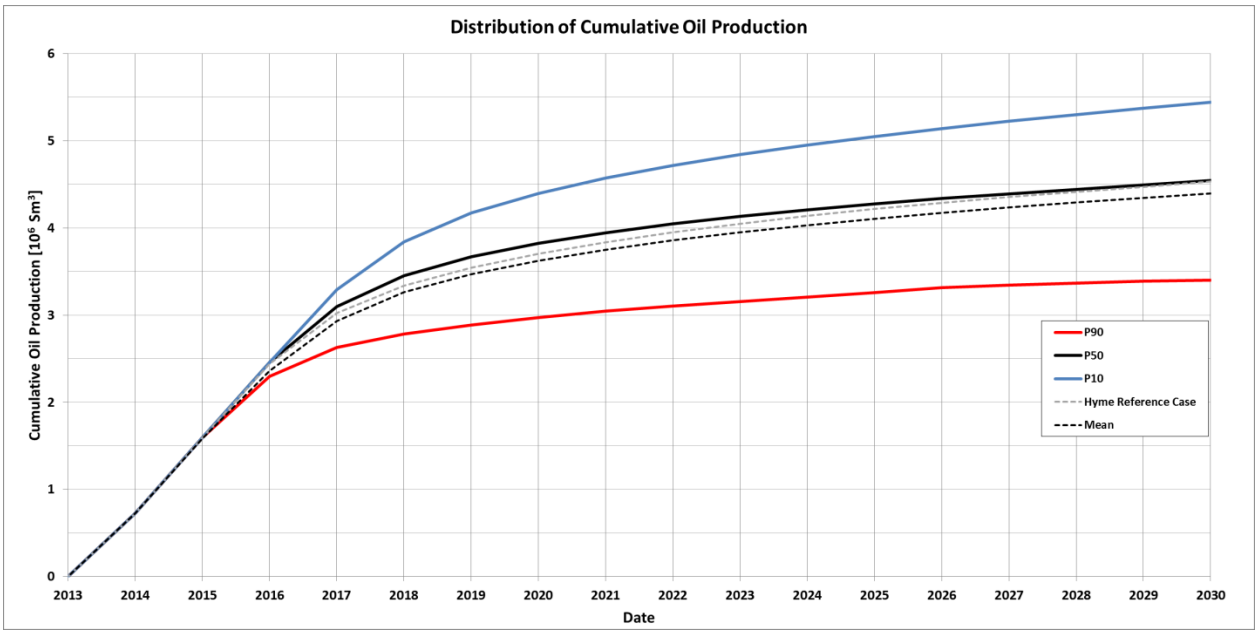

Figure 4-19: Distribution of cumulative oil production based on pre-production simulation results.

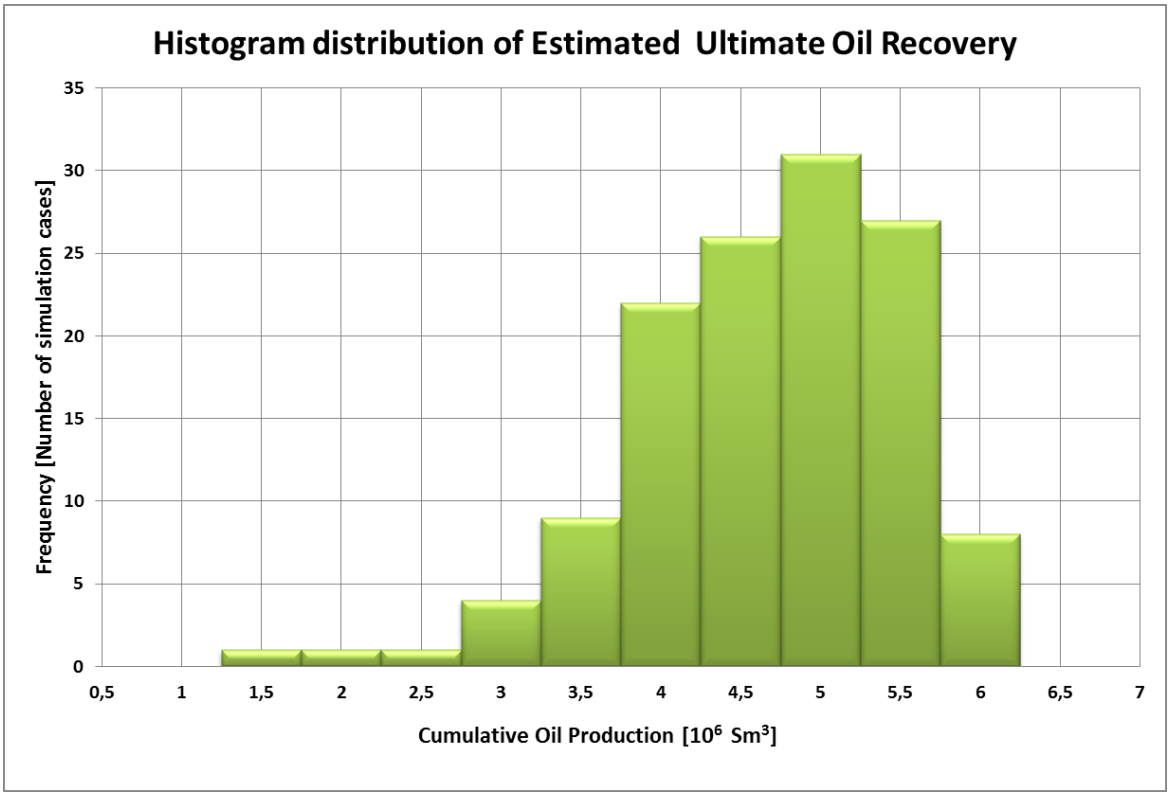

Figure 4-20: Pre-Production histogram distribution of estimated ultimate oil recovery.

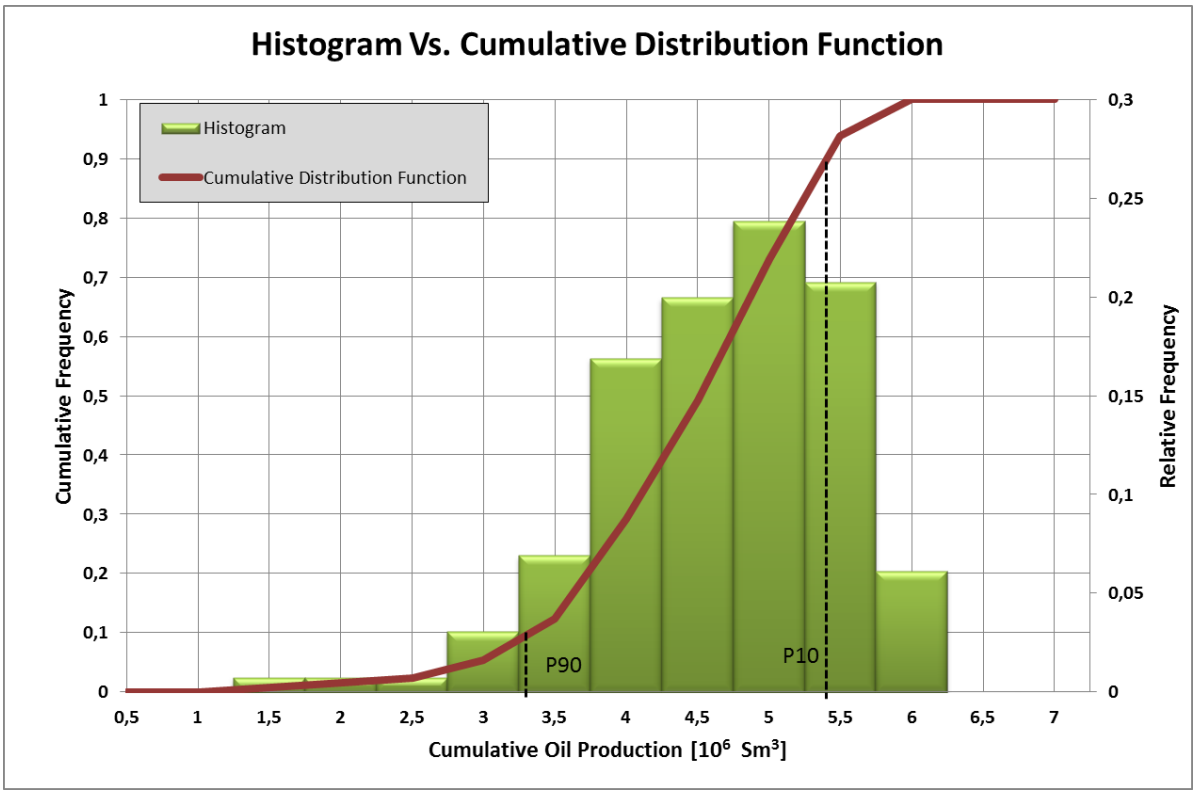

Figure 4-21: Pre-Production histogram versus cumulative distribution function

Based on the results from Table 4-15 and Figure 4-19, there are general alignment between the Hyme reference case and the P50. The mean value is about 3% lower than the P50 which mainly are related to the downside in in-place volumes. The estimated ultimate recovery is considered as the total cumulative oil production at 1st of January 2030. The distribution of the estimated ultimate oil recovery is illustrated by the histogram in Figure 4-20.

From Figure 4-20 it can be observed that the simulations resulted in an estimated ultimate oil recovery range of 1.5 to 6 million Sm^3. In order to capture the uncertainty range between P90 and P10 within the histogram, a probability distribution histogram with a cumulative distribution function was created (Figure 4-21). This was done by normalizing the frequency to relative frequency. A cumulative distribution function was added in order to observe the different percentiles within the histogram. The cumulative distribution function can be defined as the cumulative relative frequency.

Based on the P90 and P10, which provides a 90% confidence interval, from Figure 4-19, Figure 4-21 and Table 4-15 , the estimated ultimate oil recovery should be within the uncertainty range of 3.40 to 5.44 million Sm^3.

5. Post-production Uncertainty Study

A post-production uncertainty study will be performed based on the Hyme reference case established in chapter 3, sensitivity analysis performed in chapter and available production data. The workflow is described in Figure 5-1.

5.0.1 History Matching

History matching can be defined as the process of adjusting parameters in a reservoir simulation model until the simulated performance matches the measured performance within an accepted tolerance (Caers, 2005). Alternatively, history matching can be defined as the process of conditioning the reservoir model on dynamic, as well as static observations. The aim of this process is to create reservoir models which have an improved prediction power for prediction of future resources and reserves.

In traditional history matching, deterministic models are being considered, where properties are changed in order to calibrate the model. These modified properties are parameters that are considered uncertain (Almeida Netto et. al, 2003). This means that the engineer has to manually change the selected parameters by the trial-and-error principle. Common performance data to be matched are (Kleppe, 2010):

- Reservoir Pressure; average pressure and pressure distributions.
- Fluid movement, saturation from cores, tracer tests, arrival times for injected fluids at producers.
- Well observations; rates, pressures, water cut, gas oil ratio.

At the time this study was performed, 2 months of production was data available from the Hyme field. These data were the oil production rates and bottom hole pressure data. As oil production rate is at plateau rate during the 2 months period, it was decided that bottom hole pressure is the key observation data that will be utilized in history matching for this study.

Another less time consuming approach is to use computer assisted history matching software instead of manual adjusting. Such software is integrated in the simulation workflow, and allows the user to use an experimental design. Assisted history matching can

be defined as a process where the quality of a model is improved by gradually changing the input variables such that the simulated output becomes closer to the observed production data (Reis et al., 2009).

This study used the assisted history matching software Olyx developed by Resoptima. Olyx is a plug-in used with Petrel and is designed for history matching and optimization of reservoir simulation models. The software enables the user to integrate any kind of geological and geophysical property as a variable in addition to more familiar reservoir engineering variables (Resoptima, 2012). For this study, it is a great advantage that Olyx is a plug-in for Petrel, as it allows keeping the same workflow as in pre-production study and therefore the same experimental design.

5.0.2 Objective function

The procedure for performing a computer assisted history match has two major steps. The first step is to define an objective function, which is defined as a mathematical expression describing the difference between simulated and observed data. The next step will be minimizing the objective function by using an optimization algorithm (Reis et al., 2009). Olyx defines the objective function as

$$Q_i = m_i \sqrt{\sum_{J}^{N_i} \frac{1}{N_i} \left(\frac{Sim_{i,j} - Obs_{i,j}}{\sigma_{i,j}} \right)^2},$$

where

- i is the objective element index
- j is the observed sample point index
- Q_i is the objective function
- m_i is the multiplier of objective element i
- N_i is the number of valid observed sample points for objective element i
- $Sim_{i,j}$ is the simulated value for objective element at observed point j
- $Obs_{i,j}$ is the observed value for objective element I at observed point j
- $\sigma_{i,j}$ is the measurement error of objective element I at observed point j

As the only objective element of this study is bottom hole pressure, the objective element index can be denoted with bhp. It will not be used any multipliers since all data points will be

weighted equally. Accordingly, this will be set to the value 1. In addition to this, measurement errors in the bottom hole pressure was estimated to be 1 bar for simplicity, since it is assumed not to affect the purpose of this study. With these assumptions in mind, the objective function used in this study can be expressed as

$$Q_{bhp} = \sqrt{\sum_{J}^{N_{bhp}} \frac{1}{N_{bhp}} \left(Sim_{bhp,j} - Obs_{bhp,j}\right)^2},$$

where

- *bhp* is the objective element index
- *j* is the observed bottom hole pressure sample point index
- Q_{bhp} is the objective function
- N_{bhp} is the number of valid bottom hole pressure sample points
- $Sim_{i,j}$ is the simulated bottom hole pressure value at observed point j
- $Obs_{i,j}$ is the observed bottom hole pressure value at observed point j

5.0.3 Integration of history matching in uncertainty study

With a well-established objective function, it is possible to start the history matching using an optimization algorithm embedded in Olyx. This study uses an algorithm called Genetic algorithm. The Olyx software makes it possible to use the same workflow that was used in pre-production uncertainty analysis. This means that the history matching will rely on the same uncertainty ranges as described in Table 4-9.

The Genetic algorithm is designed so that it generates a specified number of stochastic simulation cases based on Monte Carlo sampling from the set of the specified uncertainty ranges. Based on the objective function values of these simulation cases, a new number of cases are generated. The purpose of this is to minimize the objective function. This process is repeated a specified number of times.

After all simulations are performed, each case will have an objective function value associated with it. A traditional method is to use the model with the lowest objective function value for further analysis. Another possibility is to set an upper limit to the objective function so that all cases with lower value are analyzed further (Reis et al., 2009). The advantage of this method is that the model is history matched in addition to the simulation cases can be part of a post-production analysis, where the results can be treated statistically. This methodology are used as described for this study, using the workflow in Figure 5-1 with bottom hole pressure values listed in section 5.1.

5.0.4 Workflow for Post-production uncertainty study

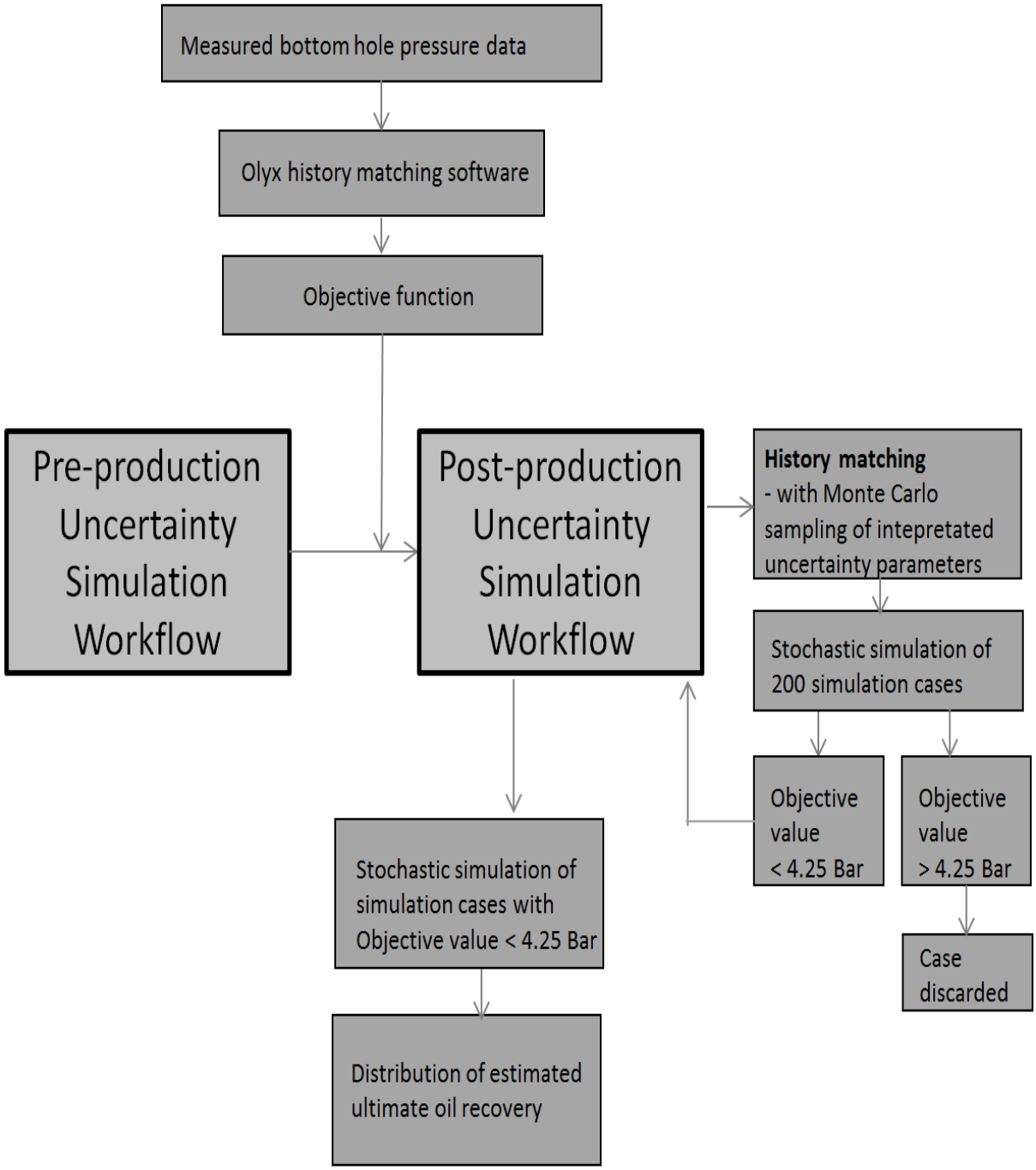

Figure 5-1: Workflow for Post-production uncertainty study

5.1 Bottom hole pressure data

Table 5-1 shows the bottom hole pressure data available for the post-production uncertainty study. These data will define the objective function that will be used further for history matching.

Table 5-1: Bottom hole pressure from Hyme in the period 02.03-24.04 2013

Date	Bottom hole pressure[Bar]	Date	Bottom hole pressure[Bar]
02.03.2013	218	29.03.2013	202.6
03.03.2013	211.5	30.03.2013	202.4
04.03.2013	202.2	31.03.2013	202.2
05.03.2013	213.3	01.04.2013	202
06.03.2013	213.3	02.04.2013	201.9
07.03.2013	209.9	03.04.2013	201.7
08.03.2013	210.2	04.04.2013	201.5
09.03.2013	209.9	05.04.2013	201.3
10.03.2013	210.3	06.04.2013	201.3
11.03.2013	210.6	07.04.2013	201
12.03.2013	209	08.04.2013	200.8
13.03.2013	208.5	09.04.2013	200.6
14.03.2013	208.2	10.04.2013	200.4
15.03.2013	207.9	11.04.2013	200.3
16.03.2013	207.6	12.04.2013	204.3
17.03.2013	207.4	13.04.2013	202.1
18.03.2013	207.2	14.04.2013	201.4
19.03.2013	206.2	15.04.2013	204.2
20.03.2013	204.8	16.04.2013	202.6
21.03.2013	204.5	17.04.2013	200.4
22.03.2013	204.2	18.04.2013	199.8
23.03.2013	203.9	19.04.2013	199.2
24.03.2013	203.6	20.04.2013	199
25.03.2013	203.4	21.04.2013	198.8
26.03.2013	203.2	22.04.2013	198.5
27.03.2013	203	23.04.2013	198.3
28.03.2013	202.8	24.04.2013	198.1

5.1.1 Determination of objective value criteria for history matching

Based on the measured values of the bottom hole pressure in Table 5-1 and the simulation results from Hyme reference case, an objective value criteria for history matching was determined. The objective value for Hyme reference case was calculated by Olyx to be 4.25 bar. This value can be considered as a good match, which can be observed in Figure 5-2.

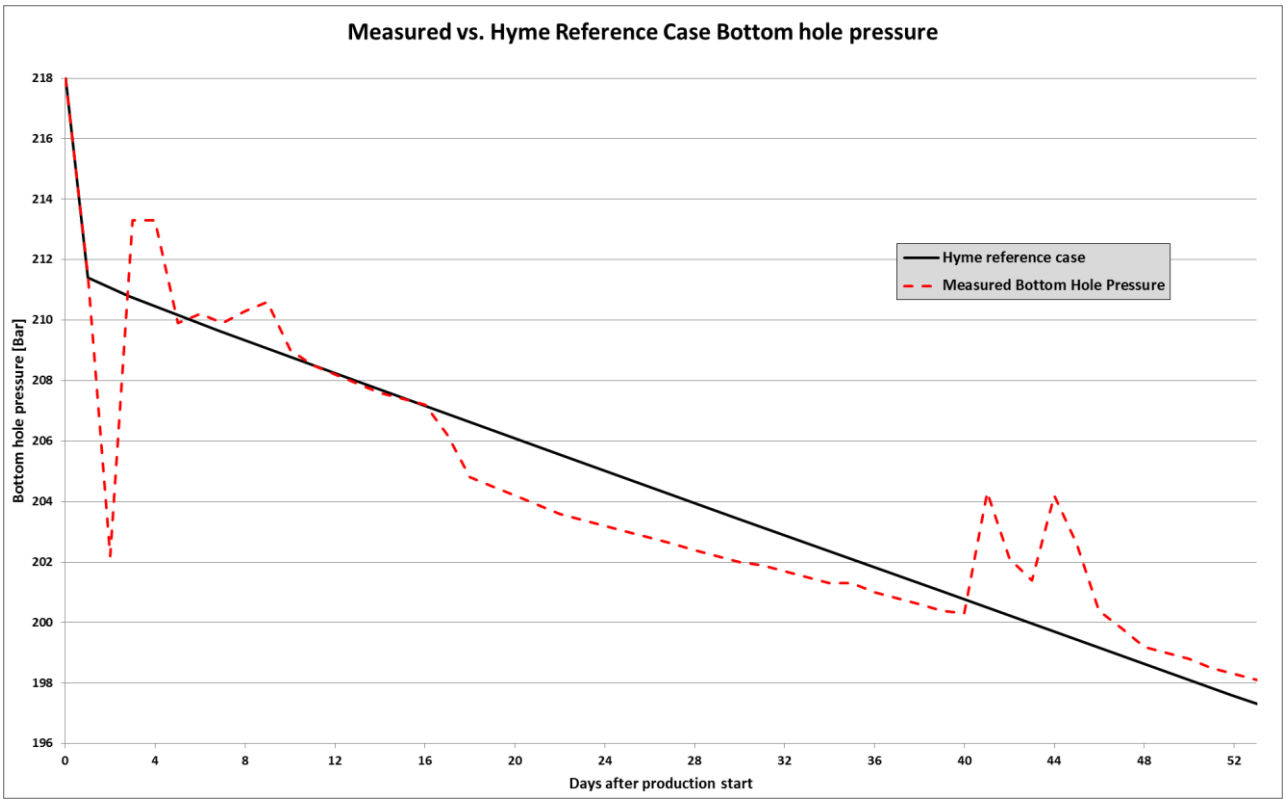

Figure 5-2: Measured bottom hole pressure compared with Hyme reference case where day 0 is April 2 2013.

Since the reference case turned out to be a god match with the observed data, the criteria was determined to be every objective value less 4.25 bar. This means that out of the 230 simulated cases, all cases with an objective value less than 4.25 bar will be included in the post-production uncertainty analysis.

5.2 Post-production uncertainty analysis results

There was in total 50 cases that complement the objective function value of less than 4.25 bar, which makes the basis for the results of the post-production uncertainty study. The study is divided into three parts, where the first part consists of the uncertainty ranges for the input parameters to the post-production study. The second part consist plots of the stochastic simulation results, and the second part shows the statistical treatment of the simulation results for cumulative oil production, in alignment with chapter 4.

5.3 Post-production uncertainty input parameters

After the history matching process was performed, 50 cases matched the preset criteria. These cases were generated by Monte Carlo sampling from the same table as for the pre-production study (Table 4-9). Based on the 50 cases it was possible to create new ranges for the uncertainty input, based on maximum and minimum values for each of the sampled parameters. For the discrete input, the percentage was calculated based on appearance relative to number of cases included. The uncertainty input ranges are listed in Table 5-2.

Table 5-2: Ranges for post-production uncertainty input parameters

Uncertainty	Low	Reference	High	Description
Pore volume eastern segment	0.66	1	1.55	Multiplier
Pore volume western segment	0.49	1	1.36	Multiplier
Horizontal Permeability	0.32	1	3.46	Multiplier
Vertical Permeability	0.01	0.1	0.5	Multiplier
Transmissibility multiplier Z1	0	0	0.1	Multiplier
Transmissibility multiplier Z2	0	0	0.1	Multiplier
Transmissibility multiplier Z3	0	0.0001	0.1	Multiplier
Transmissibility multiplier Z4	0	0	0.1	Multiplier
Relative permeability	22 % (oil-wet)	40 % (mixed wet)	28 % (water-wet)	Discrete
Fault seal	20 % (tight)	40 % (reference)	40 % (open)	Discrete

From Table 5-2 it can be observed that some of the ranges are smaller compared with Table 4-9, which will be discussed more in chapter 6. For faults, the reference and high case suggest communications, which implies that 80 % of the cases included in this study, had communication.

5.4 Post-production simulation results

Out of the 230 simulation cases generated by through the workflow, 50 cases had an objective function value less than 4.25 bar. These cases were run to 1st of January 2030 in alignment with the pre-production study. The raw simulation results for the 50 cases are organized in plots and they are compared with the Hyme reference case. Simulation results are displayed with a grey color, while the Hyme reference case has an actual color in alignment with the pre-production study.

Oil production is displayed in Figure 5-3 and Figure 5-4 with the Hyme reference case in green. It can be observed from the oil production rates (Figure 5-3) that the variations in how long the production is on the plateau rate of 2500 Sm^3/d, are less compared with the pre-production study. This affects the cumulative oil production (Figure 5-4) where the spread in the results looks smaller compared with pre-production study. The reference case seems to be in the middle; however there is a larger density of cases above it, implying potential for higher oil rate. The same trends can be observed in gas production (Figure 5-5 and Figure 5-6) where the reference case is illustrated with red.

Water production is displayed in Figure 5-7 and Figure 5-8 with the Hyme reference case in blue. The water rates (Figure 5-7) still reaches the production constraint of 3500 Sm3/d within few years resulting in small variations in cumulative water production (Figure 5-8). However there is less spread in the water rates and a larger density of cases with less water production compared with the pre-production study.

Water injection is illustrated in Figure 5-9 and Figure 5-10 with the Hyme reference case in blue. The results for water injection are very similar to the pre-production study, but the spreading are diminished, both injection rates and hence cumulative injection.

5.4.1 Production (Oil, gas, and water)

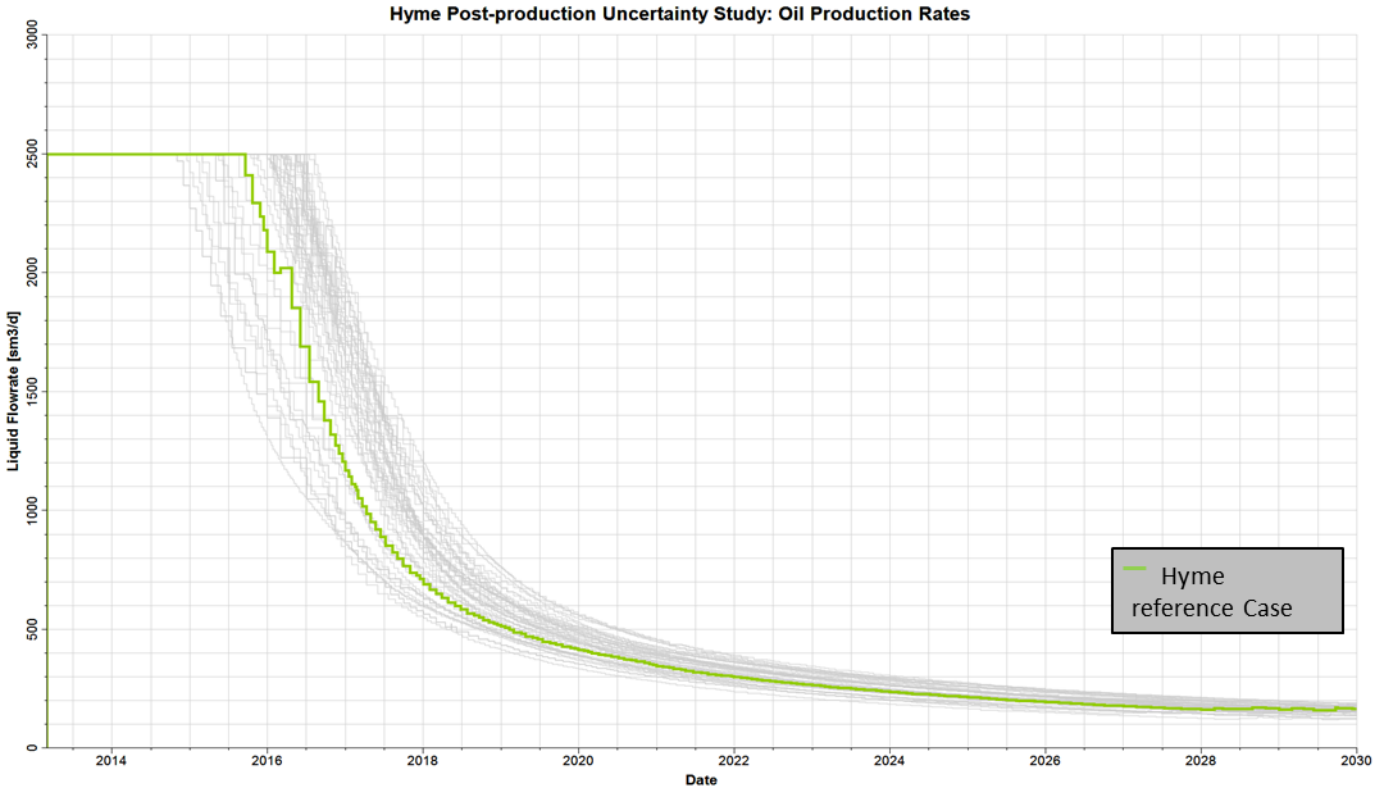

Figure 5-3: Oil production rates from post-production simulations

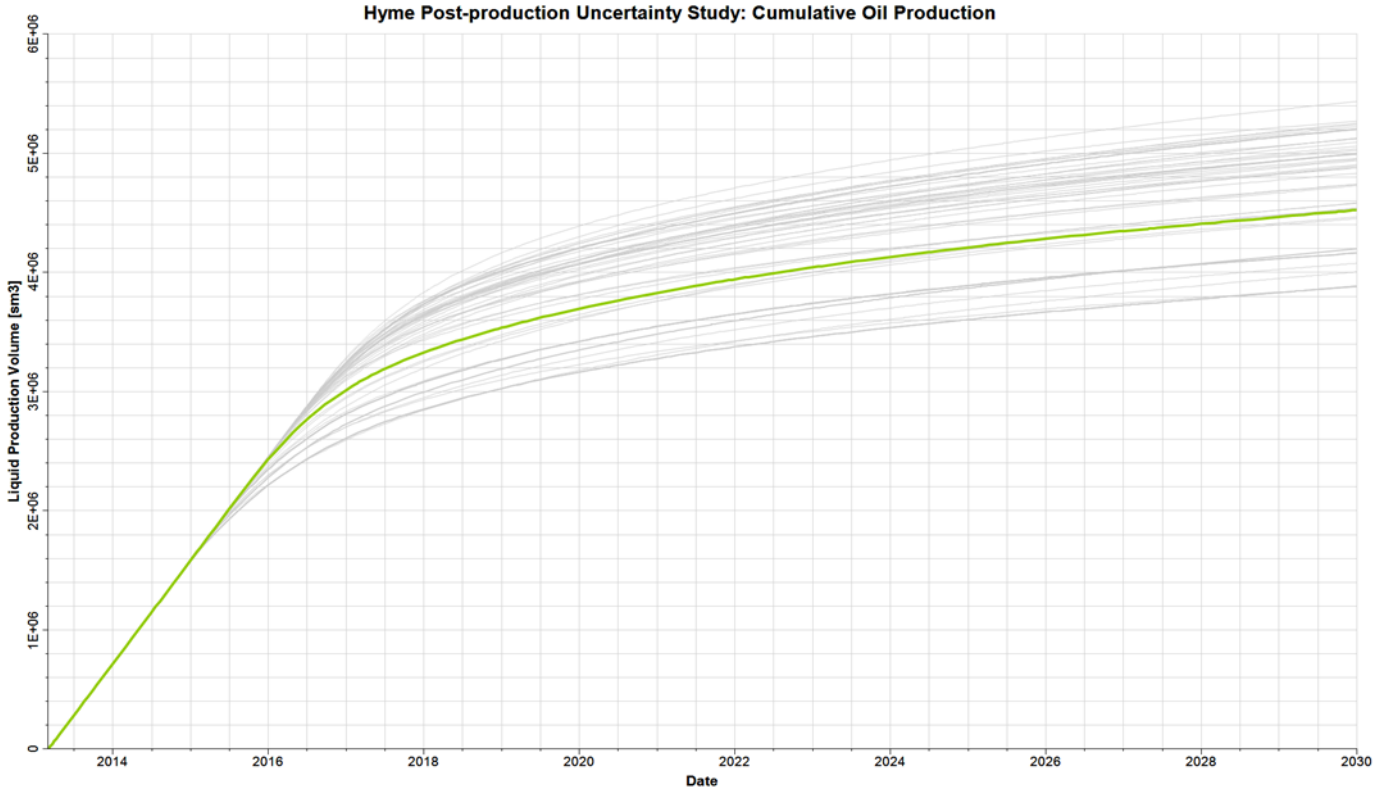

Figure 5-4: Cumulative oil production from post-production simulations.

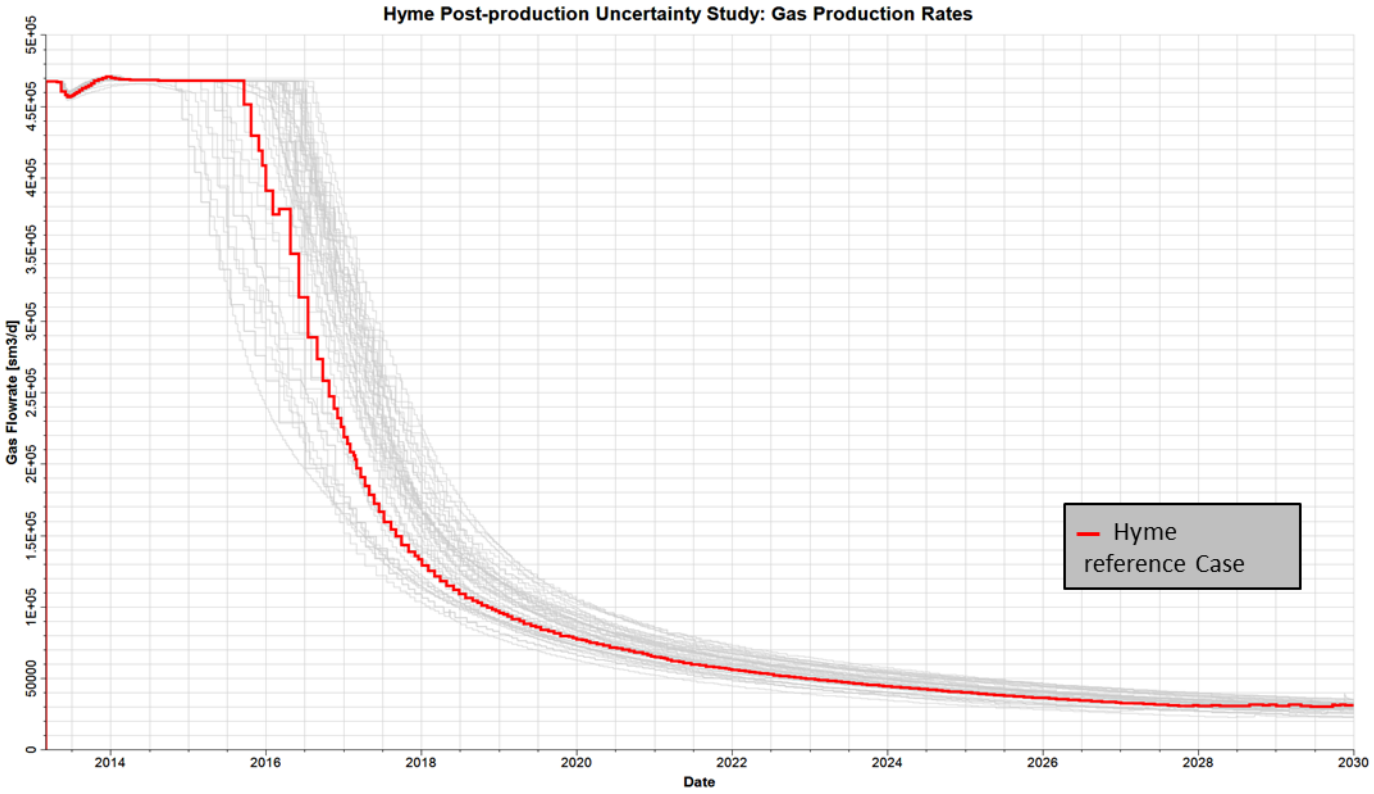

Figure 5-5: Gas production rates from post-production simulations

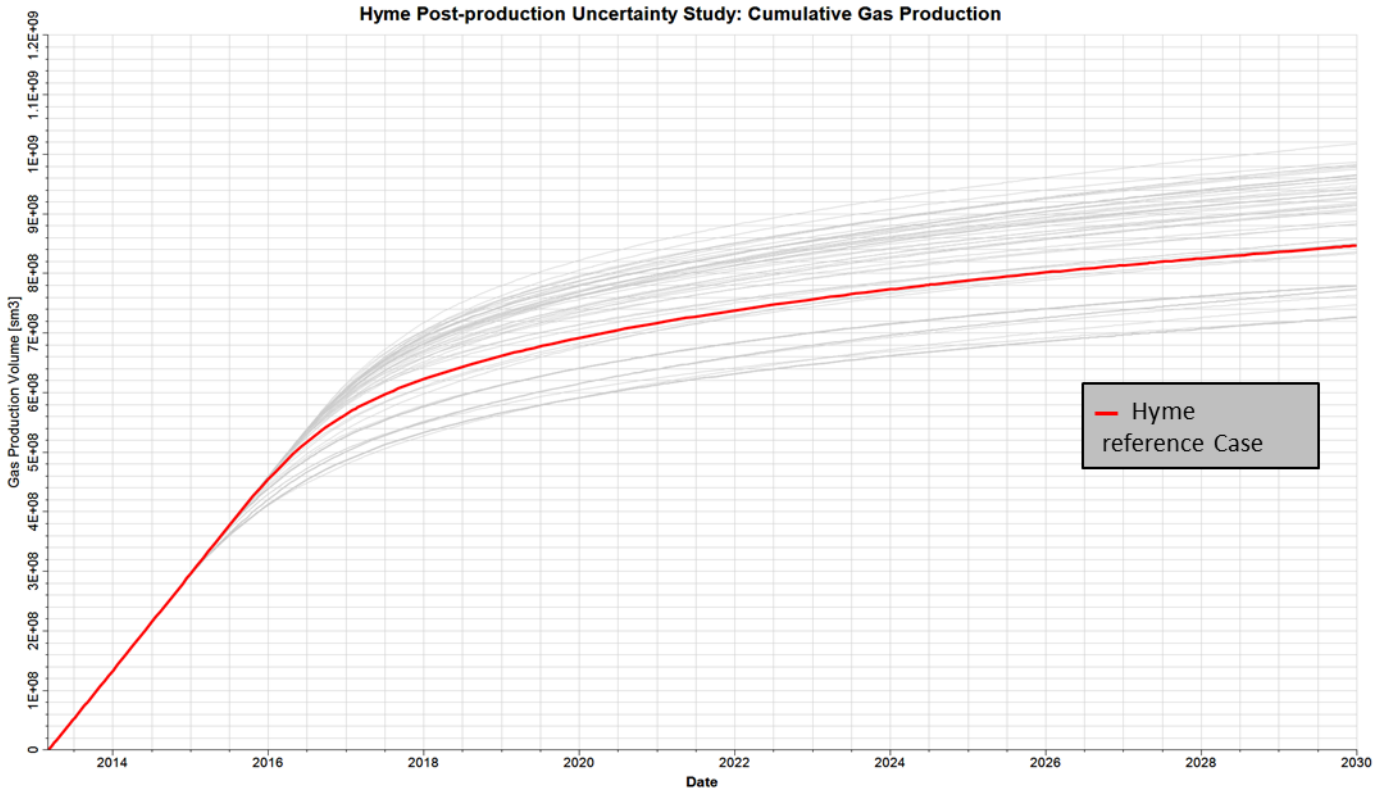

Figure 5-6: Cumulative gas production from post-production simulations.

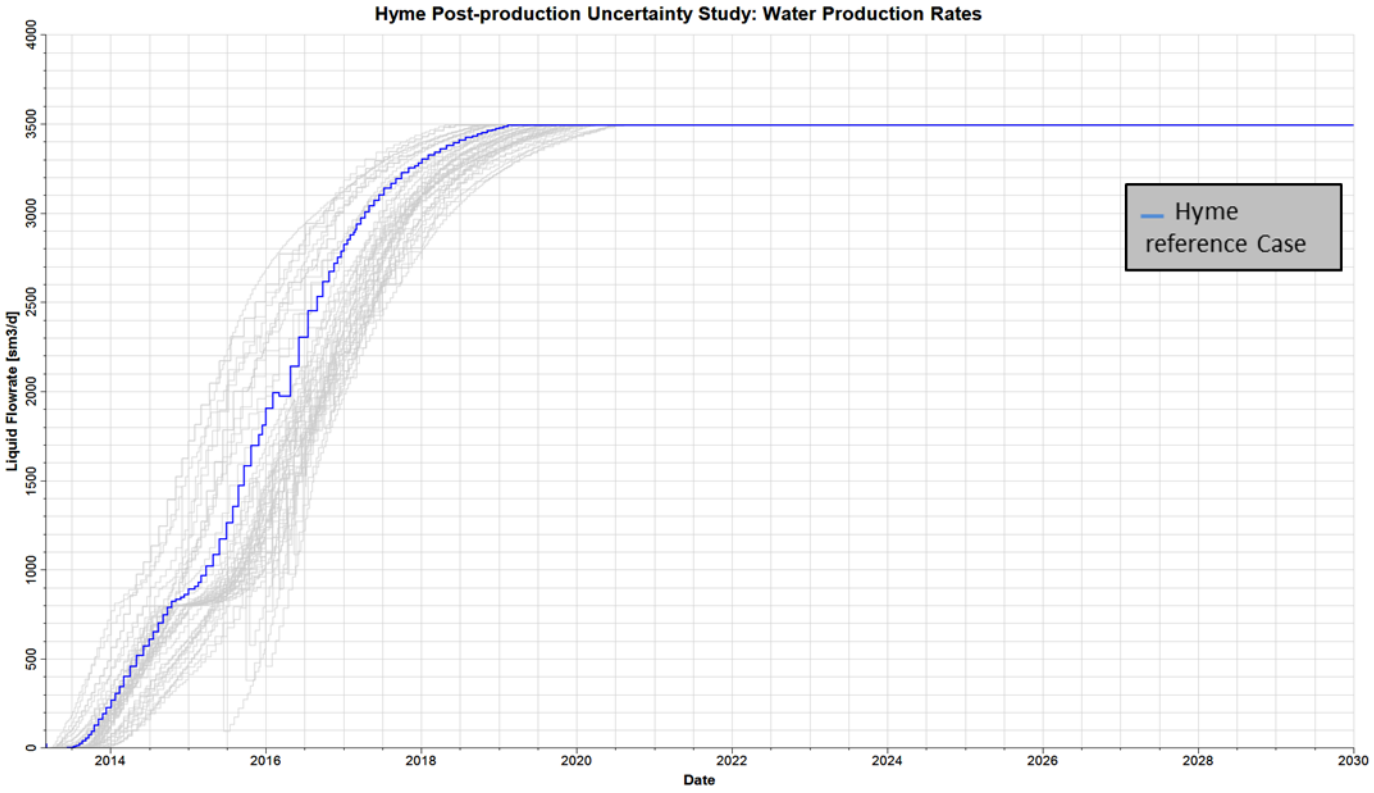

Figure 5-7: Water production rates from post-production simulations

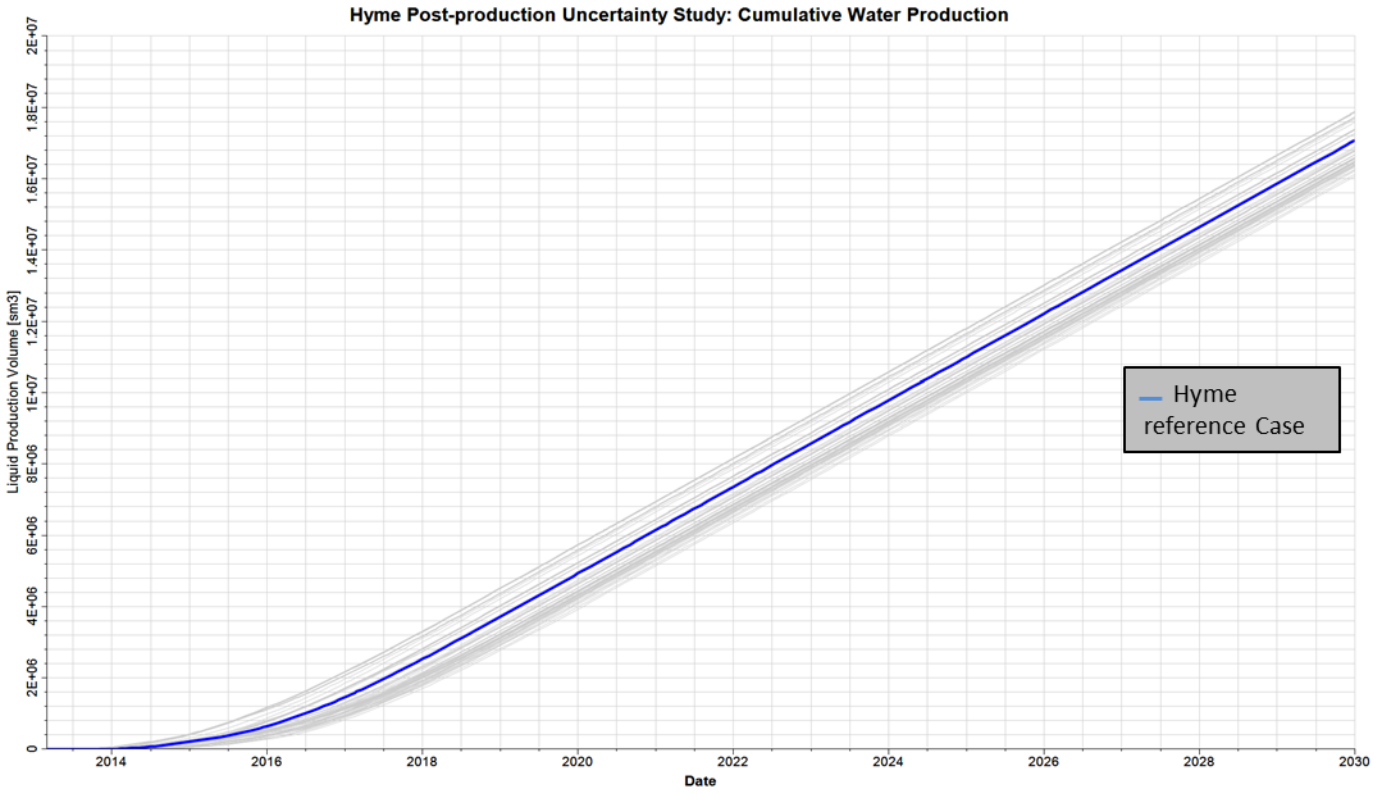

Figure 5-8: Cumulative water production from post-production simulations.

5.4.2 Injection (Water)

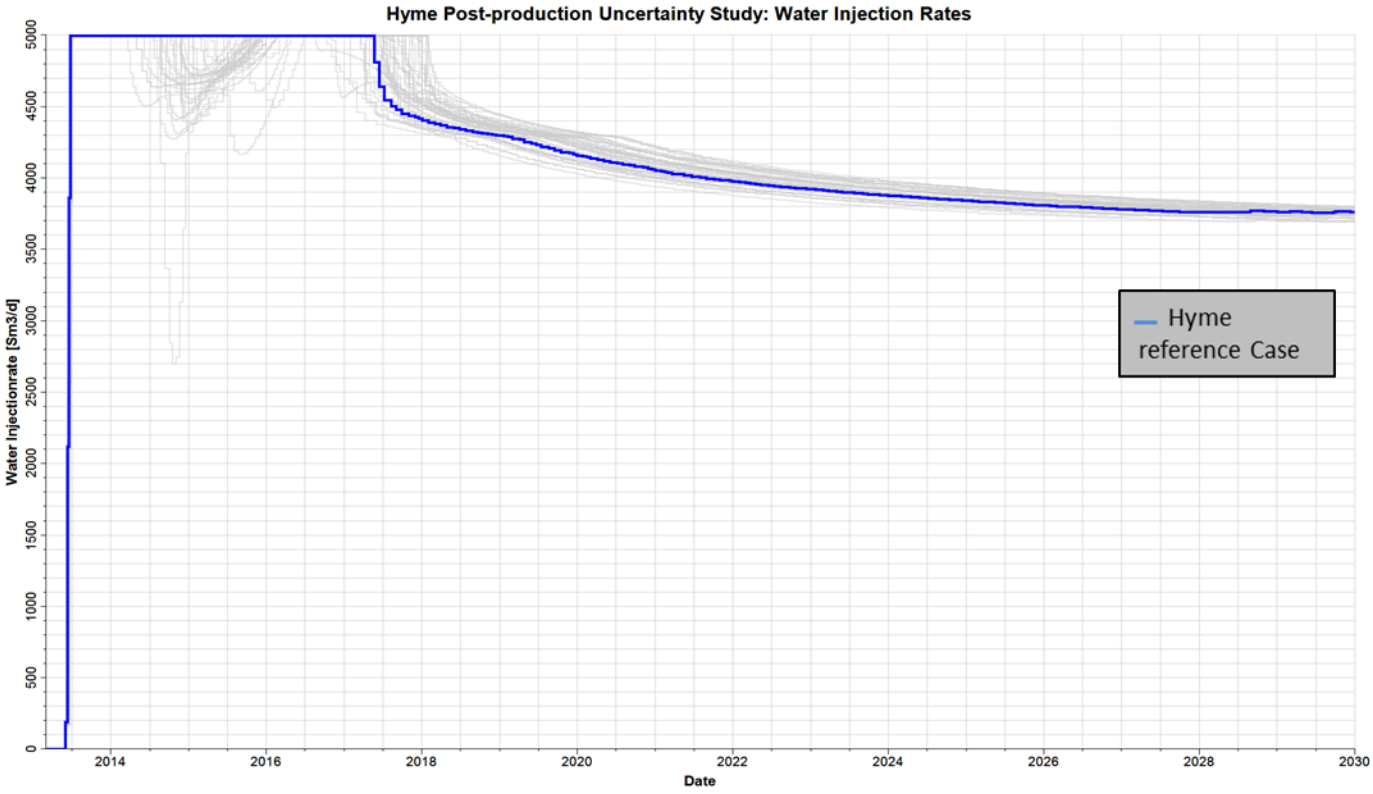

Figure 5-9: Water injection rates from post-production simulations

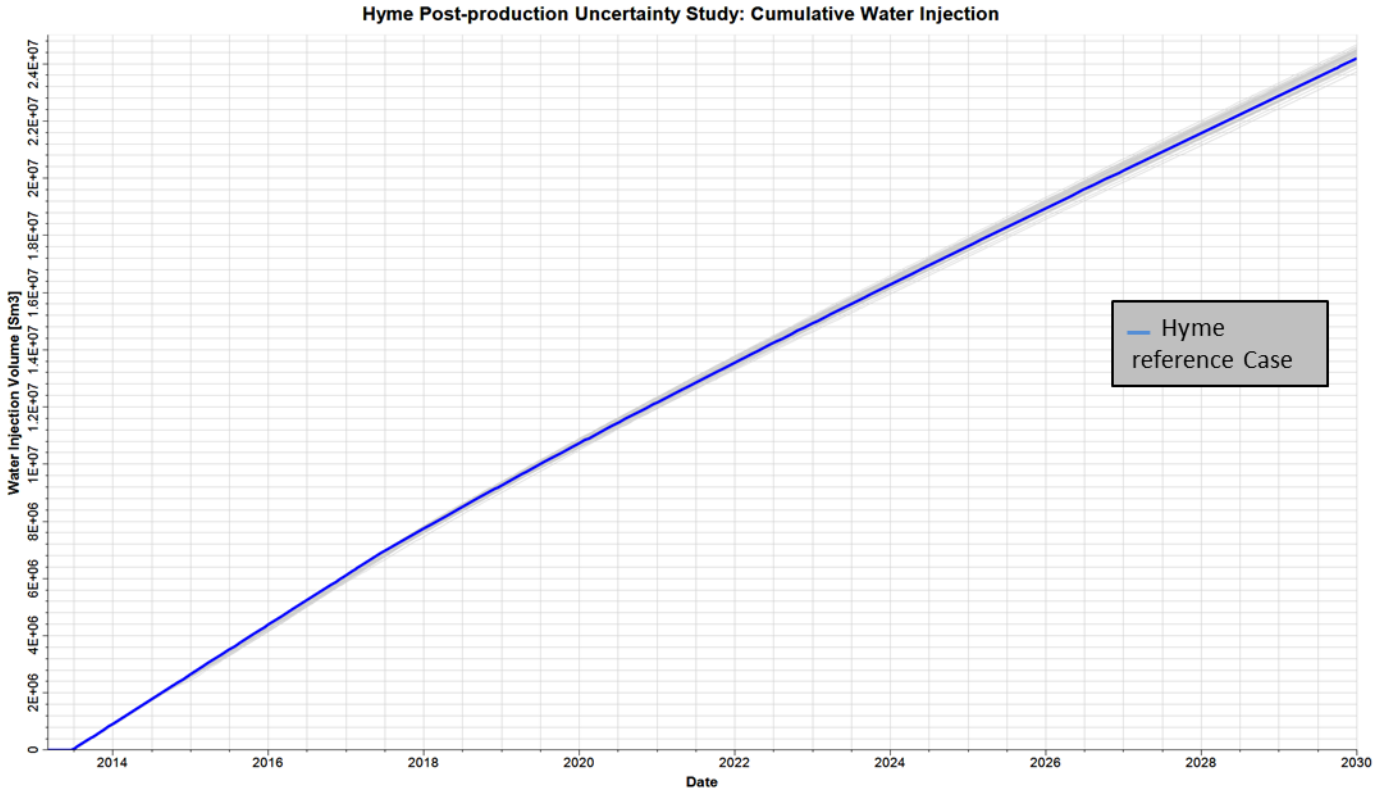

Figure 5-10: Cumulative water injection from post-production simulations.

5.5 Post-production estimated ultimate oil recovery

The post-production results were treated statistically in alignment with the pre-production study. Based on the 50 simulation cases with an objective value lower than 4.25 bar, a distribution of the cumulative oil production was created.

The distribution consists of the average cumulative oil production, P10, P50 and P90 which are based on the cumulative oil production at 1st of January 2030. The percentiles were determined in the same way as for the pre-production uncertainty study (Section 4.5). Hyme reference case is also included for comparison, and the results are listed in Table 5-3 .

Table 5-3: Distribution of cumulative oil production based on post-production simulation results

Distribution of cumulative oil production						
Date	Mean	P90	P50	P10	Reference Case	Unit
01.01.2014	0.72	0.72	0.72	0.72	0.72	[10^6 Sm^3]
01.01.2015	1.59	1.59	1.59	1.59	1.59	[10^6 Sm^3]
01.01.2016	2.42	2.23	2.45	2.46	2.44	[10^6 Sm^3]
01.01.2017	3.06	2.60	3.11	3.24	3.02	[10^6 Sm^3]
01.01.2018	3.44	2.85	3.47	3.70	3.34	[10^6 Sm^3]
01.01.2019	3.67	3.03	3.67	3.99	3.54	[10^6 Sm^3]
01.01.2020	3.84	3.19	3.82	4.21	3.70	[10^6 Sm^3]
01.01.2021	3.98	3.31	3.94	4.38	3.84	[10^6 Sm^3]
01.01.2022	4.10	3.43	4.04	4.53	3.95	[10^6 Sm^3]
01.01.2023	4.20	3.52	4.13	4.66	4.05	[10^6 Sm^3]
01.01.2024	4.29	3.61	4.21	4.76	4.14	[10^6 Sm^3]
01.01.2025	4.38	3.69	4.28	4.86	4.22	[10^6 Sm^3]
01.01.2026	4.45	3.77	4.35	4.94	4.29	[10^6 Sm^3]
01.01.2027	4.52	3.83	4.41	5.02	4.35	[10^6 Sm^3]
01.01.2028	4.58	390	4.47	5.09	4.41	[10^6 Sm^3]
01.01.2029	4.64	3.96	4.53	5.15	4.47	[10^6 Sm^3]
01.01.2030	4.70	4.01	4.59	5.21	4.53	[10^6 Sm^3]

The results from Table 5-3 are illustrated in Figure 5-11. There are general alignment with P50 and Hyme reference case; however the mean is significantly higher. This is mainly due to larger density of cases with higher oil production which was observed in section 5.2. The distribution of the estimated ultimate oil recovery is illustrated by the histogram in Figure

5-12. In order to observe the P10 and P90, and to make it comparable with the pre-production results, a probability distribution histogram with a cumulative distribution function was created.

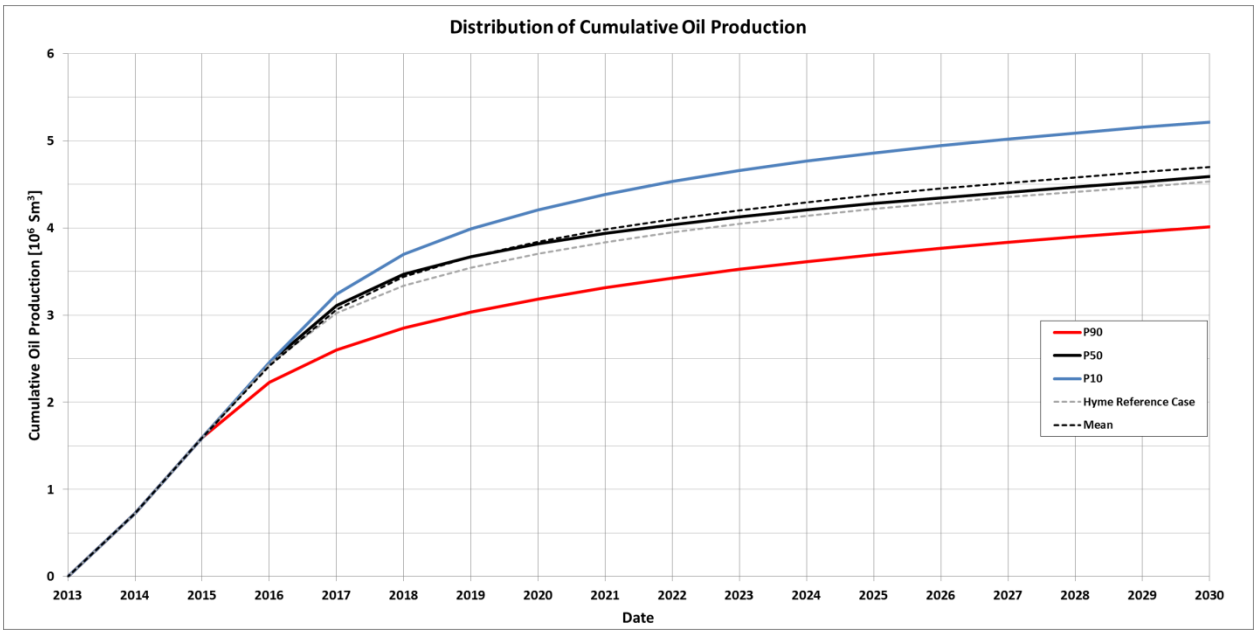

Figure 5-11: Distribution of cumulative oil production based on post-production simulation results

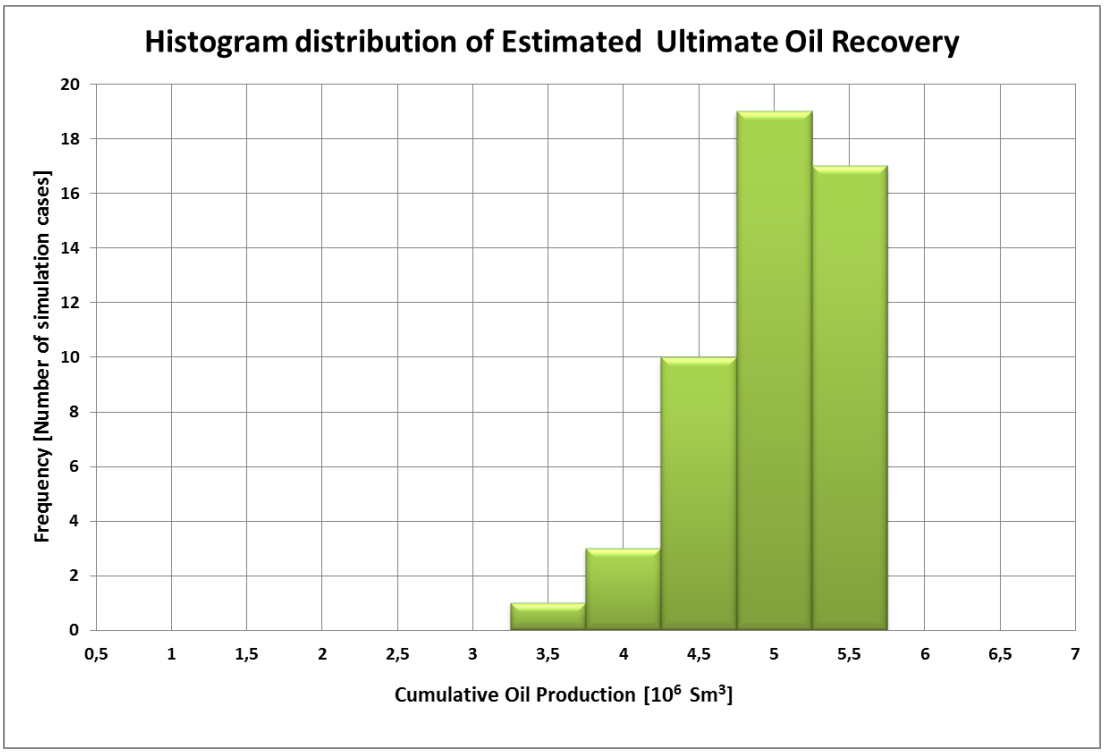

Figure 5-12: Post-Production histogram distribution of estimated ultimate oil recovery

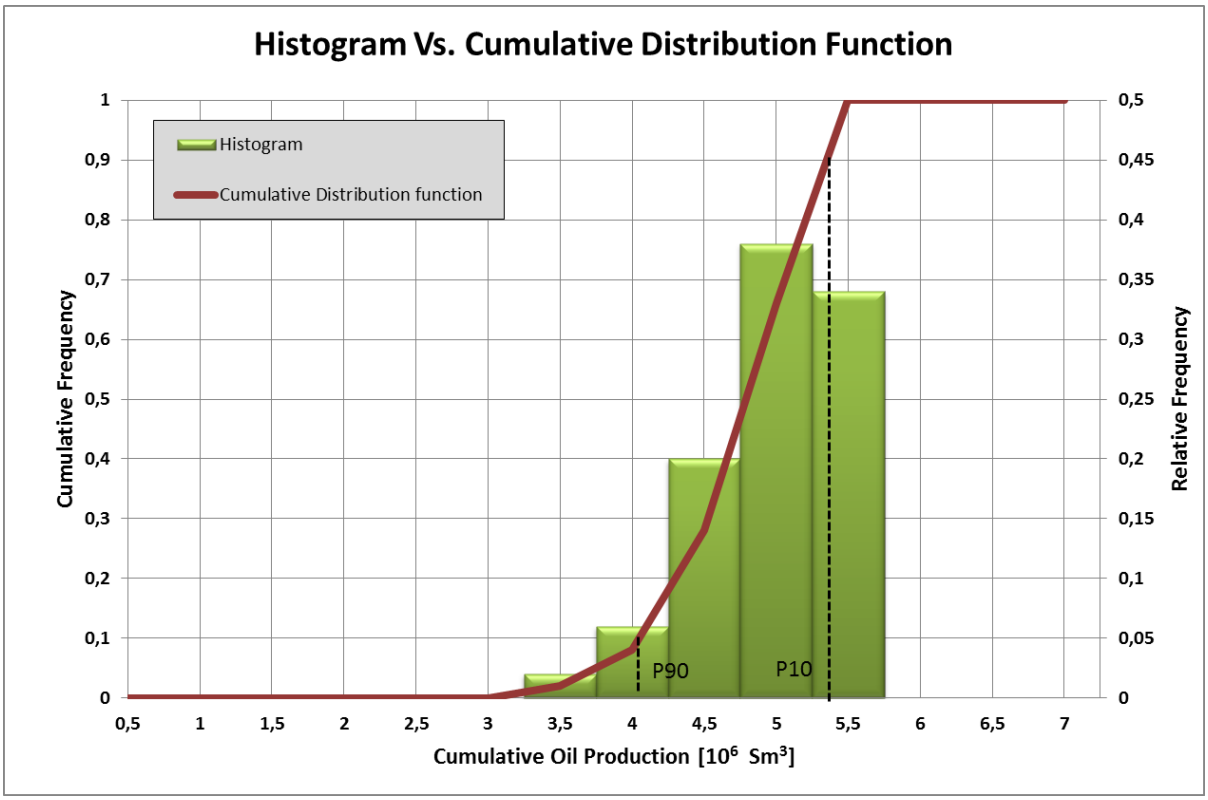

Figure 5-13: Post-Production histogram versus cumulative distribution function

Based on the P10 and P90 from last column of Table 5-3, Figure 5-11 and Figure 5-13 , the estimated ultimate oil recovery should be within the uncertainty range of 4.01 to 5.21 million Sm^3. This is reduced compared with the pre-production uncertainty study, and will be discussed further in chapter 6.

6. Pre/post-production uncertainty discussion

The sensitivity results in section 4.3 stated that the pore volume multipliers were the parameters that affected oil volume in-place and cumulative oil production the most. In addition to this, the horizontal permeability and relative permeability had significant effect. From the pre-production to the post-production results, the uncertainty in these parameters is reduced, which can be observed on the deltas in Table 6-1 and Table 6-2.

Table 6-1: Comparison of pre/post-production low case input parameters

Uncertainty	**Low case**			
	Pre	**Post**	**Delta**	**Description**
Pore volume eastern segment	0.50	0.66	0.16	Multiplier
Pore volume western segment	0.20	0.49	0.29	Multiplier
Horizontal Permeability	0.20	0.32	0.12	Multiplier
Vertical Permeability	0.01	0.01	0	Multiplier
Transmissibility multiplier Z1	0	0	0	Multiplier
Transmissibility multiplier Z2	0	0	0	Multiplier
Transmissibility multiplier Z3	0	0	0	Multiplier
Transmissibility multiplier Z4	0	0	0	Multiplier
Relative permeability	30 %	22 %	8 %	Discrete
Fault seal	30 %	20 %	10 %	Discrete

Table 6-1 shows a comparison between the pre and post-production low case input parameters. It can be observed that the deltas between the pore volume multipliers are large, especially for the western segment with a delta of 0.29. The uncertainty in horizontal permeability is also reduced, implied by the delta of 0.12. For the transmissibility multipliers there are no changes, which can be explained by that the ranges were small initially.

For the discrete input parameters it can be observed the relative frequency of low case relative permeability and sealed fault are less in the post-production study compared with the pre-production study. This can imply that the probability of an oil wet reservoir and a sealed fault are less than initially expected.

Table 6-2: Comparison of pre/post-production high case input parameters

Uncertainty	High case			
	Pre	**Post**	**Delta**	**Description**
Pore volume eastern segment	1.62	1.55	0.07	Multiplier
Pore volume western segment	1.4	1.36	0.04	Multiplier
Horizontal Permeability	5.00	3.46	1.15	Multiplier
Vertical Permeability	0.6	0.5	0.1	Multiplier
Transmissibility multiplier Z1	0.1	0.1	0	Multiplier
Transmissibility multiplier Z2	0.1	0.1	0	Multiplier
Transmissibility multiplier Z3	0.1	0.1	0	Multiplier
Transmissibility multiplier Z4	0.1	0.1	0	Multiplier
Relative permeability	30 %	28 %	2 %	Discrete
Fault seal	30 %	40 %	10 %	Discrete

For the high cases shown in Table 6-2 it can be observed that the deltas between pre and post-production not are as large as for the low cases. The pore volume multipliers are almost the same, with a delta reduction of 0.07 for eastern and 0.04 for western segment. However there is a significant reduction in horizontal permeability uncertainty, with a delta reduction of 1.15. There are no changes in the vertical transmissibility multipliers here either, which also can be explained by the small initial ranges.

The relative permeability does not change much, with a reduction of 2 %, which can imply that the probability of the reservoir to be water-wet is reduced by 2 %. For the fault seal, it can be observed that there is an increase of 10 %, however it is stated that both reference and high case suggest communication across the internal fault. Based on this, the probability for communication across the fault can be considered as 80 %.

The overall reduction in the uncertainty input parameters from the pre to the post-production study has also lead to a reduction in the uncertainty range of ultimate estimated oil recovery. Both the calculated P10 and P90 had a significant reduction, while the P50 remained almost the same. For comparison, a combination of Figure 4-19 and Figure 5-11 were made, and the results are displayed in Figure 6-1.

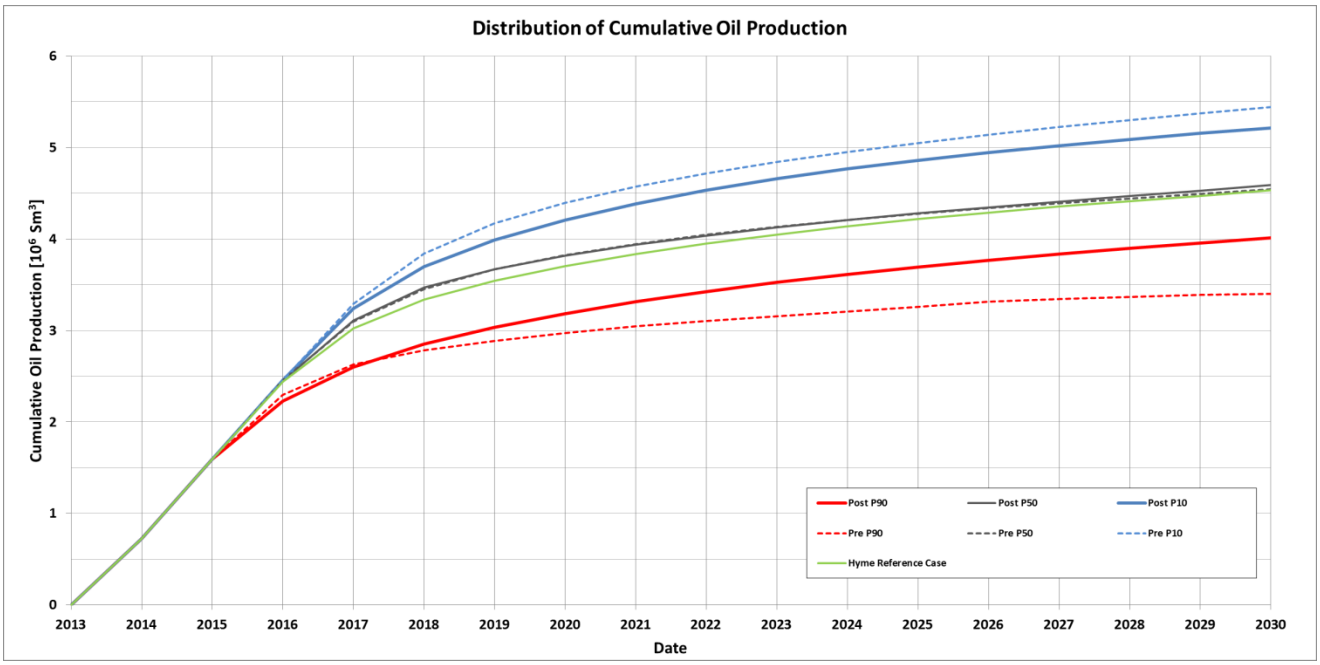

Figure 6-1: Pre/post-comparison of distribution of cumulative oil production.

From Figure 6-1 it can be observed that the P90 has the largest change, the 1st of January 2030 it has increased about 18 %. The P10 has a reduction of about 4 % while the P50 remains almost the same. It can also be observed that the Hyme reference case is in alignment with the P50. The reason why there is a larger change in the P10 is because there were larger changes in the low case input parameters (Table 6-1). This can be explained by the fact that the history matching process eliminated a great amount of the low cases, because these did not match the desired criteria of 4.25 bar.

In terms of estimated oil recovery, the changes from pre to post-production uncertainty study are displayed in Figure 6-2 . The figure was created based on the histograms in Figure 4-21 and Figure 5-13. It can be observed that the overall uncertainty for the estimated ultimate oil recovery is reduced as more data became available, especially for the low side (P90) of the range. Based on these results, the long term production potential looks better for Hyme as more data became available.

There are some limitations in this study that should be mentioned. In the pre-production study, there were 70 simulation cases that failed to run until 1st of January 2030 due to convergence failure with the material balance equations. As described in section 4.4, this

could be due to large variations in pore volume and permeability. In order to avoid this problem, it could be implemented a correlation factor between the eastern and western segment. This can again avoid too large variations in the eastern and western pore volume at the same time, and possible cause less failed simulation cases.

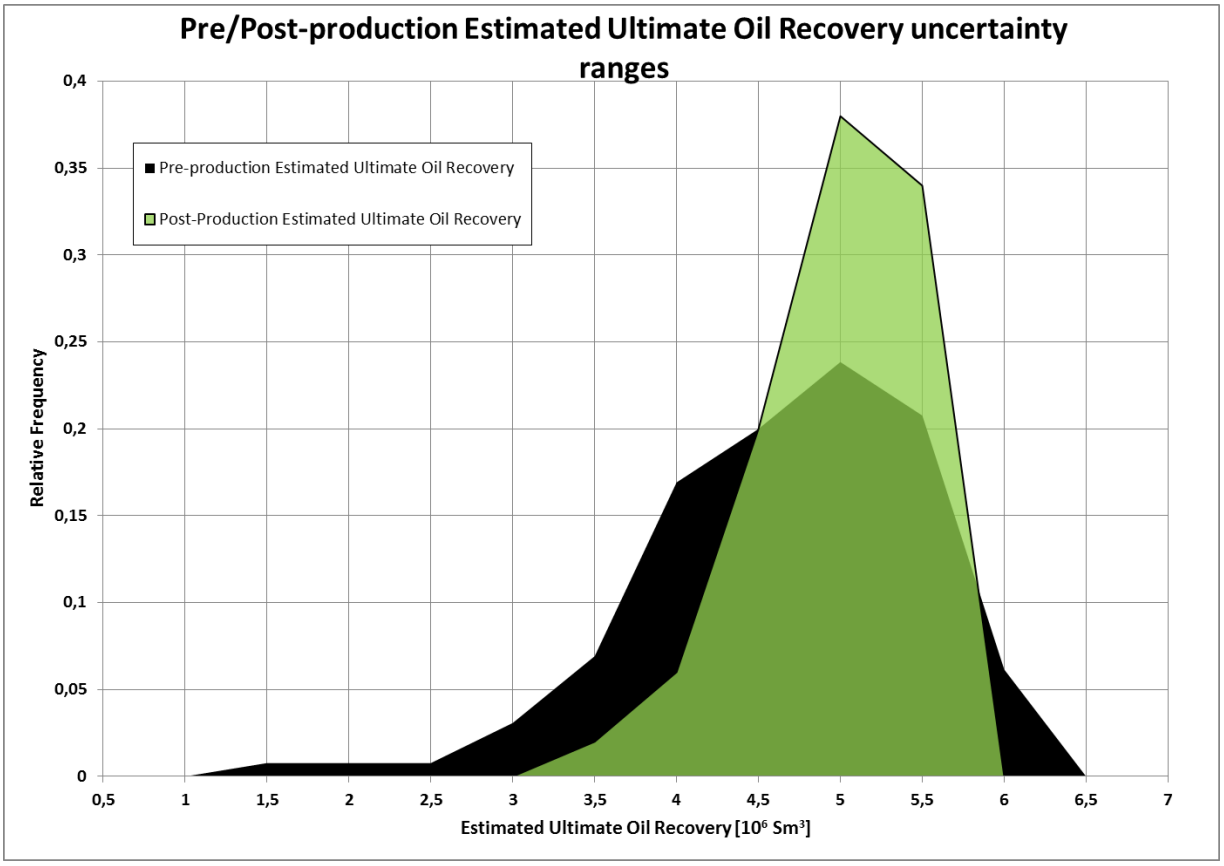

Figure 6-2: pre/post-production estimated ultimate oil recovery uncertainty ranges

Another issue is that the post-production study consist of production data from only 54 days and are only matched with bottom hole pressure. With more bottom hole pressure data available, the results could probably change. There is also a great possibility for the results to change, when other types of data becomes available, such as water production and injection.

7. Conclusions

A pre/post production uncertainty study was performed on the Hyme field in order to quantify how predicted uncertainty will change as more data becomes available. This was done by first performing a pre-production uncertainty study based on stochastic simulations with Monte Carlo sampling from interpreted uncertainty ranges for input parameters. Secondly, the study was performed again by including actual production data in a history matching process. Results from these studies was treated statistically, and compared in terms of the uncertainty ranges of the ultimate estimated oil recovery.

The results from the pre-production uncertainty study indicated that the pore volume multipliers are the most sensitive parameters. These parameters had a deep impact on both oil volumes in-place and the cumulative oil production. Additionally, the horizontal permeability and relative permeability also have a significant impact on the cumulative oil production.

Based on the results from both pre and post-production studies, it can be concluded that the uncertainty ranges for the pore volume multipliers have been reduced, especially on the low side. The uncertainty range was also reduced for the horizontal permeability. For the relative permeability it can be concluded that the probability for an oil-wet reservoir has been reduced. In addition to this, it can be concluded that there is 80 % probability for communication across the internal fault.

Results for the pre/post-uncertainty study have led to a significant reduction in the uncertainty range of the estimated ultimate oil recovery. A conclusion that can be drawn from this is that there is less uncertainty, hence a lower risk in the Hyme long term production potential as more data becomes available.

The model and workflow used in this thesis has been constructed, tested and is ready for use as a tool for VNG in future evaluation of Hyme. For the future, it is recommended to include more bottom hole pressure data and integration of other production data as they become available.

8. References

- Almeida Netto, S.L, Schiozer, D.J., Ligero, E.L. and Maschio, C.: "History Matching using Uncertainty Analysis" Canadian International Petroleum Conference, Jun 10 - 12, 2003, Calgary, Alberta
- Archie, G.E.: "The electrical resistivity log as an aid in determining some reservoir characteristics" Petroleum Transactions of AIME (January 1942) pp.54-62.
- Breitenbach, E.A.: "Reservoir Simulation: State of the Art", JPT(September 1991), pp. 1033- 1036
- Caers, J.: "Petroleum Geostatics", 2005, SPE, ISBN 978-1-55583-106-2, pp. 53-63
- Dalland, A., Worsley, D. and Ofstad, K. 1988: "A lithostratigrafic scheme for the Mesozoic and Cenozoic succession offshore mid- and northern Norway", NPD-bulletin No 4 (January 1988), pp.10-12.
- Damsleth, E., Hage, A. and Volden,R.: "Maximum Information at Minimum Cost: A North Sea Field Development Study With an Experimental Design", JPT(November 1992, Vol.44, No 12, pp. 1350-1356
- Haldorsen, H.H. and Damsleth, E.: "Stochastic modeling", JPT(April 1990), pp.404-412
- Kleppe, H.:"Notes RESERVOIR SIMULATION", University of Stavanger (2010), pp. 1-39 and pp.112-114
- Lehne, K.A.:"Geologisk brønnlogging", 1985, Universitetsforlaget AS, ISBN 82-00-06875-7, pp. 17-50
- Lépine, O.J., Bissell, R.C., Aanonsen, S.I., Pallister, I.C. and Barker, J.W.: "Uncertainty in Predictive Reservoir simulation using gradient information" SPE Journal, Vol. 4, No 3 (September 1999), pp.251-259
- Li-Bong, W.L., Krum, G.L., Yao, T., Wattenbarger, R.C. and Landis, L.H.: Application of Model-Based Uncertainty Analysis" , Abu Dhabi International Petroleum Exhibition and Conference, 5-8 November 2006, Abu Dhabi, UAE, pp.1-5
- Lisboa, E. and Duarte, R.: "Uncertainty Analysis Considering the Production History: Evaluation of a Real Field", SPE Latin American and Caribbean Petroleum Engineering Confrence, 1-3 December 2010, Lima, Peru, pp. 1-10

- Martinius, A.W., Ringrose, P.S., Næss, A., Wen, R.: “Multi-Scale Characterization and Modeling of Heterolithic Tidal Systems, Offshore Mid-Norway”, 1999. In: "Advanced Reservoir Characterization for the 21st Century" Hentz, T. F. (ed), Proceedings of GCSSEPM Research Conference, pp. 193-204. Houston, U.S.A, (December 5-8, 1999)
- Mattax, C.C and Dalton, R.L.: “Reservoir Simulation” , JPT (June 1990), pp. 692-695
- Reid, B.E., Høyland, L.A., Olsen S.R. and Petterson, O.: “The Heidrun Field – Challenges in Reservoir Development and Production”, OTC (May 1996), pp.521-534
- Reis, L.C, dos Reis, L.E, da Silva, L.C. and Becerra, G.G.: “History Matching: Is it Necessary to Optimize?”, Latin American and Caribbean Petroleum Engineering Conference, 31 May -3 June 2009, Cartagena de Indias, Colombia, pp. 1-11
- Resoptima: “ Olyx User guide”, 2012, version 1.3.0
- Schlumberger:”Petrel Help Manual”, 2012
- Skjaeveland, S.M., Siqveland, L.M., Kjosavik, A., Hammervold Thomas, W.L. and Virnovsky, G.A.: "Capillary Pressure Correlation for Mixed-Wet Reservoirs" SPE Reservoir Eval. & Eng., Vol. 3, No 1 (February 2000), pp. 60-67
- Statoil: “Book 201 Petroleum Technology Report - Hyme Project DG3”, 2012, pp. 1-274
- Steagall, D.E and Schiozer, D.J.: “Uncertainty Analysis In Reservoir Production Forecast During Apraisal And Piliot Production Phases”, SPE 66399 (February 2001), pp.1-8
- Stoian, E.: ”Fundamentals and Applications of the Monte Carlo Method”, Journal of Canadian Petroleum, Vol. 4, No 1 (July-September 1965), pp.120-129
- Walstrom, J.E., Mueller, T.D. and McFarline, R.C.: “Evaluating Uncertainty in Engineering Calculations” , JPT(December 1967), Vol. 19, No 12, pp. 1595-1603

9. Appendix A

Hyme Reference case: – Eclipse 100 simulation deck

This section is a copy of the Eclipse 100 simulation deck of the Hyme reference case. The main deck has several include files, and many of them are too long to be included in this paper. Include files from props and schedule sections are included

RUNSPEC

```
MESSAGES
3*  15 /
TRACERS
 1* 1 /
WSEGDIMS
 1 264 2 /
VFPIDIMS
 15 10 3 /
EQLDIMS
 8 /
ENDSCALE
 /
WPOTCALC
no  /
TITLE
Hyme Reference Case
WELLDIMS
 2 246 3 2 6* 3 /
START
 2 MAR 2013 /
VAPOIL
DISGAS
WATER
OIL
```

GAS

GRIDOPTS

NO 8 /

PETOPTS

INITNNC /

MONITOR

MULTOUT

METRIC

DIMENS

77 114 156 /

TABDIMS

2 3 42 1* 8 7* 1 /

REGDIMS

8 2 /

NSTACK

200 /

NUPCOL

15 /

GRID

INCLUDE

'MB_REFERENCE_GRID.INC' /

NOECHO

GDFILE

MB_REFERENCE_GRID.EGRID /

INCLUDE

'MB_REFERENCE_PROP_PERMX.GRDECL' /

INCLUDE

'MB_REFERENCE_PROP_PERMY.GRDECL' /

INCLUDE

'MB_REFERENCE_PROP_PERMZ.GRDECL' /

INCLUDE

'MB_REFERENCE_PROP_NTG.GRDECL' /

INCLUDE

'MB_REFERENCE_PROP_PORO.GRDECL' /

INCLUDE

'MB_REFERENCE_PROP_ACTNUM.GRDECL' /

INCLUDE

'MB_REFERENCE_PROP_MULTNUM.GRDECL' /

ECHO

EDIT

INCLUDE

'MB_REFERENCE_EDIT.INC' /

PROPS

INCLUDE

'MB_REFERENCE_PROPS.INC' /

REGIONS

NOECHO

NCLUDE

'MB_REFERENCE_PROP_SATNUM.GRDECL' /

INCLUDE

'MB_REFERENCE_PROP_PVTNUM.GRDECL' /

INCLUDE

'MB_REFERENCE_PROP_ROCKNUM.GRDECL' /

INCLUDE

'MB_REFERENCE_PROP_EQLNUM.GRDECL' /

INCLUDE

'MB_REFERENCE_PROP_FIPNUM.GRDECL' /

INCLUDE

'MB_REFERENCE_PROP_FIPFAULT.GRDECL' /

ECHO

SOLUTION

INCLUDE

'MB_REFERENCE_SOL.INC' /

SUMMARY

INCLUDE

'MB_REFERENCE_SUM.INC' /

SCHEDULE

INCLUDE

'MB_REFERENCE_SCH.INC' /

'MB_REFERENCE_PROPS.INC' /

```
SCALECRS
  YES/
TRACER
  TR1 WAT /
/
ROCKOPTS
  1* 1* ROCKNUM /
ROCK
       216.8   7.833E-005 /
PVTW
       198.2      1.0303  3.9868E-005     0.33034  8.9588E-005 /
       198.2      1.0303  3.9868E-005     0.33034  8.9588E-005 /
       198.2      1.0303  3.9868E-005     0.33034  8.9588E-005 /
PVTO
        17.2         20      1.1152       0.574
         50      1.1098       0.612
         100      1.1019       0.678
         150      1.0949       0.746
        198.2      1.0889       0.812
         250      1.0831       0.883
         300      1.0781       0.951
         350      1.0736       1.019
         400      1.0694       1.086
         450      1.0656       1.152
         500      1.0621       1.217
         550      1.0588       1.281
         600      1.0558       1.345 /
        45.8         50       1.214       0.456
```

100 1.2024 0.501

150 1.1925 0.548

198.2 1.1841 0.594

250 1.1761 0.644

300 1.1693 0.693

350 1.1631 0.742

400 1.1575 0.79

450 1.1524 0.838

500 1.1477 0.886

550 1.1434 0.933

600 1.1394 0.979 /

89.5 100 1.3482 0.336

150 1.3325 0.361

198.2 1.3196 0.385

250 1.3076 0.41

300 1.2974 0.435

350 1.2884 0.458

400 1.2804 0.482

450 1.273 0.505

500 1.2664 0.528

550 1.2603 0.55

600 1.2547 0.572 /

135.4 150 1.4804 0.264

198.2 1.4611 0.281

250 1.4437 0.299

300 1.4291 0.317

350 1.4164 0.333

400 1.4052 0.35

450 1.3951 0.366

500 1.3861 0.381

550 1.3778 0.397

600 1.3703 0.411 /

187.3 198.2 1.6288 0.214

250 1.6033 0.228

300 1.5825 0.241

350 1.5647 0.254

400 1.5491 0.266

450 1.5354 0.278

500 1.5231 0.29

550 1.5121 0.302

600 1.5021 0.313 /

/

17.2 20 1.1152 0.574

50 1.1098 0.612

100 1.1019 0.678

150 1.0949 0.746

198.2 1.0889 0.812

250 1.0831 0.883

300 1.0781 0.951

350 1.0736 1.019

400 1.0694 1.086

450 1.0656 1.152

500 1.0621 1.217

550 1.0588 1.281

600 1.0558 1.345 /

45.8 50 1.214 0.456

100 1.2024 0.501

150 1.1925 0.548

198.2 1.1841 0.594

250 1.1761 0.644

300 1.1693 0.693

350 1.1631 0.742

400 1.1575 0.79

450 1.1524 0.838

500 1.1477 0.886

550 1.1434 0.933

600 1.1394 0.979 /

89.5 100 1.3482 0.336

150 1.3325 0.361

198.2 1.3196 0.385

250 1.3076 0.41

300 1.2974 0.435

350 1.2884 0.458

400 1.2804 0.482

450 1.273 0.505

500 1.2664 0.528

550 1.2603 0.55

600 1.2547 0.572 /

135.4 150 1.4804 0.264

198.2 1.4611 0.281

250 1.4437 0.299

300 1.4291 0.317

350 1.4164 0.333

400 1.4052 0.35

450 1.3951 0.366

500 1.3861 0.381

550 1.3778 0.397

600 1.3703 0.411 /

187.3 198.2 1.6288 0.214

250 1.6033 0.228

300 1.5825 0.241

350 1.5647 0.254

400 1.5491 0.266

450 1.5354 0.278

500 1.5231 0.29

550 1.5121 0.302

600 1.5021 0.313 /

/

17.2 20 1.1152 0.574

50 1.1098 0.612

100 1.1019 0.678

150 1.0949 0.746

198.2 1.0889 0.812

250 1.0831 0.883

300 1.0781 0.951

350 1.0736 1.019

400 1.0694 1.086

450 1.0656 1.152

500 1.0621 1.217

550 1.0588 1.281

600 1.0558 1.345 /

45.8 50 1.214 0.456

100 1.2024 0.501

150 1.1925 0.548

198.2 1.1841 0.594

250 1.1761 0.644

300 1.1693 0.693

350 1.1631 0.742

400 1.1575 0.79

450 1.1524 0.838

500 1.1477 0.886

550 1.1434 0.933

600 1.1394 0.979 /

89.5 100 1.3482 0.336

150 1.3325 0.361

198.2 1.3196 0.385

250 1.3076 0.41

300 1.2974 0.435

350 1.2884 0.458

400 1.2804 0.482

450 1.273 0.505

500 1.2664 0.528

550 1.2603 0.55

600 1.2547 0.572 /

135.4 150 1.4804 0.264

198.2 1.4611 0.281

250 1.4437 0.299

300 1.4291 0.317

350 1.4164 0.333

400 1.4052 0.35

450 1.3951 0.366

500 1.3861 0.381

550 1.3778 0.397

600 1.3703 0.411 /

187.3 198.2 1.6288 0.214

250 1.6033 0.228

300 1.5825 0.241

350 1.5647 0.254

400 1.5491 0.266

450 1.5354 0.278

```
      500      1.5231       0.29
      550      1.5121      0.302
      600      1.5021      0.313 /
 /
PVTG
       20  0.00001308    0.062612    0.013107
  0.00001307    0.063071    0.013145 /
       50  0.00001309    0.023645    0.014157
  0.00001307    0.063323    0.013385 /
      100  0.00002551    0.011215    0.016177
  0.00001307    0.011241    0.013403 /
      150  0.00007430    0.007312    0.019292
  0.00001307    0.023922    0.013399 /
     198.2  0.00017392     0.00559    0.024293
  0.00001307    0.063339    0.013399 /
 /
       20  0.00001308    0.062612    0.013107
  0.00001307    0.063071    0.013145 /
       50  0.00001309    0.023645    0.014157
  0.00001307    0.063323    0.013385 /
      100  0.00002551    0.011215    0.016177
  0.00001307    0.011241    0.013403 /
      150  0.00007430    0.007312    0.019292
  0.00001307    0.023922    0.013399 /
     198.2  0.00017392     0.00559    0.024293
  0.00001307    0.063339    0.013399 /
 /
       20  0.00001308    0.062612    0.013107
  0.00001307    0.063071    0.013145 /
       50  0.00001309    0.023645    0.014157
```

```
  0.00001307    0.063323    0.013385 /
       100  0.00002551    0.011215    0.016177
  0.00001307    0.011241    0.013403 /
       150  0.00007430    0.007312    0.019292
  0.00001307    0.023922    0.013399 /
      198.2  0.00017392     0.00559    0.024293
  0.00001307    0.063339    0.013399 /
 /
DENSITY
      815.4      1028.1      1.1042 /
      815.4      1028.1      1.1042 /
      815.4      1028.1      1.1042 /
INCLUDE
'MB_REFERENCE_PROP_PROPS.GRDECL' /
FILLEPS
SWOF
         0          0          1      0.0001
     0.02075      1E-006     0.89232     9.5E-005
      0.0415     1.3E-005     0.79388   9.025E-005
     0.06225     5.2E-005     0.70411  8.5738E-005
       0.083    0.000142     0.62243  8.1451E-005
     0.10375    0.000311     0.54832  7.7378E-005
      0.1245    0.000588     0.48127  7.3509E-005
     0.14525    0.001009     0.42077  6.9834E-005
       0.166     0.00161     0.36636  6.6342E-005
     0.18675    0.002431     0.31758  6.3025E-005
      0.2075    0.003516     0.27402  5.9874E-005
     0.22825    0.004908     0.23525   5.688E-005
       0.249    0.006655     0.20088  5.4036E-005
     0.26975    0.008807     0.17056  5.1334E-005
```

0.2905 0.011414 0.14392 4.8767E-005

0.31125 0.014532 0.12063 4.6329E-005

0.332 0.018215 0.10039 4.4013E-005

0.35275 0.02252 0.082891 4.1812E-005

0.3735 0.027508 0.067863 3.9721E-005

0.39425 0.033238 0.055045 3.7735E-005

0.415 0.039775 0.044194 3.5849E-005

0.43575 0.047181 0.035085 3.4056E-005

0.4565 0.055524 0.027508 3.2353E-005

0.47725 0.064871 0.021269 3.0736E-005

0.498 0.075291 0.016191 2.9199E-005

0.51875 0.086855 0.01211 2.7739E-005

0.5395 0.099634 0.008878 2.6352E-005

0.56025 0.1137 0.00636 2.5034E-005

0.581 0.12914 0.004437 2.3783E-005

0.60175 0.14601 0.002999 2.2594E-005

0.6225 0.16441 0.001953 2.1464E-005

0.64325 0.1844 0.001216 2.0391E-005

0.664 0.20608 0.000716 1.9371E-005

0.68475 0.22951 0.000392 1.8403E-005

0.7055 0.25479 0.000196 1.7483E-005

0.72625 0.282 8.6E-005 1.6608E-005

0.747 0.31122 3.2E-005 1.5778E-005

0.76775 0.34254 9E-006 1.4989E-005

0.7885 0.37605 1E-006 1.424E-005

0.80925 0.41184 0 1.3528E-005

0.83 0.45 0 1.2851E-005

1 1 0 1E-005

/

0 0 1 0.0001

0.022	5.9E-005	0.8811	9.5E-005
0.044	0.000335	0.77378	9.025E-005
0.066	0.000924	0.67719	8.5738E-005
0.088	0.001897	0.59049	8.1451E-005
0.11	0.003315	0.51291	7.7378E-005
0.132	0.005229	0.44371	7.3509E-005
0.154	0.007687	0.38218	6.9834E-005
0.176	0.010733	0.32768	6.6342E-005
0.198	0.014408	0.27958	6.3025E-005
0.22	0.01875	0.2373	5.9874E-005
0.242	0.023795	0.2003	5.688E-005
0.264	0.029577	0.16807	5.4036E-005
0.286	0.036129	0.14013	5.1334E-005
0.308	0.043483	0.11603	4.8767E-005
0.33	0.051669	0.095367	4.6329E-005
0.352	0.060716	0.07776	4.4013E-005
0.374	0.070652	0.062855	4.1812E-005
0.396	0.081505	0.050328	3.9721E-005
0.418	0.093301	0.039884	3.7735E-005
0.44	0.10607	0.03125	3.5849E-005
0.462	0.11983	0.024181	3.4056E-005
0.484	0.1346	0.018453	3.2353E-005
0.506	0.15043	0.013866	3.0736E-005
0.528	0.16731	0.01024	2.9199E-005
0.55	0.18529	0.007416	2.7739E-005
0.572	0.20438	0.005252	2.6352E-005
0.594	0.2246	0.003626	2.5034E-005
0.616	0.24598	0.00243	2.3783E-005
0.638	0.26853	0.001573	2.2594E-005
0.66	0.29228	0.000977	2.1464E-005

0.682 0.31725 0.000577 2.0391E-005

0.704 0.34346 0.00032 1.9371E-005

0.726 0.37093 0.000164 1.8403E-005

0.748 0.39967 7.6E-005 1.7483E-005

0.77 0.42971 3.1E-005 1.6608E-005

0.792 0.46106 1E-005 1.5778E-005

0.814 0.49375 2E-006 1.4989E-005

0.836 0.52779 0 1.424E-005

0.858 0.5632 0 1.3528E-005

0.88 0.6 0 1.2851E-005

1 1 0 1E-005

/

SGOF

0 0 1 0

0.022 0.000469 0.89232 0

0.044 0.001875 0.79388 0

0.066 0.004219 0.70411 0

0.088 0.0075 0.62243 0

0.11 0.011719 0.54832 0

0.132 0.016875 0.48127 0

0.154 0.022969 0.42077 0

0.176 0.03 0.36636 0

0.198 0.037969 0.31758 0

0.22 0.046875 0.27402 0

0.242 0.056719 0.23525 0

0.264 0.0675 0.20088 0

0.286 0.079219 0.17056 0

0.308 0.091875 0.14392 0

0.33 0.10547 0.12063 0

0.352 0.12 0.10039 0

0.374 0.13547 0.082891 0

0.396 0.15188 0.067863 0

0.418 0.16922 0.055045 0

0.44 0.1875 0.044194 0

0.462 0.20672 0.035085 0

0.484 0.22687 0.027508 0

0.506 0.24797 0.021269 0

0.528 0.27 0.016191 0

0.55 0.29297 0.01211 0

0.572 0.31688 0.008878 0

0.594 0.34172 0.00636 0

0.616 0.3675 0.004437 0

0.638 0.39422 0.002999 0

0.66 0.42188 0.001953 0

0.682 0.45047 0.001216 0

0.704 0.48 0.000716 0

0.726 0.51047 0.000392 0

0.748 0.54188 0.000196 0

0.77 0.57422 8.6E-005 0

0.792 0.6075 3.2E-005 0

0.814 0.64172 9E-006 0

0.836 0.67688 1E-006 0

0.858 0.71297 0 0

0.88 0.75 0 0

/

0 0 1 0

0.022 0.000469 0.89232 0

0.044 0.001875 0.79388 0

0.066 0.004219 0.70411 0

0.088 0.0075 0.62243 0

0.11	0.011719	0.54832	0
0.132	0.016875	0.48127	0
0.154	0.022969	0.42077	0
0.176	0.03	0.36636	0
0.198	0.037969	0.31758	0
0.22	0.046875	0.27402	0
0.242	0.056719	0.23525	0
0.264	0.0675	0.20088	0
0.286	0.079219	0.17056	0
0.308	0.091875	0.14392	0
0.33	0.10547	0.12063	0
0.352	0.12	0.10039	0
0.374	0.13547	0.082891	0
0.396	0.15188	0.067863	0
0.418	0.16922	0.055045	0
0.44	0.1875	0.044194	0
0.462	0.20672	0.035085	0
0.484	0.22687	0.027508	0
0.506	0.24797	0.021269	0
0.528	0.27	0.016191	0
0.55	0.29297	0.01211	0
0.572	0.31688	0.008878	0
0.594	0.34172	0.00636	0
0.616	0.3675	0.004437	0
0.638	0.39422	0.002999	0
0.66	0.42188	0.001953	0
0.682	0.45047	0.001216	0
0.704	0.48	0.000716	0
0.726	0.51047	0.000392	0
0.748	0.54188	0.000196	0

0.77	0.57422	8.6E-005	0
0.792	0.6075	3.2E-005	0
0.814	0.64172	9E-006	0
0.836	0.67688	1E-006	0
0.858	0.71297	0	0
0.88	0.75	0	0

/

'MB_REFERENCE_SCH.INC' /

```
RPTSCHED
  FIP=3 WELLS=2 /
RPTRST
  BASIC=3 FLOWS FREQ=10 /
WSEGITER
  /
WELSPECS
  PRMAIN PROD 51 42 1* OIL /
  /
INCLUDE
'MB_REFERENCE_SCH_WELSEGS.INC' /
WSEGVALV
  PRMAIN 2 1 0.012667 /
  PRMAIN 3 1 0.012667 /
  /
WLIST
  '*PRODUCT' NEW
  PRMAIN /
  '*WELLS F' NEW
  PRMAIN /
  /
INCLUDE
'MB_REFERENCE_SCH_COMPDAT.INC' /
INCLUDE
'MB_REFERENCE_SCH_COMPSEGS.INC' /
INCLUDE
'MB_REFERENCE_SCH_PRMAIN.INC' /
GRUPTREE
```

```
 INJ FIELD /
 PROD FIELD /
 /
WECON
 PRMAIN 1* 1* 0.9500 1* 1* CON 1* 1* RATE 1* 1* 1* 100.00 /
 /
WCONPROD
 PRMAIN 1* GRUP 5* 70.0000 /
 /
GRUPTREE
 PROD   FIELD   /
/
GCONPROD
 PROD NONE 2500.00 3500.00 900000.00 4000.00 RATE 1* 1* 1* RATE RATE
 RATE /
 /
GEFAC
 PROD 0.9500 /
 INJ 0.9500 /
 /
TUNING
 1  5*  0.01  /
  /
   2*  200  /
WSEGITER
-- MXWSIT   mxnrtimes      RedFac  IncFac
  70           70              0.25        3  /
DATES
 1 JUN 2013 /
 /
```

```
WELSPECS
 INJREF INJ 55 23 1* WATER /
 /
WLIST
 '*INJECTI' NEW
 INJREF /
 '*WELLS F' ADD
 INJREF /
 /
WCONINJE
 INJREF WATER 1* GRUP 5000.00 1* 225.0000 /
 /
GPMAINT
 FIELD WINS 0 1* 215.0000 10.0000 1.0000 /
 /
WSEGFLIM
 'PR*'  3 3  WAT  800 200 /
 'PR*'  2 2  WAT  3500 200 /
/
ACTIONS
 REDEAST2 'PR*'   3   SWCT > 0.7   2 /
 /
WSEGFLIM
 'PR*'  3 3  WAT  0 200 /
 /
ENDACTIO
DATES
 1 OCT 2013 /
 /
DATES
```

1 JAN 2014 /

/

DATES

2 MAR 2014 /

/

DATES

1 NOV 2014 /

/

DATES

1 JAN 2015 /

/

DATES

2 MAR 2015 /

/

DATES

1 JAN 2016 /

/

DATES

2 MAR 2016 /

/

DATES

1 JAN 2017 /

/

DATES

2 MAR 2017 /

/

DATES

1 JAN 2018 /

/

DATES

2 MAR 2018 /

/

DATES

1 JAN 2019 /

/

DATES

2 MAR 2019 /

/

DATES

1 JAN 2020 /

/

DATES

2 MAR 2020 /

/

DATES

1 JAN 2021 /

/

DATES

2 MAR 2021 /

/

DATES

1 JAN 2022 /

/

DATES

2 MAR 2022 /

/

DATES

1 JAN 2023 /

/

DATES

2 MAR 2023 /

/

DATES

1 JAN 2024 /

/

DATES

2 MAR 2024 /

/

DATES

1 JAN 2025 /

/

DATES

2 MAR 2025 /

/

DATES

1 JAN 2026 /

/

DATES

2 MAR 2026 /

/

DATES

1 JAN 2027 /

/

DATES

2 MAR 2027 /

/

DATES

1 JAN 2028 /

/

DATES

2 MAR 2028 /

/

DATES

1 JAN 2029 /

/

DATES

2 MAR 2029 /

/

DATES

1 JAN 2030 /

/